# Palladium-catalysed Suzuki-Miyaura cross coupling; understanding of site selectivity using different palladium pre-catalysts

Hyewon Han

MSc by research

University of York
Chemistry

March 2024

## *Abstract*

This study focused on the Pd-catalysed Suzuki-Miyaura cross-coupling reaction (SMCC) to understand site selectivity and reactivity involving 2,4-dihalopyridine substrates. This study brings two pieces of work together between Willans and Neufeldt's studies. The principal aimis to better understand the nature of the active Pd species in these site-selectives reactions, focusing mainly on palladium-*N*-heterocyclic carbene (PEPPSI) catalysts. The SMCC reaction will screening of regioselective using 2,4-dibromopyridine or 2,4-dichloropyridine and *p*-fluorophenylboronic acid with PEPPSI complexes. Furthermore, other Pd-catalysts were examined in the SMCC reactions to understand pre-catalyst activation.

*N*-Heterocyclic Carbenes (NHCs) were chosen to explore the effect of ligand sterics and electronics on catalytic activity and site-selectivity. Screening of the PEPPSI complexes showed that bulky PEPPSI complexes bring about good reactivity and most of the product was di-arylated product (2,4-Ar). The ligand sterics affect the reaction lead to higher catalyst activity. Non-bulky PEPPSI ligated Pd complexes exhibit lower activity. Additionally, when comparing two substrates, namely 2,4-dibromopyridine and 2,4-dichloropyridine, using Willans' conditions it was found that 2,4-dichloropyridine reacted well, comparable to 2,4-dibromopyridine in the SMCC reactions examined.

In addition, the bis(diisopropylamino)cyclopropenylidene (BAC) ligand was explored, along with a $[Pd_3(\mu\text{-}Cl)(\mu\text{-}PPh_2)(PPh_3)_3][Cl]$ cluster catalyst species (the Coulson cluster). These were examined in the SMCC using both Fairlamb's and Willans' reaction conditions. The BACligand showed less effect in the SMCC reactions; the Coulson cluster exhibited high reactivityin both reactions and showed greater C*4* selectivity in the SMCC using Fairlamb's reaction conditions.

## Author’s Declaration

I declare that this thesis is an original work and I am the sole author. This work has not previously been presented for a degree or other qualification at this University or elsewhere. All sources are acknowledged as references.

Hyewon Han

February 2024

## *Table of contents*

## List of Figures

## List of Schemes

## List of Graphs

## Acknowledgements

I am grateful to my supervisors Ian Fairlamb and Charlotte Willans for support and caring during my MScR studies. I was inexperienced and not sure to complete my Master but two supervisor's infinite warmth and care, which helped me to complete successfully. I learned a lot about many things include chemistry and life. It makes me to draw more big future in chemistry and also being a great person.

Second, I would like to thank Fairlamb's and Willans' groups in York. Everyone made me feel welcome, enabling me to adapt well. It was friendly and my memories will be one of the most precious and unforgettable moments of my life. Especially, thanks to Marine Labonde, my laboratory mentor, who always took care of me, taught me a lot and is now one of my best friends. In addition, thank you for running melting point for me. Also, thanks to Dr. Neil W.J. Scott, for supporting me throughtout my project. I admire his commitment and for showing me the pathway to being a real chemist. I also would like to thank Dr. Chris Horbaczewskyi, Dr. James Firth and Dr. Abigail Firth who support me in this project and in York. For the best friends, Sara Bonfante, Neda Jeddi and Lorna (Qingyun) became friends for the whole of this journey and the time we spent together was so much fun, precious and happy and I will never forget it. Also, thanks for this wonderful memory to my team members I really appreciate it.

Thirdly, thanks to the technical team in York, Charlotte Lee (Technician), Heather Fish (NMR), Karl Heaton (MS) for providing amazing support for my project. Dr. Ed Bergstrom (MS) and Dr. Jackie Mosely (MS) who gave a special opportunity to learn new technical skills in MALDI- MS, which I really appreciated.

Lastly, I especially would to thankful and grateful to my parents who have given me full funding, emotional support even long distance to complete my MScR and also for my future PhD. Even my parents give funding for my academic journey but they always make me confident and give more chance to being greater person. Also, thanks to Sohyeon Park and Junghwan Kim, I could always rely on both in London and in my mind, as a resting place when things got tough.

# Table of Abbreviations

| | |
|---|---|
| 2,4-Ar | 2,4-Bis(*p*-fluorophenyl)pyridine |
| 2-Ar | 2-(*p*-Fluorophenyl)-4-bromopyridine |
| 4-Ar | 2-Bromo-4-(*p*-fluorophenyl)pyridine |
| D | Double multiplicity (NMR) |
| DCM | Dichloromethane |
| DFT | Density Functional Theory |
| ESI | Electrospray Ionisation |
| EtOAc | Ethyl Acetate |
| HOMO | Highest occupied molecular orbital |
| *IMes* | 1,3-Di(adamantly)imidazole-2-ylidene |
| *IPr* | 1,3-Bismesityl-imidazol-2-ylidene' |
| L | Ligand |
| LUMO | Lowest unoccupied molecular orbital |
| M | Multiplet multiplicity (NMR) |
| MALDI | Matrix-assisted laser desorption/ionization |
| MS | Mass spectrometry |
| m/z | Mass to charge ratio |
| MHz | Megahertz |
| NHC | N-heterocyclic carbene |
| NMR | Nuclear Magnetic Resonance |
| Pd | Palladium |
| PEPPSI | Pyridine-Enhanced Precatalyst, Preparation, Stabilisation and Initation |
| ppm | Parts per million |
| RT | Room Temperature |
| S | Singlet multiplicity (NMR) |
| SMCC | Suzuki-Miyaura cross-coupling |
| T | Triplet Multiplicity (NMR) |

# Chapter 1- Introduction

## 1.1 Suzuki-Miyaura Cross-Coupling reaction (SMCC)

Transition metal-catalysed Suzuki-Miyaura Cross-Coupling (SMCC) reactions involve, organic boron compounds and organic halides (Scheme 1). They are widely used in many industrial and pharmaceutical applications.[1] The SMCC reaction, was reported by Suzuki and his student Miyaura in 1979.[2] It is a carbon-carbon bond cross-coupling reaction, similar to the Negishi and Kumada cross-coupling reactions, but its properties are slightly different in that itrequires a base. The SMCC reactions is largely unaffected by the presence of water, is tolerant of a wide range of functional groups, and can proceed regioselectivity and stereoselectively.[3]Additionally, the inorganic by-products of the reaction are typically non-toxic and easily removed from the reaction mixture, so SMCC reactions are suitable for laboratory as well as industrial processes.

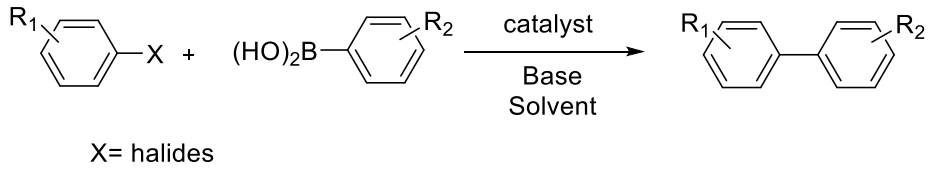


Scheme 1. General reaction scheme of the SMCC reaction.

The SMCC reaction often uses a palladium catalyst (though other metals such as the more abundant nickel can be used) and a wide range of organoboron reagents and aryl halides/ pseudo halides.[4] The reaction mechanism mainly consists of three key steps: oxidative addition (OA), transmetalation (TM), and reductive elimination (RE) (Scheme 2). Thepalladium catalyst, which is usually active in the zero oxidation state, oxidizes from Pd(0) to Pd(II), reducing the aryl halide (as an example) and forming an (aryl) Pd(II) halide intermediate. A transmetalation step with the organo-boron followed by reductive elimination yields theproduct and Pd(0) is regenerated.[5]

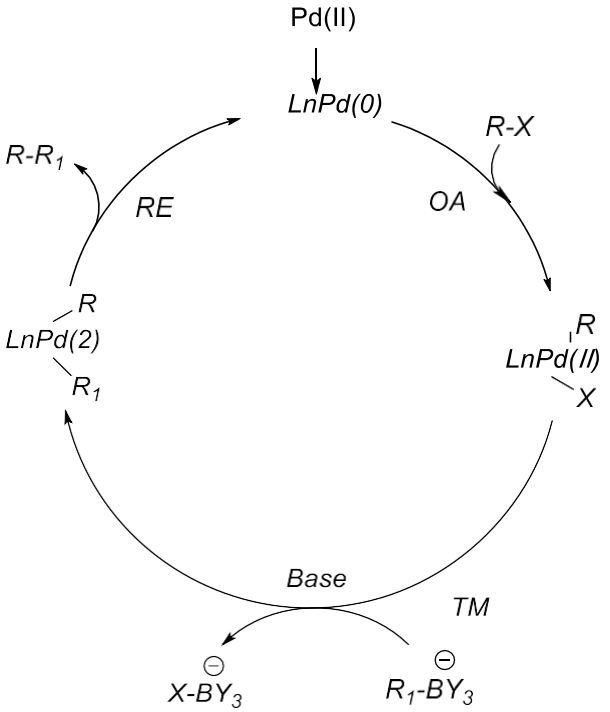


Scheme 2. General mechanism of SMCC reaction; Oxidative addition, transmetalation, reductive elimination and regeneration of the catalyst species.

In SMCC reactions, ligands play an important role at Pd in determining the rate of the oxidative addition step. Phosphine ligands are generally used because they are strong σ-donors hence will promote oxidative addition (being more electron rich at Pd).[6] However, due to the more strongly electron-donating power and greater steric shielding, N-heterocyclic carbene (NHC)ligands have been studied widely in the SMCC reaction. The steric shielding property of NHCsalso helps stabilize the active Pd(0) catalyst.[7] Many studies have shown that bulky NHC ligands bound to Pd increase reactivity and selectivity in the SMCC reaction.[8,9] Although studies have shown that the reaction can be performed without exogenous ligands, this workhas been shown using triflates as a reagents rather than bromides and chlorides, thus supporting the rationale that certain ligands provide improved product selectivity.

## 1.2 *N*-Heterocyclic Carbenes (NHCs)

NHCs have become common ligands for transition metals in organometallic and inorganic coordination chemistry and stabilize metal centres in different key catalytic steps of organic synthesis, such as in C−H activation, C−C and C−O bond-forming reactions.[10] NHCs belong to the Ficher-type carbene and usually consist of 5-membered rings with carbenic centre incorporated between two nitrogen atoms. NHCs are a strong σ-donors and bind stably to metal centres and the substituents can orient towards the metal centre. Adjacent σ-electron withdrawing and π-electron donating nitrogen atoms stabilize NHCs inductively by lowering the energy of the occupied σ-orbitals and mesomerically by donatingelectron density to the empty nitrogen *p*-orbitals and this effect leads to the planer geometry of the carbenes centres (Figure 1).[7 11]

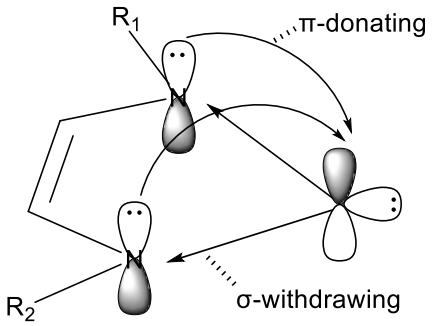


Figure 1. The σ-withdrawing and π-donating effects of the nitrogen heteroatoms stabilising thecarbonic centre of NHCs.

The first free isolated NHC (Figure 2) was reported by Arduengo in 1991 by deprotonation of 1,3-di(adamantly)imidazole-2-ylidene and it was easily isolated and stable in air.[12] Some isolated NHCs research demonstrated better catalytic effectiveness by promoting both oxidative addition and reductive elimination steps, assisted by their strong σ-donating properties and ability to sterically influence the Pd centre.[13,14]

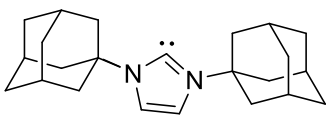


Figure 2. The first reported isolate NHC structure of 1,3-di(adamantly)imidazole-2-ylidene in 1991.[1]

NHCs generally form stable M-C bonds, are easily used as a metal catalyst. Excessive amounts of ligand (as seen with some phosphines) can be avoided. After the first NHC compound was reported, it was quickly recognised as an alternative to phosphine ligands. NHCs are typically more stabilised than phosphines, leading to thermodynamically stronger metal–ligand bonds (Scheme 3).[15] Moreover, the substituents, the backbone modifications, and heterocyclic system of the NHC motif can be modified individually, allowing electronic andsteric parameters to be varied independently.[15]

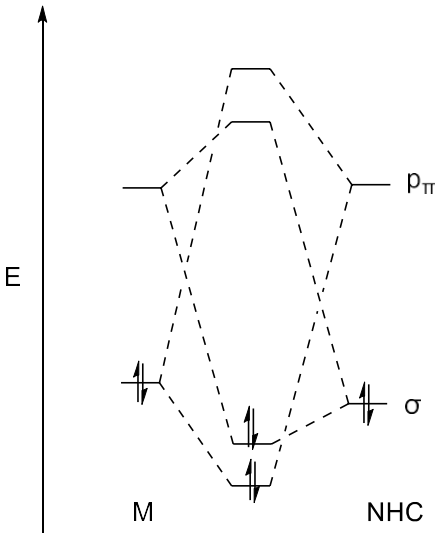


Scheme 3. Molecular orbital displayed of singlet state of an NHC with a metal centre, showing the stabilising orbitalization interactions by σ-withdrawing NHC carbene and π-donating components of the two nitrogen atoms.

## 1.3 Cyclopropenylidene

NHC ligands have been widely recognized for their usefulness and stability in the field of organometallic chemistry, with related new catalysts also being developed. Cyclopropenylidene, the smallest aromatic compound with a unique carbene centre, has attracted attention as a promising non-heterocycle-based candidate. The first cyclopropenone, diphenylcyclopropenone, was reported in 1959,[16] with Bertrand and colleagues successfully isolating bis(diisopropylamino)cyclopropenylidene (BAC) in 2006 (Scheme 4).[17]

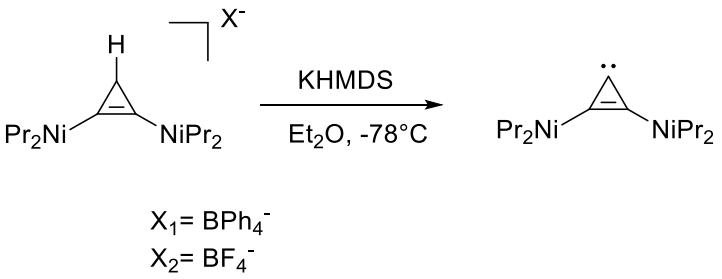


Scheme 4. The first isolated cyclopropenylidenes by Bertrand. et al, 2006[17]

The X-ray single crystal structure (Scheme 4) reveals significant π-donation of the amino group to the cyclopropene ring and a C-Ccarbene-C bond angle of 57.2° showing that it is a very strong σ-donor system. Although this compound is not stable in air, it is proven to be thermally stable, revealing its potential as a unique carbene-type ligand.[17]

The substantial resonance stabilization, or aromaticity, that arises from the symmetry of the cyclopropenium π-system gives these cations the advantage of high stability over typical carbohydrate cations.[18] A type of cyclopropenylidiene, aminocyclopropenium–metal complexes have been reported for catalytic application studies in various chemical transformations.[19,20] Overall, the bonds of the cyclopropenium complex can be broadly divided into four types: (a) TDAC π-complex[21,22], (b) bis(dialkylamino)cyclopropenium (BDAC) σ-complex,[17] (c) cyclopropenimine nitrogen(I) based ligand,[23] and (d) BDAC.[24]

Generally, cyclopropenylidiene research has focused on the catalytic investigation of how thesteric size of BACs affected the outcome of the Stetter reaction. Tucker who tested two BACswith differing steric properties, found that the steric bulk of the catalyst (Figure 2) used as a precatalyst was critical to high catalyst activity. There is a lack of research testing BAC as analternative ligand more common five-membered NHC ligand.

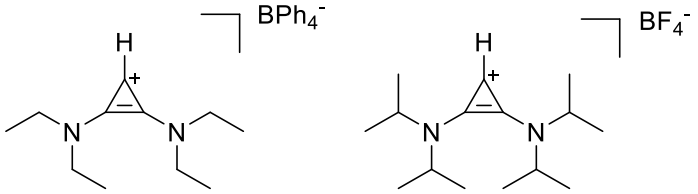


Figure 2. Di(amino)cyclopropenium complex and bis(alkylamino)cyclopropenylidine systems.

## 1.4 Pd-NHC complexes in catalysis

In 1995, Herrmann reported the first application of an NHC as a ligand in the Mizoroki-Heck reaction (Figure 3).[25] Pd-NHC complexes were synthesized using [Pd(OAc)]2 and 1.3- dimethylimidazolium iodide or 3.3'-dimethyl-l,1'-methylenediimidazolium di-iodide, with the complexes being stable to heat, oxygen, and moisture.

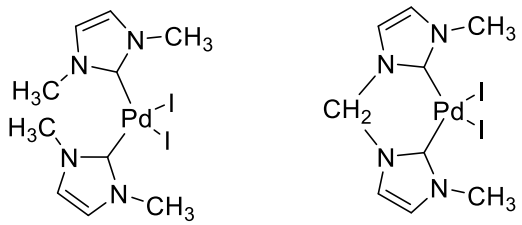


Figure 3. Initial application of NHC complexes in 1995[25]

Historically, Pd-phosphine type catalysts have dominated cross-coupling chemistry. However, the requirement for a large excess of phosphine ligands is a disadvantage, and they are sensitive to both water and air. Following early developments by Öfele[26] and Wanzlick,[27] who introduced some transition metal complexes containing NHC ligands, they were initially not widely used due to their low stability. Following the discovery of free and isolated sterically- hindered NHCs,[12] the powerful advantage of the ligand could be harnessed to increase catalytic stability and consequently reduce the rate of catalytic decomposition due to strong metal-ligand bonds. The distinct steric and electronic effects of NHCs on the metal centre contributed to improved catalytic activity. NHCs are established as a good replacement for phosphine ligands in recognition of their efficiency.[7]

The Pd complexes with NHC ligands with bulky N-substituents are the most widely applied (Figure 4), particularly those bearing 1,3-bis(2,6-diisopropylphenyl)-imidazol-2-ylidene (*IPr*) and 1,3-bismesitylimidazol-2-ylidene (*IMes*).[28]

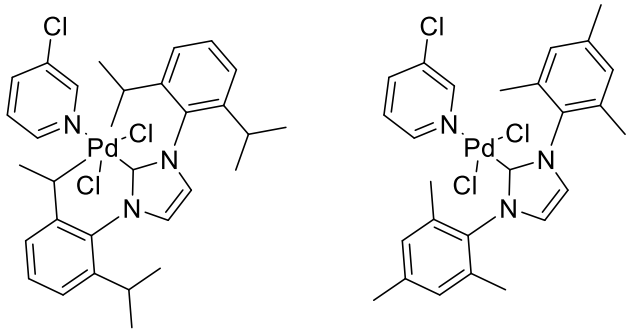


***P1*** ***P2***

Figure 4. General NHCs; ***P1*** {N-substituent: 1,3-bis(2,6-diisopropylphenyl)-imidazol-2-ylidene (*IPr*)} and ***P2*** {N-substituent: 1,3-bismesitylimidazol-2-ylidene (*IMes*)}

PEPPSI (Pyridine-Enhanced Pre-catalyst, Preparation, Stabilization, and Initiation) complexes, which are Pd(II) complexes bearing NHC and 3-chloropyridine ligands are highlystable pre-catalysts that exhibit excellent activity in a raft of cross-coupling reactions. PEPPSI complexes are considered to be excellent catalysts in cross-reactions because the strong σ donation around the metal centre and the variable steric bulk promote oxidative addition and reductive elimination. Herrmann,[29–31] Nolan,[32–34] Beller,[30] and Sigman,[35] groups have presented integrated Pd-NHC complexes that exhibit high levels of activity in Pd-catalysed reactions, but all of these Pd catalysts have the disadvantage of having to be manufactured under strict anhydrous reactionconditions.

Organ and co-workers in 2006 published a method for synthesizing stable $Pd^{II}$ species, or Pd-NHC pre-catalysts, that hold contain an NHC ligand, two anionic ligands (e.g., Cl, Br, OAc) ontothe Pd centre and a fourth "single-use" ligand in the air.[32] (Scheme 5). The authors showed rapid quantitative formation at room temperature when Pd-NHC complexes were used in SMCCs and interestingly, Negishi alkyl-alkyl cross-coupling reactions.[32] The research resultsof the process indicated that the bulky NHC ligand induces rapid reduction removal, thereby inhibiting unwanted adverse reactions or catalytic degradation in a manner similar to the bulky phosphine.[9] These studies demonstrated the high stability and excellent catalytic activity of the PEPPSI complex, and became the basis for it to be one of the commonly used pre- catalysts this day.

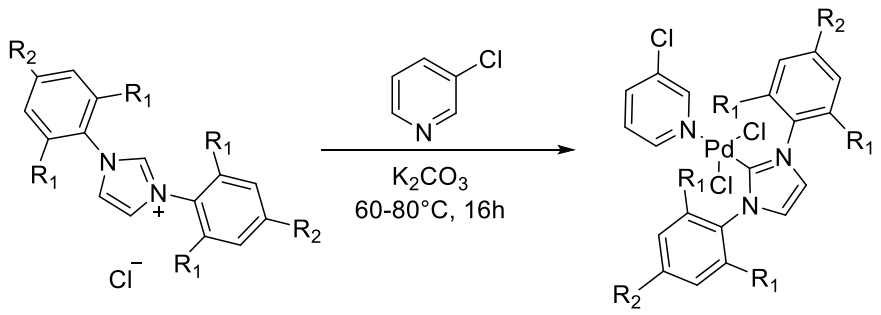


$R_1$: *IPr*
or $R_2$: *IMes*

Scheme 5. General synthesis of NHC-$PdCl_2$-3-chloropyridine complexes (PEPPSI).

## 1.5 Pd nanoparticles (Pd NPs) and clusters

Using metal nanoparticles as efficient catalysts is considered one of the promising methods for C–C formation cross-coupling reactions under mild and environmentally friendly conditions.[36] Transition metal nanoparticles are typically small in size (diameter 1-10 nm), narrow in dispersion size, and are used for chemical synthesis with a well-defined configuration.[37,38] Advantages of using nanoparticles include catalyst recovery and reuse. They are typically, highly active and exhibit high selectivity.[36]

Generally, Pd nanoparticles can be heterogeneous catalysts, and mechanisms have been reported in which palladium atoms can be extracted from the Pd nanoparticles surfaces, for example by oxidative addition enabling the leaching of [Pd(Ar)X] type species (Scheme 6).[36]

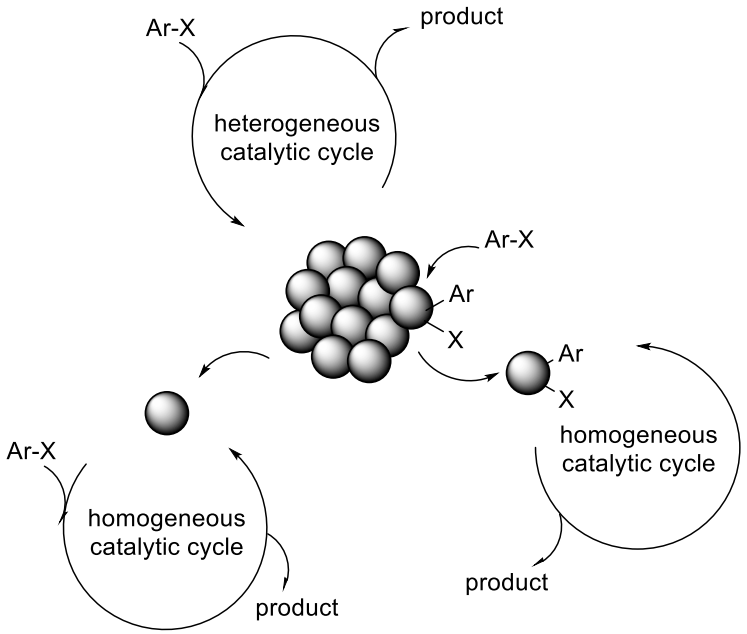


Scheme 6. General mechanisms for the Pd nanoparticles catalysed C–C coupling reactions.[36]

Metal nanoparticles (M-NPs) are generally synthesized through metal salt reduction and decomposition of organometallic complexes. M-NPs are stabilised using protective agents to prevent the formation of larger particles. Stabilisation is divided into two types: electrostatic stabilization using ionic compounds, and steric stabilization using neutral molecules such as polymers or large ligands, including oligopeptides.[36]

Fairlamb *et al*. synthesized and characterized NHC protected Au and Pd nanoparticles. The Pd-NHC nanoparticles were found to have limited stability in solution. However, the nanoparticles do exhibit interesting catalyst properties (Scheme 7, a).[39] Tilley and co-workers reported that nanoparticles stabilized with NHCs were stable enough to require no post-treatment procedures, affording a narrow size distribution, even when using a relatively weakreducing agent (Scheme 7, b).[40] The steric bulk properties of the substituents on the NHC ligand can control the NPs size and explained that AuNPs can be formed when the size of the NHC ligand is reduced.

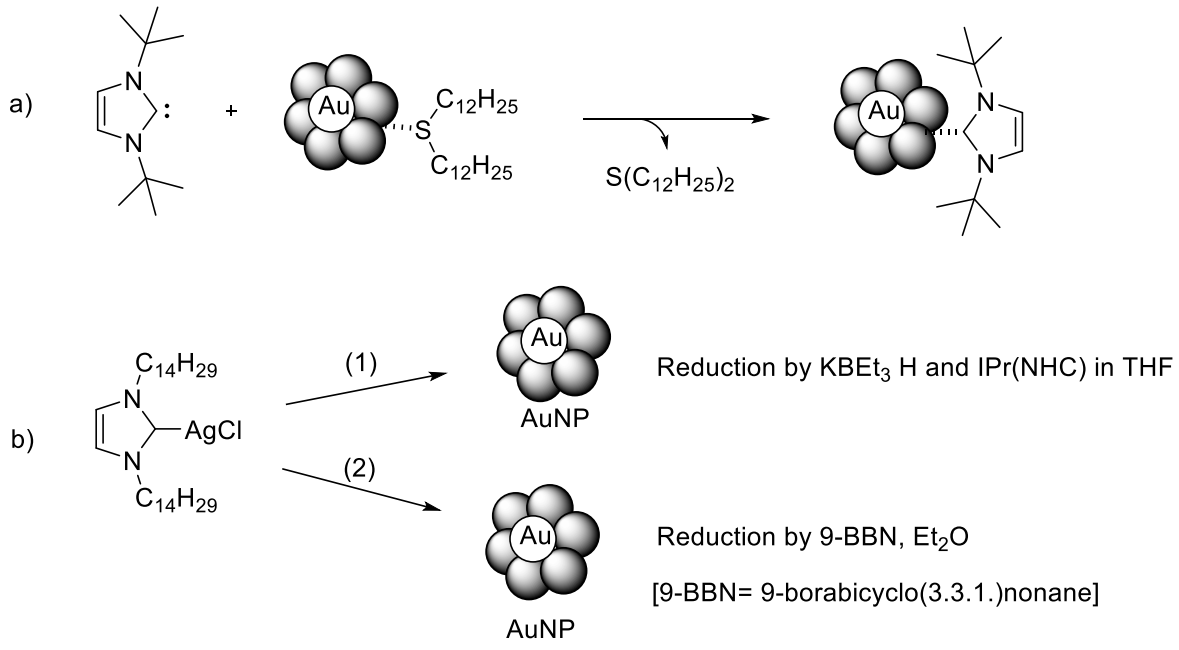


Scheme 7. a) Synthesis of NHC-protected Au nanoparticles by Fairlamb and co-workers[39], b) Reduction and synthesis of AuNPs with (1) $KBEt_3H$, THF and (2) 9-BBN, $Et_2O$ (9-BBN = 9-borabicyclo[3.3.1]nonane) by Tilley and co-worker.[40]

Li *et al*. reported an intramolecular continuous reaction in a liquid phase using the Au nanocluster as an electron transfer catalyst.[41] In addition, Li *et al.* reported the generation of robust $Pd_3$ clusters which is $[Pd_3Cl(PPh_2)_2(PPh_3)_3]^+$ (which refer to as the 'Coulson cluster') and showed as a facile and efficient catalyst in the SMCC reaction under ambient and aerobic conditions (Scheme 8).[42] The Coulson cluster resulted in excellent results with short reaction time, at room temperature, and with low Pd concentration. It was suggested that the Coulson cluster first reacted with phenylboronic acid to form the intermediate $Pd_3$-Ar (transmetalation-first step), indicating deviation from the "traditional" mechanism of the SMCC reaction (which is oxidative addition-first).

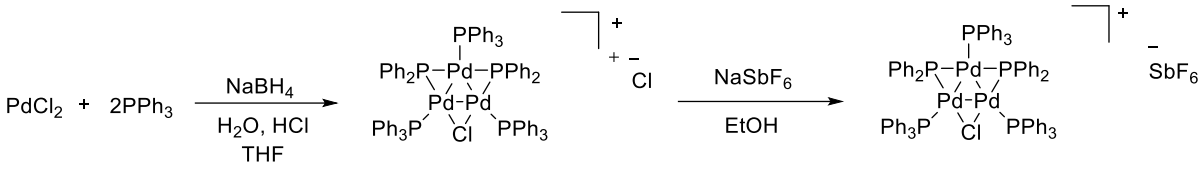


Scheme 8. Reported synthesis of $[Pd_3Cl(PPh_2)_2(PPh_3)_3]^+$ (Coulson) cluster, pre-catalyst for SMCC reactions reported by Li *et al.* (yield = 1%).[42]

Following this, Fairlamb *et al*. reported that the Coulson cluster can be generated by aggregation of mononuclear Pd species to form higher-order Pd species that can mediate further substrate conversion, suggesting that this is more similar to σ-bonding complexation to oxidative addition.[43] They explained that PdNPs are derived from a $Pd_3(OAc)_6/6PPh_3$ pre- catalyst by reaction with organic halide and published a study on the effect of PdNPs on converting positional selectivity from typical C*2* to C*4* employing 2,4-dibromopyridine in SMCC and Kumada-Corriu type reactions (Scheme 9). The Fairlamb group were also able to form the Coulson cluster in ~95% using the original reported procedure.

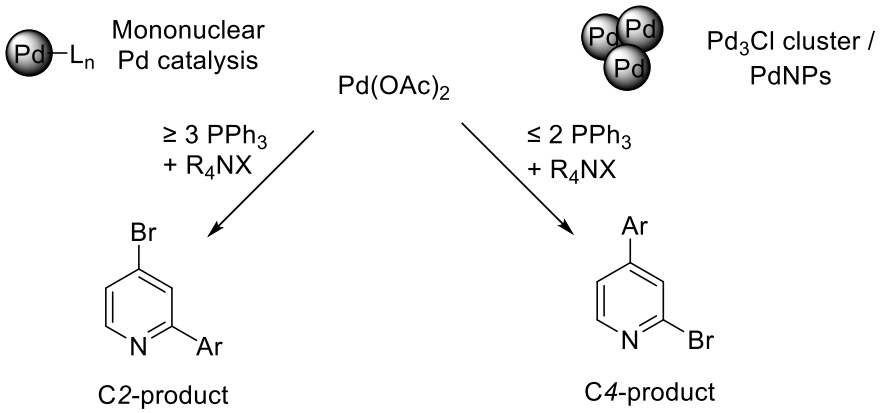


Scheme 9. Site-selectivity in SMCCs using dihalogenated pyridines (2,4-dibromopyridine) and related derivatives, reported by Fairlamb *et al.* [43]

## 1.6 Site-selectivity in SMCC

Pd-catalysed cross-coupling reactions have a variety of parameters that affect product site-selectivity (reaction outcomes), including solvent choice, base, and ligand. Fairlamb *et al*. focused on the ratio of Pd and ligand and reported that different ratios provide different site-selectivities in the cross-coupling reactions of aryl boronic acids with 2,4-dibromopyridine. $Pd_3$-type clusters and Pd nanoparticle catalysts derived from the $Pd(OAc)_2/nPPh_3$ pre-catalyst system were investigated. Changing the ratio of ligand ($PPh_3$) to $Pd(OAc)_2$ switched between higher-order Pdn catalysts and mononuclear Pd1 catalysts by catalytic speciation (Scheme 10).[7] They determined that selectivity could be controlled, with $Pd(OAc)_2/PPh_3$ (1:2) being theoptimal ratio for arylation of the 4-position, and a greater excess of $PPh_3$ (>3) switches the site-selectivity to obtain the C*2*-arylated product.

Several research groups have reported the diversity of site-selectivity for Pd-catalysed cross-coupling reactions due to the influence of the ligand, solvent, or substrate. Willans and co- workers reported that several Pd-NHC complexes are suitable catalysts for SMCC reactions, interestingly exhibiting a switch from the normal positional selectivity (C*2*) observed in the reaction of 2,4-dibromopyridine to give C*4*-arylated products.[44] Additionally, Zhou *et al.* showed highly regioselective of C*2* by 2,3 or 4-dihalopyridines and phenylboronic acid in palladium-catalysed cross-coupling reactions.[45]

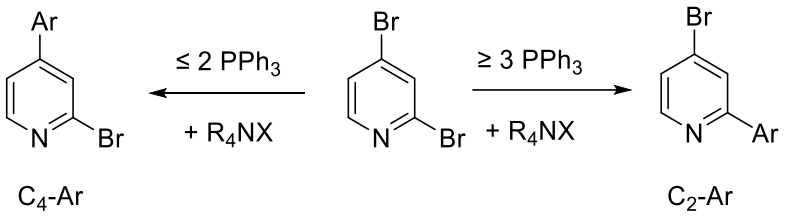


Scheme 10. Different ratio of ligands showed different site selectivity by Fairlamb *et al.*[43]

Neufeldt *et al*. showed 12e- and 14e- electron Pd(0) catalysts have disparate mechanisms foroxidative addition due to different HOMO symmetries (Scheme 11).[28] When using 2,4-dichloropyridine and the catalytic PEPPSI complex, they reported that the π-type HOMO of $PdL_2$ donates two electrons, while the σ-type HOMO of PdL donates one atom, resulting in different site-selectivity. For the 2,4-dichloropyridine substrate, it has π-symmetry with nodal planes on both sides, and they found that PdL and $PdL_2$ exhibit different site

selectivities in binding to the PEPPSI complex. They also reported their findings on ligand-induced atypical selectivity, showing that the steric hindrance varies with the size of the ligand, resulting in different site-selectivities. As shown in Scheme 15, the bulky *IPr* ligand showed C*4*-selectiveby favouring the lower coordination 12e-(PdL) in the oxidative addition step, while the non- bulky ligand lead to C*2*-selectivity by choosing the 14e-($PdL_2$) coordination due to less steric hindrance. To substantiate their findings with experimental results, they performed DFT calculations using a model system and reported a size dependency for the NHC ligands withthe observed site-selectivity.

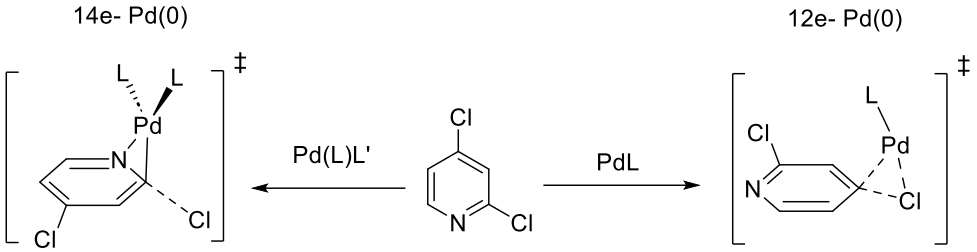


Scheme 11. Ligand-controlled divergent site selectivity by Neufeldt *et al*.[28]

It has been shown that reaction rate and site-selectivity in the Pd-catalysed SMCC reaction isaffected by many factors, including the type and ratio of the ligand Pd-NHC PEPPSI complexes.

## 1.7 Aims and Objectives

Whilst studies have been conducted to examine ligand effects in the site-selectivity SM reaction, comparing data across the studies in not possible due to the effects of other parameters that have been changed as solvent, reactor type and stir speeds. The main goal of this project is to investigate site-selectivity in the SMCC reaction of 2,4-dibromopyridine with p-fluorophenylboronic acid using a robust method that enables the data to be directly comparable for PEPPSI complexes bearing different NHC ligands. In addition, the reactivity of Pd clusters bearing BAC ligands is explored for the first time. 2,4-Dichloropyridine is compared directly to 2,4-dibromopyridine; previous studies have examined only one of these substrates. They appear to show dramatically different reactivity. Appropriate techniques willbe used for these studies including time-course sampling (reaction monitoring), specifically NMR spectroscopic analysis to follow the reactions and MALDI mass-spectrometry to observe reaction intermediates.

# Chapter 2- Catalytic Screening of [$PdCl_2(NHC_R)$(3-Cl-Pyr)] complexes in site-selective SMCC Reactions

## 2.1 Introduction

Among the NHC ligand types typically used in cross-coupling reactions, *IPr* is commonly usedbecause of its steric bulk which stabilize the metal centre.[46] As mentioned earlier in Chapter 1, NHC ligands are typically formed through deprotonation of an imidazolium salt to form a free carbene that can be coordinated to a metal centre. A five-membered unsaturated heterocycle (imidazole-based) was chosen as the basic ring architecture of the investigated NHC ligands studied (Figure 5). As ring size increases, the angle between the NHC *N*- substituents and the metal carbene bond will decrease, increasing the proximity of the N- substituents to the metal centre.[47] In general, the way to change the TEP value (an electronicproperty) for NHCs of fixed heterocycle architecture is to change the backbone substituents,[48] which is the strategy applied in this study.

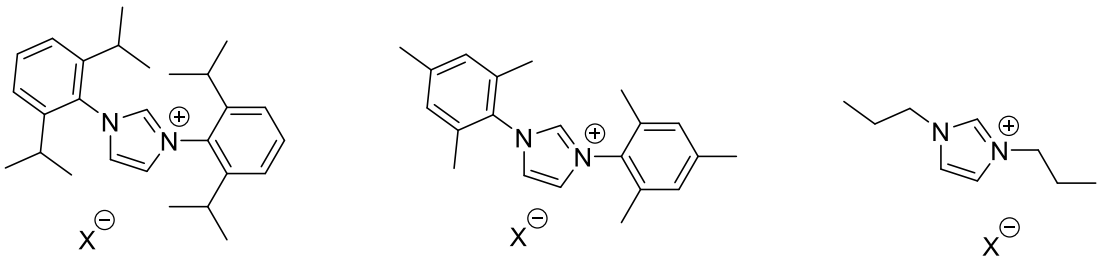


*IPr* *IMes* *n-propyl*

Figure 5. Imidazolium salts, precursors to; *IPr*, *IMes* and *n-propyl* ligands used in this study.

A series of *N*-substituents of NHC ligands were selected, ranging from bulky to non-bulky sizes. Norman *et al*. reported NHC steric effects in the SMCC reactions, when testing dihalogenated substrates and arylboronic acids. The *IPr* ligand displayed higher C*4*-selectivity compared to *IMes*. Using computational studies (free energy DFT calculations) they were able to show that *IPr* is bulkier than *IMes*.[28] The author also showed that *IMes* provides lower C*4*-selectivity dueto the high proportion of double bonds in unsaturated backbone in the ligand. They also studied the properties of PEPPSI complexes as well as the optimal substrates used together in the reactions. Following the DFT calculations, they reported that under conditions that promote oxidative addition to the unsaturated in

12e- PdL species, there would be a difference in selectivity based on the difference between the LUMO coefficients at the two positions of the dihaloheteroarene. It was assumed that the LUMO contribution in 2,4-dichloropyridine is muchlarger at the C*4* site in the SMCC reaction of 2,4-dichloropyridine with PEPPSI complexes, giving good C*4*-selectivity (Scheme 12).[49] The carbon atom on the C*2* position is more electronegative than C*4* due to weaker C–Cl bond, which is the bond adjacent to nitrogen and has a lower bond dissociation energy (BDE). Therefore, oxidative addition is more favourable at this C*2* position compared to C*4* position. Based on these results, 2,4-dibromopyridine, the benchmark substrate of Willans' benchmark reactions, and 2,4-dichloropyridine which using in the Neufeldt's studies, were both selectivity in the Pd-catalysed SMCC reactions to compare their reactivity and selectivity.

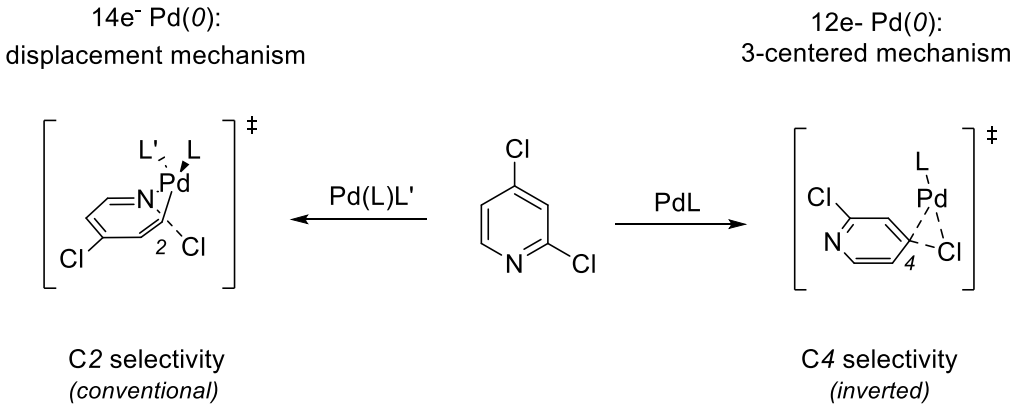


Scheme 12. Proposed different oxidative addition mechanisms for 12- and 14-electron Pd(0)$L_n$-species for 2,4-dichloropyridine in SMCC reactions (L and L' can be the same or different).[28]

## 2.2 Synthesis of NHC ligand precursors

A 5-membered unsaturated heterocyclic ring (imidazole-based) was chosen as the base ringin the reference complex used in William's study and others. The authors provided evidence on how increasing the size of the NHC ring can decrease angles between the NHC *N*- substituents and the metal carbene bond and can increase the proximity of the *N*-substituentsto the metal centre (Figure 6, a). Willams studies showed how the TEP values changes through modification of the NHC backbone substituents; 4,5-methylimidazole was chosen asthe structure with the largest degree of electron donation. (Figure 6, b)

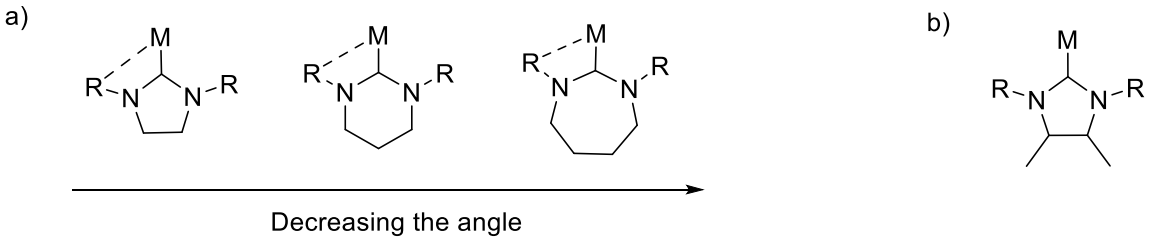


Figure 6. a) Illustration showing how increasing the NHC ring size increase the proximity of the *N*-substituent from the metal centre; b) The 4,5-dimethylimidazole ring structure with the strongest electron donating ability.

Generally, the synthesis of NHC ligand precursor require two steps to make the imidazolium salts (Scheme 13). The first step was established by Nolan and co-workers, involving reactions of the amine derivative of the desired imidazolium N-substituent with glyoxal in the presence of an acid catalyst to form an N-functionalized diimine.[50] In the second step, a ring closure ofthe diimine and paraformaldehyde takes place under acidic condition using hydrochloric acidin dioxane to form the unsaturated imidazolium chloride.

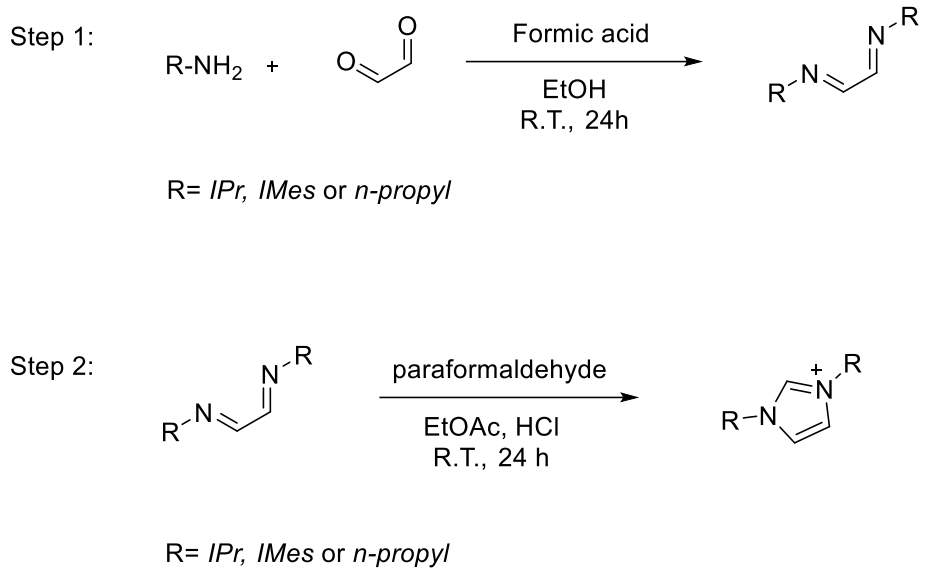


Scheme 13. General procedures to formed imidazolium salts in two steps reactions.

In this study, ***I1*** (*IPr*) and ***I2*** (*IMes*) N-substituents were chosen. Also, ***I3*** (*n-propyl*) N-substituents were selected to reduce the overall steric bulk of the NHC ligand (Figure 7).

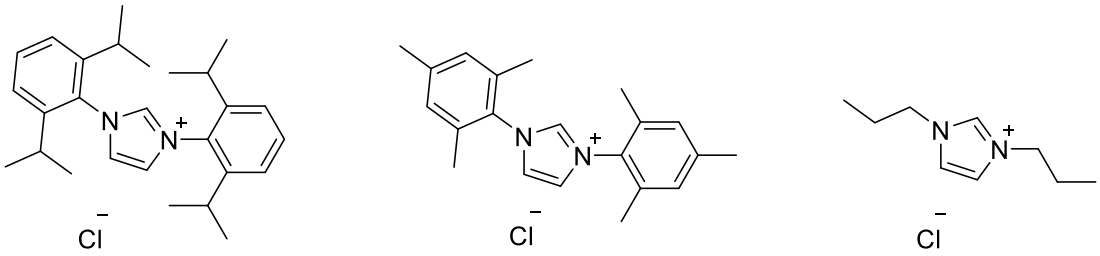


Figure 7. a) ***I1*** (*IPr*) as a bulky ligand and b) ***I2*** (*IMes*) NHC ligands considered as a less-bulky ligand and c) ***I3*** (*n-propyl*) considered as a non-bulky NHC ligands to determined steric effects.

All imidazolium salts ***I1-3*** were synthesised and characterised by $^{1}H$, $^{13}C$ NMR spectroscopy and the characterisation data compared well with the literature.[51–53] The characteristic C*2* proton signal in the $^{1}H$ NMR spectra was observed between 11 and 9.5 ppm. For example, after synthesis of ***I1*** and confirmed by $^{1}H$ NMR spectrum (Figure 8) using general procedure in Scheme 13.

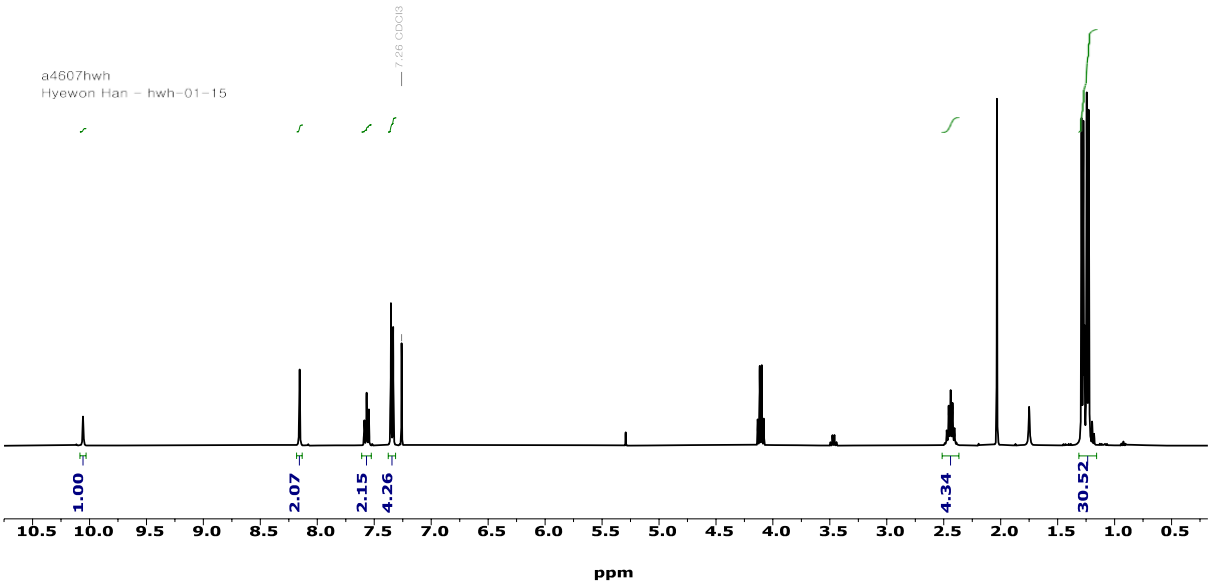


Figure 8. $^{1}$H NMR spectrum (chloroform-d, 400 MHz) of ***I1***, illustrating the characteristic C*2* proton (H, 10.5 ppm) and backbone protons (2H, 8.16 ppm) of imidazolium salts ($^{1}$H, 7.6-7.51 ppm, H, 7.36-7.30 ppm and H, 2.50-2.36 ppm and H, 1.30-1.15 ppm). Impurities confirmed for $CH_2Cl_2$ (5.28 ppm)and residual ethyl acetate (4.10, 2.0 and 1.3 ppm) and $H_2O$ (1.74 ppm).

For ***I3***, the solvent was switched to toluene and glyoxal was added as a reagent whose role isto accelerate the intramolecular ring closure (Scheme 14). The $^{1}$H NMR spectrum is shown in Figure 9.

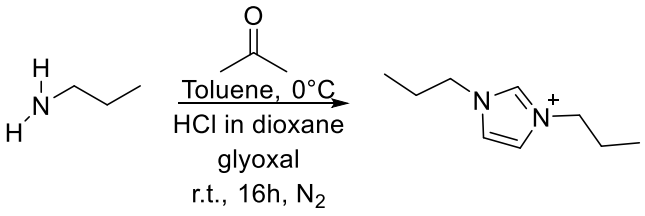


Scheme 14. General procedure to the synthesis of ***I3*** using n-propylamine with paraformaldehyde, glyoxal, HCl in toluene.

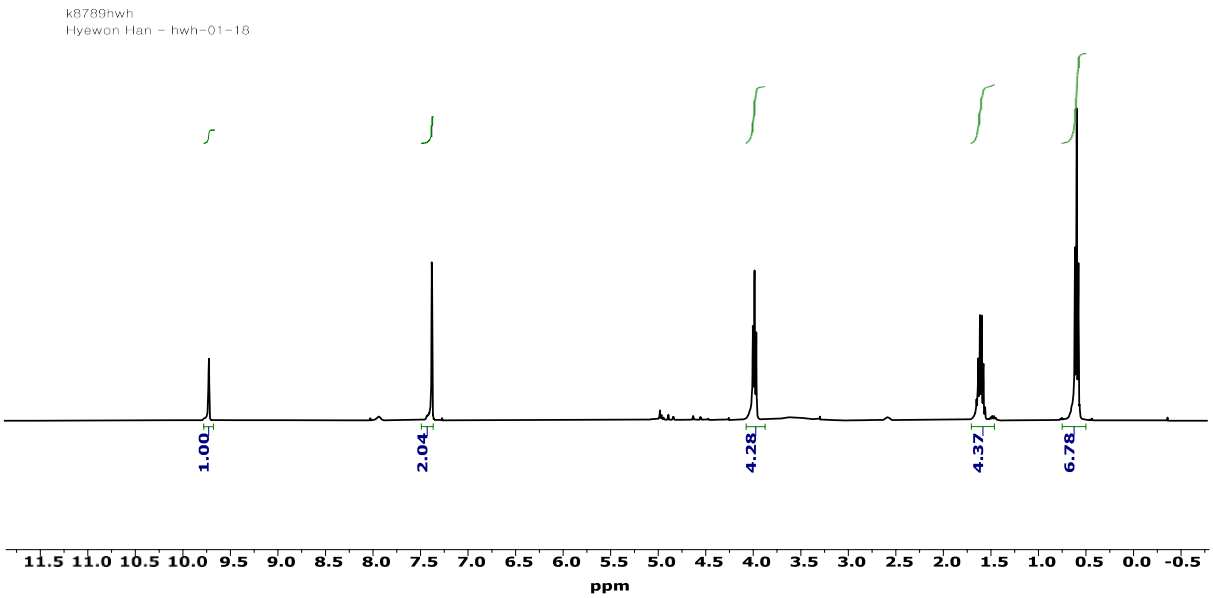


Figure 9. $^{1}$H NMR (400 MHz, chloroform-d) of *I3* δ 9.76-9.66 (s, 1H, H1), 7.47-7.35 (d, J = 1.3 Hz, 2H, H3), 4.05-3.86 (t, J = 7.3 Hz, 4H, H4), 1.69-1.44 (m, 4H, H5), 0.73-0.48 (t, J = 7.4 Hz, 6H, H6) ppm. Impurities are confirmed $CH_2Cl_2$ (5.28 ppm)

## 2.3 Synthesis of PEPPSI [$PdCl_2(NHC_R)$(3-Cl-Pyr)] complex

Syntheses of Pd-NHC complexes have reported by groups Hermann,[29,54] Nolan,[33] Beller,[55] and Sigman.[35] Their procedures have the disadvantage of being performed under strictly anhydrous conditions. Subsequently, Organ *et al.* [56] developed a synthetic route for a stable and easy-to-handle Pd-NHC complex called PEPPSI. It is a stable $Pd^{II}$ species carrying one NHC ligand, two chlorides and 3-chloropyridine with a fourth disposable ligand. This syntheticPEPPSI complex have been commercialised successfully.

According to the method presented by Organ *et al.* following deprotonation of the imidazoliumsalt, a free NHC species was generated and coordinated to $PdCl_2$ to generate the corresponding PEPPSI complex (Scheme 15). In this synthetic route, 3-chloropyridine was used as a solvent and it is the key to the PEPPSI complex and was the optimal pyridine ligand for the reactions.[56] The importance of the 3-chloropyridine cannot be understated – it is critical for stability but also in catalysis it possesses lability and potential stabilization for key Pd intermediates.

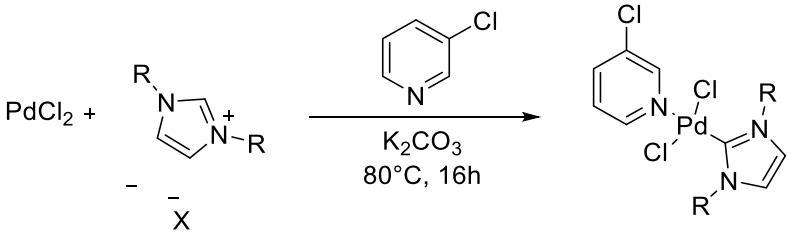


X= Cl, Br, $PF_6$ or etc.

Scheme 15. General synthetic procedure to [$PdCl_2(NHC_R)$(3-Cl-Pyr)] PEPPSIcomplexes.[56]

In addition to ***P1-3***, a novel Pd-BAC complex ***P4*** was synthesized using bis(alkylamino)cycloprophenylidine (BAC), a type of cycloprophenylidine carbene that is emerging as a similar NHC ligand (Figure 10).

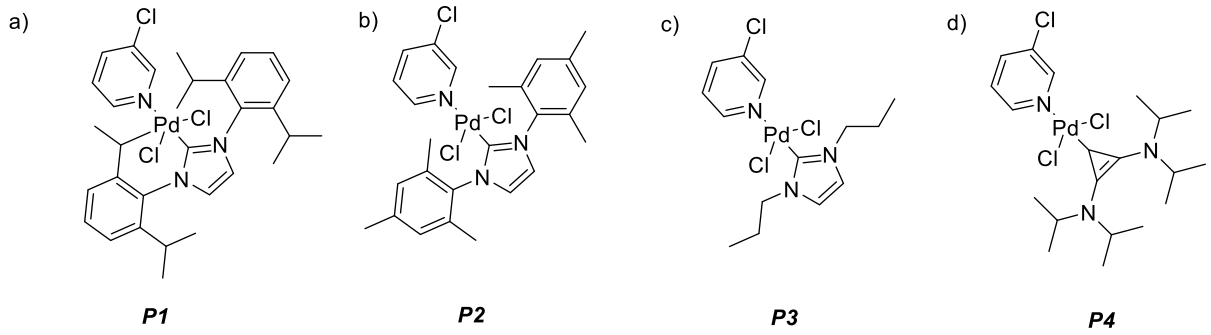


Figure 10. a) $[PdCl_2(NHC_{Dipp})(3\text{-Cl-Pyr})]$ complex (***P1***), b) $[PdCl_2(NHC_{Mes})(3\text{-Cl-Pyr})]$ complex (***P2***), c) $[PdCl_2(NHC_{n\text{-}propyl})(3\text{-Cl-Pyr})]$ complex (***P3***), d) A novel complex: $[PdCl_2(BAC_{Dipp})(3\text{-Cl-Pyr})]$ complex (***P4***)

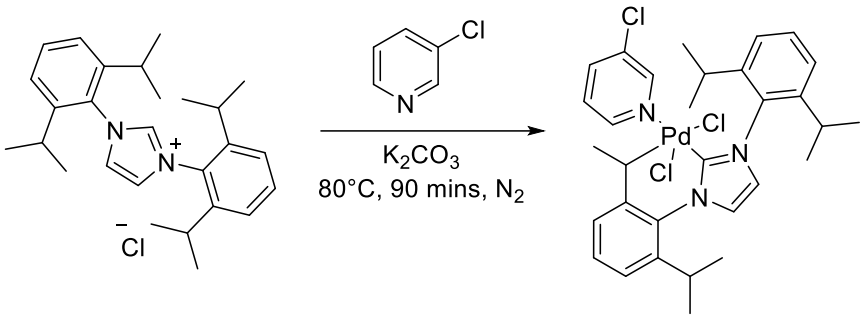


Scheme 16. Synthesis of PEPPSI complexes ***P1***-***P4***. ***P1*** complex is shown in this scheme.

All the PEPPSI complexes; ***P1***-***P4*** were characterised using $^{1}H$, $^{13}C$ NMR spectroscopy and MS. The characterisation data was compared with the available literature data. The successful formation and complexation of the NHC ligand was characterised by the loss of the imidazolium salt C*2* proton signal and a shift in the backbone corresponding complex (Scheme 16).

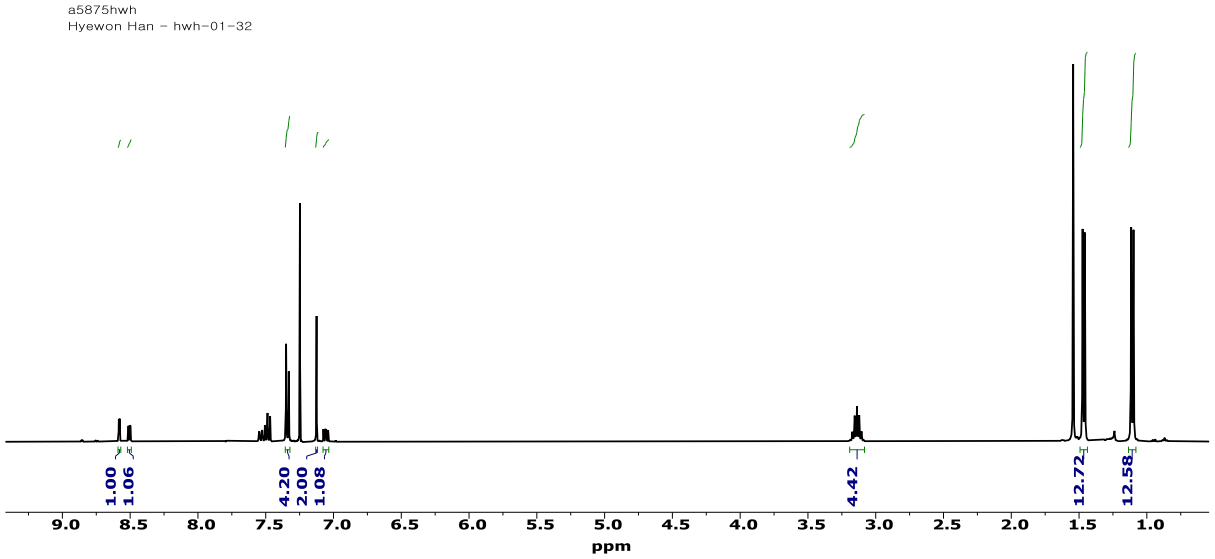


Figure 11. $^{1}H$ NMR spectrum (400 MHz, chloroform-*d*) of ***P1*** complex.

## 2.4 Examination of the PEPPSI complexes in SMCC using time course studies

### 2.4.1 Benchmark reaction conditions

Studies by Willans and co-workers have shown that PEPPSI complexes can lead to abnormal C*4*-selectivity in the SMCC reaction of 2,4-dibromopyridine with *p*-fluorophenylboronic acid in 1,4-dioxane when using bulky NHC ligands (Scheme 17).[44] In a related study, Neufeldt *et al.* reported that the LUMO of 2,4-dichloropyridine has π-symmetry with nodal planes on both thenitrogen and C*4* site. The LUMO coefficient of C*4* is considerably larger than that of C*2*, and that the larger LUMO coefficient in C*4* compared to C*2* determines the strength of the HOMO(Pd)/LUMO(substrate) overlap. Thus, providing a reason for the clear C*4*-selectivity during the PdL reaction.[28] They also analysed the energy difference between the binding intermediates of 2,4-dichloropyridine with the NHC ligand by DFT calculations. Unlike ***I1***, calculations using ***I2*** revealed that the oxidative addition intermediate involving an oxidative addition at C*2* makes the double-linked pathway energetically competitive with the single- linked pathway, which gives relatively poor C*4*-selectivity. To extend these studies, 2,4- dibromopyridine and 2,4-dichloropyridine were compared, using PEPPSI catalysts with NHCsof differing steric bulk.

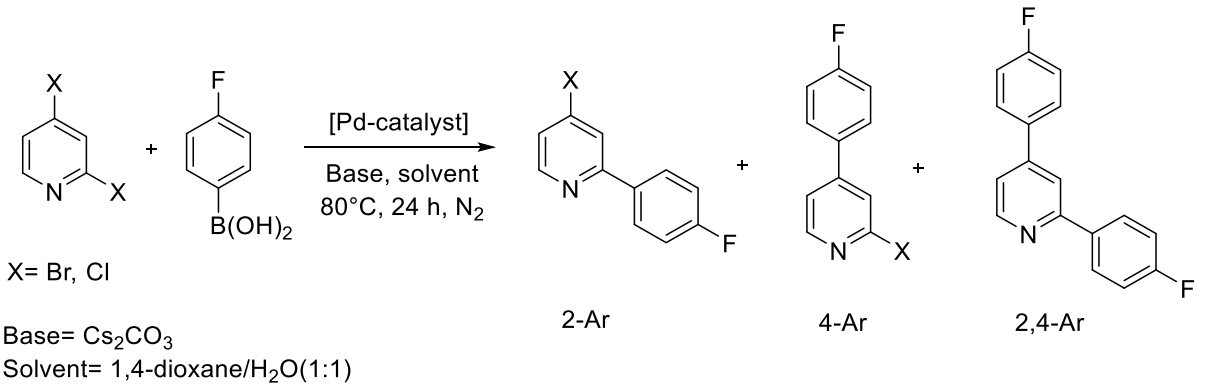


Scheme 17. Pd-catalysed SMCC reaction of 2,4-dibromopyridine or 2,4-dichloropyridine and *p*-fluorophenylboronic acid to yield 2-X-4-(p-fluorophenyl)pyridine (4-Ar), 2-(*p*-fluorophenyl)-4-X-pyridine(2-Ar) and 2,4-bis(*p*-fluorophenyl)pyridine (2,4-Ar).

The proton in the 6-position on the pyridine and the fluorine of *p*-fluorophenyl can be used to analyse the products by $^{1}$H NMR spectroscopy respectively. 1,3,5-Trimethoxybenzene (TMB) was used as an internal standard. The assay has been developed previously in the Fairlambgroup.[57]

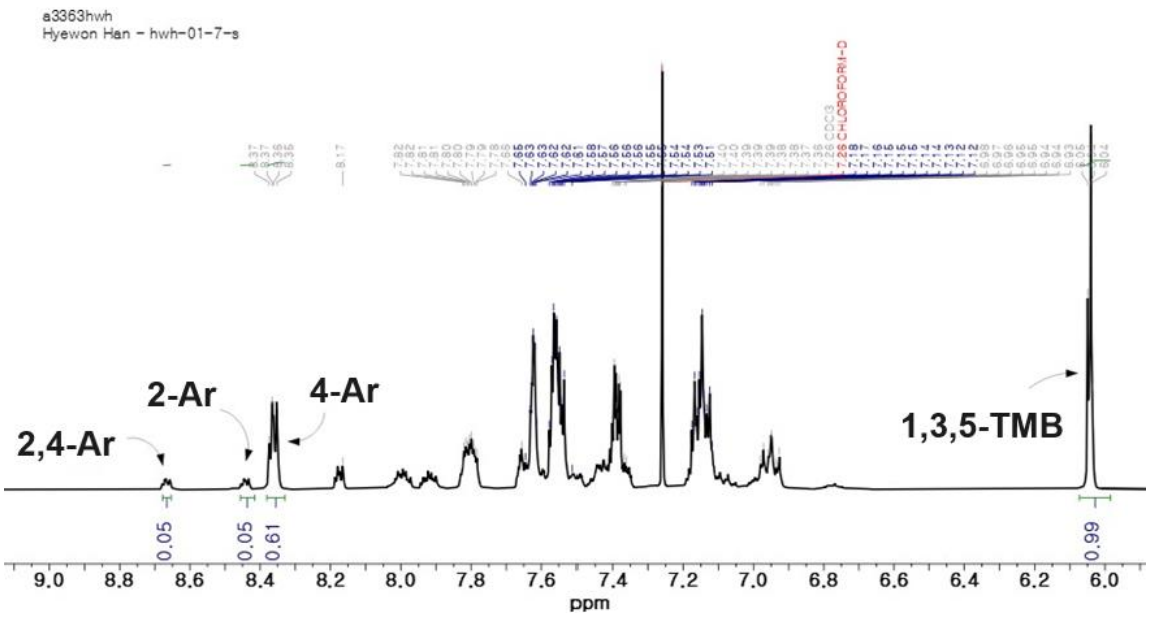


Figure 12. The $^{1}$H NMR spectrum showing that 2,4-Ar product in 8.7 ppm, 2-Ar in 8.45 ppm and 4-Ar in 8.35 ppm. 1,3,5-trimethoxybenzene was used by internal standard and the peaks showing in 6.0 ppm.

### 2.4.2 Reaction vessel selection.

Pd-catalysed SMCC reactions can be sensitive to air[5,56], and many reactions are best carried out under an inert atmosphere. In addition, these reactions must be continuously heated and the activation conditions maintained even when samples (for reaction monitoring purposes) are collected through a microsyringe. For this work silicon-capped vials were used which enables sampling whilst maintaining an appropriate inert atmosphere. It also enables reactions to be carried out in parallel and for each reaction to be identical in terms of reactor type and size.

### 2.4.3 Catalytic work-up and Filtration

For time-course sampling of the catalytic reactions, a 100 µL sample was withdrawn from thereaction mixture using a microsyringe at certain time intervals, quenched by rapid dissolutionin $CH_2Cl_2$ (1 mL) to prevent degradation and continuing to run the sample. Each sample were passed through a Celite® plug (in a glass pipette) to remove any remained palladium and unreacted arylboronic acid. The filtrate was concentrated in *vacuo* and analysed by $^{1}H$ and $^{19}F$ NMR spectroscopic analysis.

## 2.5 Examination of the PEPPSI catalysts in a regioselective SMCC reaction

### *2.5.1* Time course studies using *P1*

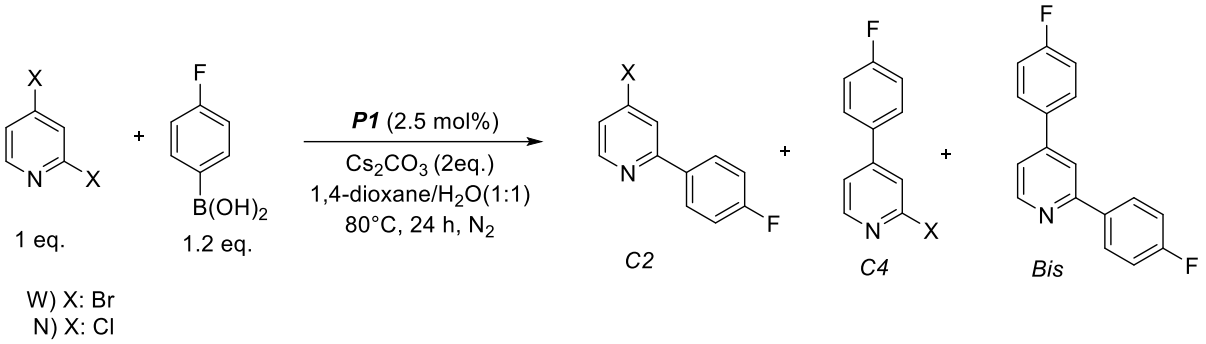


Scheme 18. Catalytic reaction of 2,4-dibromopyridine or 2,4-dichloropyridine and *p*-fluorophenylboronic acid with ***P1***. ***P1*** was used as a bulky pre-catalyst with a loading of 2.5 mol% in both reactions.

In this section, bulky PEPPSI complex ***P1*** was tested to confirm site-selectivity and reactivity.For the 2,4-dibromopyridine substrate in reaction (Scheme 18) high conversions to 2,4-Ar and4-Ar products were seen, (~4:1, 2,4-Ar:4-Ar). In this case, the limiting reagent is *p*-fluorophenylboronic acid as the 2,4-arylated product is the dominant major product. The timeto reach maximum reaction conversion appears to be relatively fast than using less-bulky size of catalysts (Graph 1). This is a viewpoint from which one can speculate on the possibility of the activity of another mechanism, or the existence of an alternative activate complexes. This result will be discussed in Chapter3 in more detail.

For comparison, 2,4-dichloropyridine was used to confirm reactivity and selectivity (Scheme 18). In contrast to 2,4-dibromopyridine, mono-arylated products were rapidly generated in thefirst few minutes (up to ~3 minutes) of the start of the reaction (Graph 1, Right). Afterwards, followed by mono-arylated products to produce 2,4-Ar products and after consumption of mono-arylated products was observed through reduction in the reaction. Similarly, the bulkier ***P1*** complex produced high conversions to 2,4-Ar and 4-Ar products. Each of products are produced relatively quickly, over relatively short times. In particular, the highest conversion of the mono-arylated products is estimated to be relatively faster than for the 2,4-Ar products.

This could indicate that the mono-arylated products are able to dissociate from the Pd centre prior to a second arylation event. Stabilization of the products is also considered to be relatively fast, and when 2,4-dichloropyridine was used in the reaction, the yield and reactionrate were shown to be superior to 2,4-dibromopyridine.

The implication of these results is that the C4-arylate product is better able to leave Pd than in the 2,4-Br system, which is one of the reasons why diarylation readily occurs in the Br system, and is particularly important in the Pd-NHC catalysed system (less important in the phosphine catalysed system).

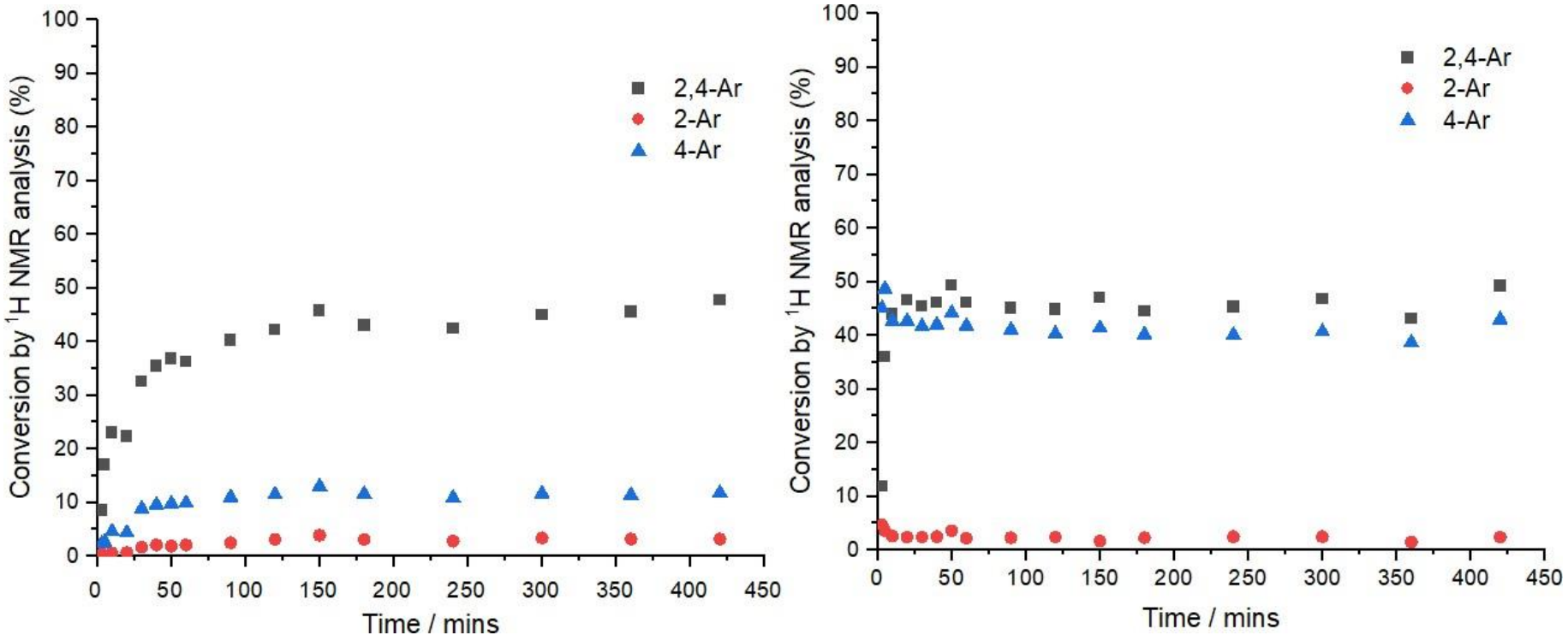


Graph 1. Left) Time-course data showing product yields of 2,4-Ar, 2-Ar and 4-Ar using 2,4-dibromopyridine and *p*-fluorophenylboronic acid with ***P1***. Right) Time-course data showing product yields of 2,4-Ar, 2-Ar and 4-Ar using 2,4-dichloropyridine and *p*-fluorophenylboronic acid with ***P1***.

### *2.5.2* Time course studies using *P2*

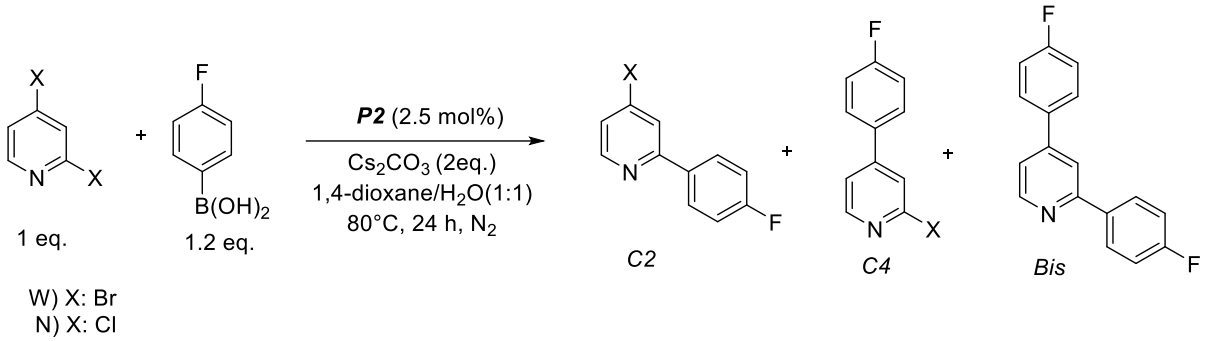


Scheme 19. Catalytic reaction of 2,4-dibromopyridine or 2,4-dichloropyridine and *p*-fluorophenylboronic acid with ***P2***. ***P2*** was used as a less-bulky pre-catalyst with a loading of 2.5 mol% in both reactions.

Using reactions in the Scheme 19, the results of using a less-bulky PEPPSI in the reaction employing 2,4-dibromopyridine resulted in the production of products relatively slower than the results of the bulkier PEPPSI reaction. Nevertheless, the reactions were typically fast (Graph 2). High conversions to 2,4-Ar product were seen; 4-Ar product was also formed, in aratio ~4:1, similar to that seen for ***P1***.

In contrast to benchmark reaction, using 2,4-dichloropyridine, mono-arylated products are rapidly generated in the first few minutes (up to ~3 minutes) of the start of the reaction (Graph 2, Right). Subsequently, the monoarylation products decreased and 2,4-Ar products were generated. Interestingly, there were some differences: the conversions of the products tendedto be stable than when using the bulky pre-catalyst and the yield of the 4-Ar product was relatively lower than when using the bulky ligand.

As a result, the comparison of PEPPSI complexes ***P1*** and ***P2*** clearly showed that steric bulksof the NHC ligands play an important role in the SMCC reaction, which is consistent with the literature evidence that the formation of 2,4-arylated product pathway in the SMCC reaction isless selective because it energetically competes with the formation of mono-arylated pathway, resulting in lower C*4* selectivity.[28]

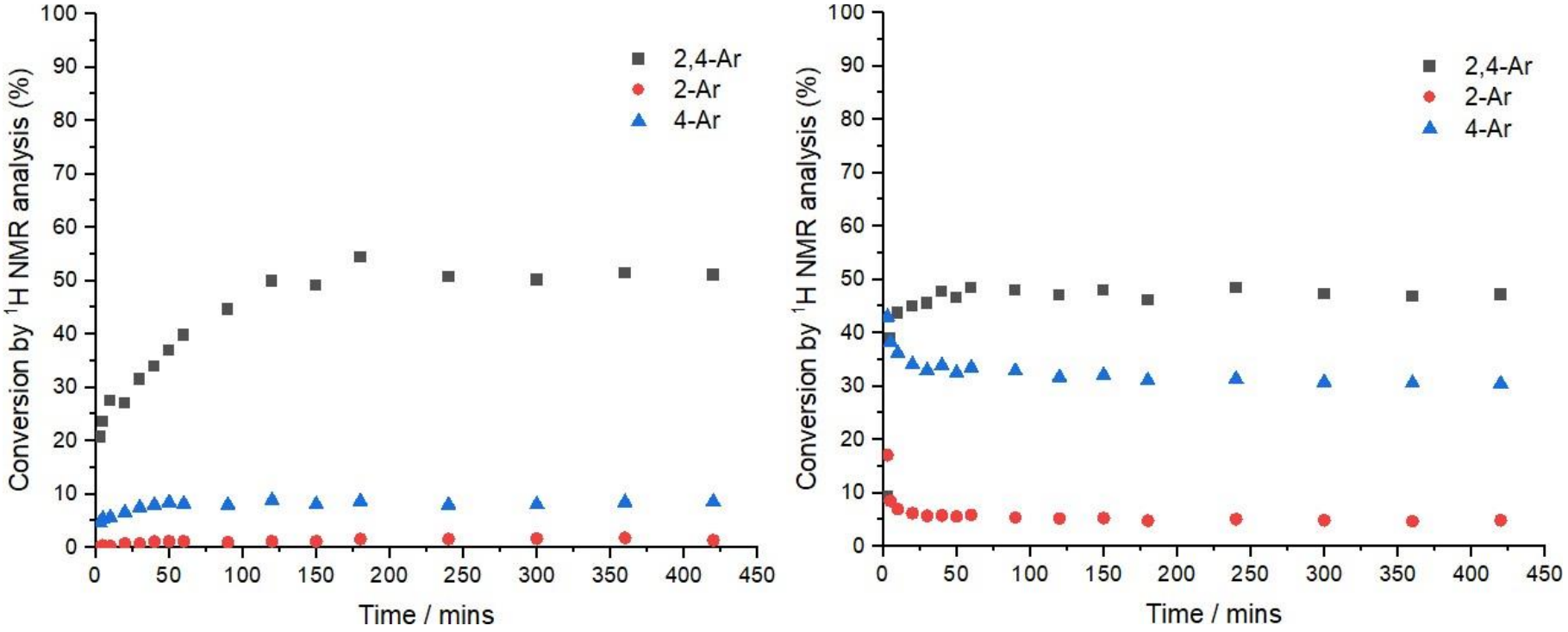


Graph 2. Left) Time-course data showing product yields of 2,4-Ar, 2-Ar and 4-Ar using 2,4-dibromopyridine and *p*-fluorophenylboronic acid with ***P2***. Right) Time-course data showing product yields of 2,4-Ar, 2-Ar and 4-Ar using 2,4-dichloropyridine and *p*-fluorophenylboronic acid with ***P2***.

### *2.5.3* Time course studies using *P3*

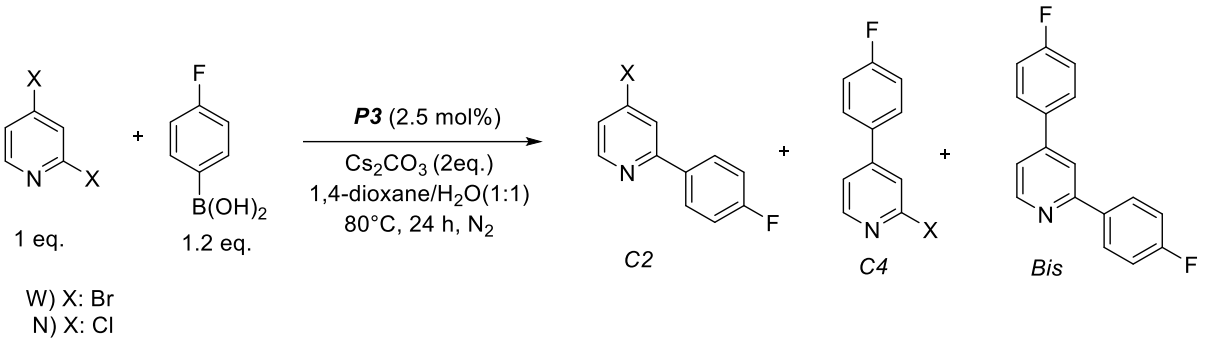


Scheme 20. Catalytic reaction of 2,4-dibromopyridine or 2,4-dichloropyridine and *p*-fluorophenylboronic acid with ***P3***. ***P3*** was used as a non-bulky pre-catalyst with a loading of 2.5 mol% in both reactions.

Using non-bulky ***P3*** complex with 2,4-dibromopyridine in the SMCC reaction (Scheme 20) and assumed that the ***P3*** would during the oxidative addition step bind toPd and that the total yields would be decreased due to the lack of steric hindrance effect unlike other bulky NHC ligands. It assumed that even when dihaloheteroarenes were used under the same conditions, the bond dissociation energies of C-X bond are different and result in different selectivity depending on the LUMO coefficient of the substrate. As a result of conducting an experiment to test this result, the yield of 2,4-Ar was the main product and theyield of mono-arylated products seemed to be significantly low (Graph 3, Left). Therefore, to prove the experimental results, the experiment was conducted by reducing the experimental time, and the results will be shown in detail after this section. Add more, analysed this graph in detail, this graph showed three subtle rising curves. It is believed that it can be hypothesized that a new mechanism occurred due to other active species.

Unlike for the other PEPPSI catalysed on the SMCC reactions, only this reaction showed C*4*-selectivity. First 150 minutes after the start of the experiment, the yield showed a decreasingtrend for a while, and then showed a slight increasing again, which can be assumed that another active species was formed or a new mechanism was created. To determine when the main reaction ends, we tested the reaction in an additional shorter time frame, which is described in more detail below section with an additional 90-minute reaction (Graph 3, Right).

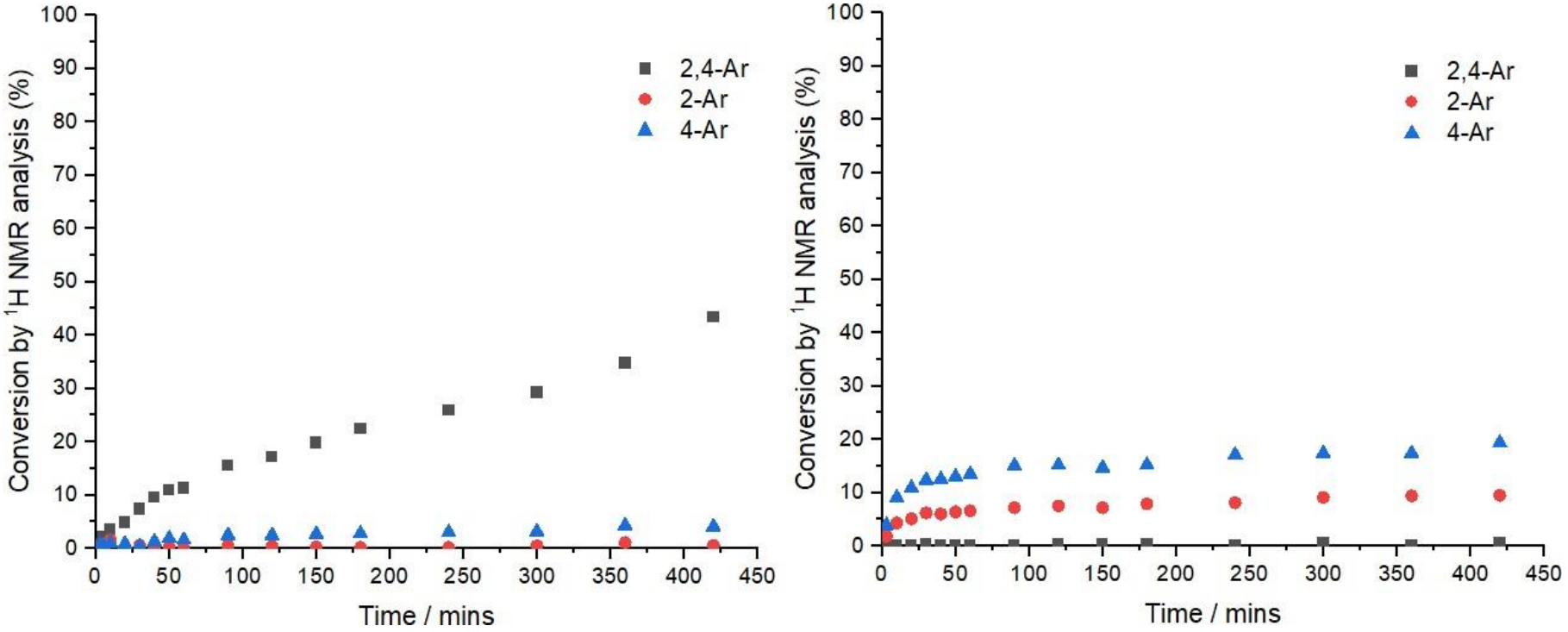


Graph 3. Left) Time-course data showing product yields of 2,4-Ar, 2-Ar and 4-Ar using 2,4-dibromopyridine and *p*-fluorophenylboronic acid with ***P3***. Right) Time-course data showing product yields of 2,4-Ar, 2-Ar and 4-Ar using 2,4-dichloropyridine and *p*-fluorophenylboronic acid with ***P3***.

## 2.6. Time variation

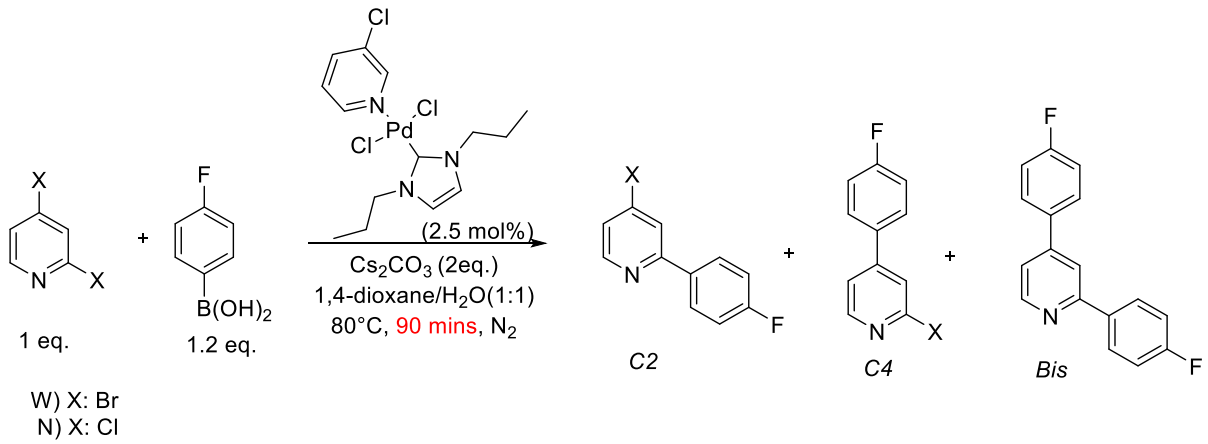


Scheme 21. Catalytic reaction of 2,4-dibromopyridine or 2,4-dichloropyridine and *p*-fluorophenylboronic acid with ***P3*** within 90 minutes. ***P3*** was used as a non-bulky pre-catalyst with a loading of 2.5 mol% in both reactions.

To extend the above 2.5.3 section, in a time course graph showed multiple curves, an experiment was conducted in which more short time samples were collected within 90 minutes to determine the point at which the reaction ends (Scheme 21). This showed that the 4-arylated product was generated as soon as the experiment started (0~2 minutes) and after that the 4-Ar product was consumed to produce the 2,4-Ar product and the 4-Ar product decreased (Graph 4, Left). After that, graph showed formation of 4-Ar products an upward curve. Overall,this reaction was progressed within 90 minutes, it confirmed, which can be assumed to lead to a different mechanism because the steric hinderance effect of the non-bulky ligand is not large than ***I1*** or ***I2*** ligand.

In the 2.5.3 section, using 2,4-dichloropyridine in the reaction showed C*4*-selectivity and multiple curves, the experiment was completed within 90 minutes to determine the end point of the reaction (Graph 3). As a result, it showed clearly C*4*-selectivity and showed a slight decreasing trend at the first 10 minutes, then increased again at the first 50 minutes, then decreased again at the 60 minutes, and then increased after 90 minutes (Graph 4, Right). Interestingly, this gave the same C*4*-selectivity as match with the above the kinetic graph in Graph 3, and it became clear that different selectivity was given depending on the differencein binding energy of the substrate and ligand.

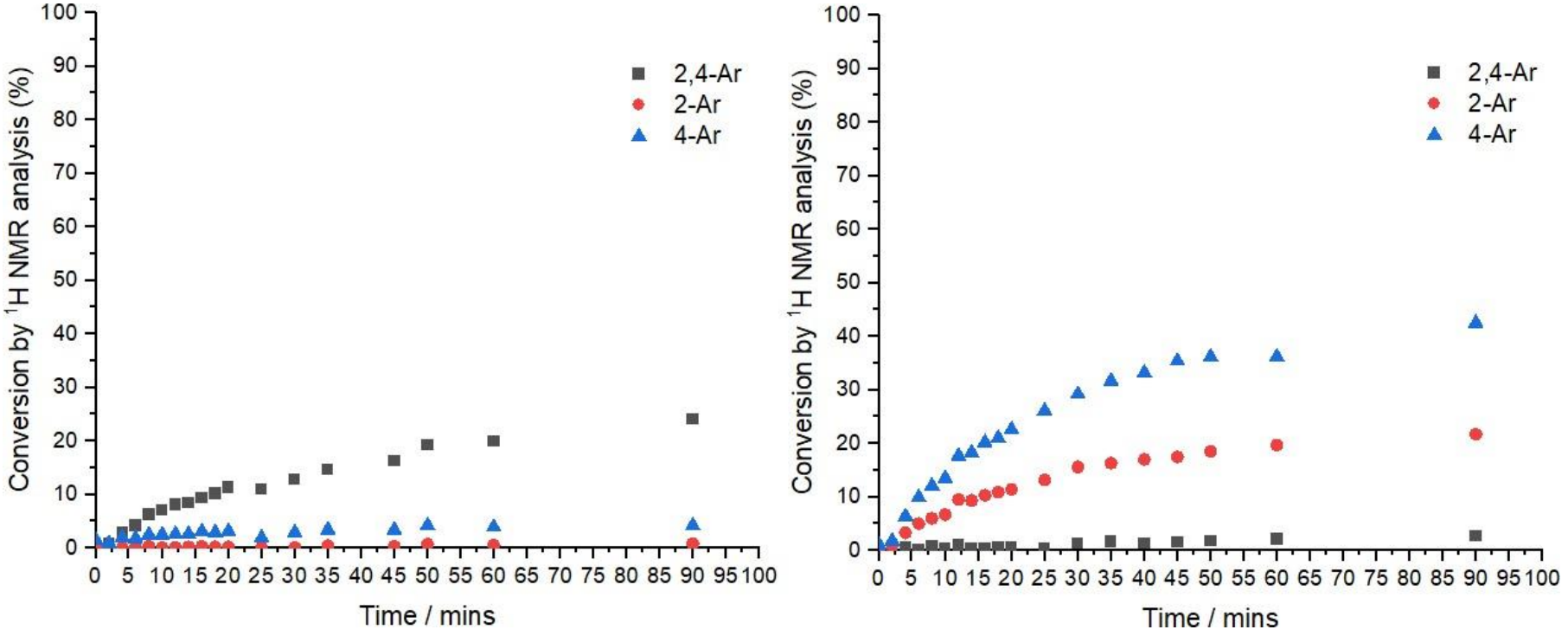


Graph 4. Left) Time-course data showing product yields of 2,4-Ar, 2-Ar and 4-Ar using 2,4-dibromopyridine and *p*-fluorophenylboronic acid with ***P3*** within 90 minutes. Right) Time-course data showing product yields of 2,4-Ar, 2-Ar and 4-Ar using 2,4-dichloropyridine and *p*-fluorophenylboronic acid with ***P3*** within 90 minutes.

## 2.7 Temperature variation

Refer to 2.5.2 section, using less-bulky catalyst (***P2***) in the SMCC reactions showed various curves which was elevated and descent of the conversions with the high temperature. In this section will be focused on temperature variation in the benchmark reactions using ***P2*** complex. Standard 80 degree condition was changed to 60, 50, and 40 degrees respectively to invest on selectivity and reactivity with 2,4-dichloropyridine substrate becauseof reactivity was better than 2,4-dibromopyridine. Hypothesis is when descended the temperature, total yields will be dropped (Figure 13).

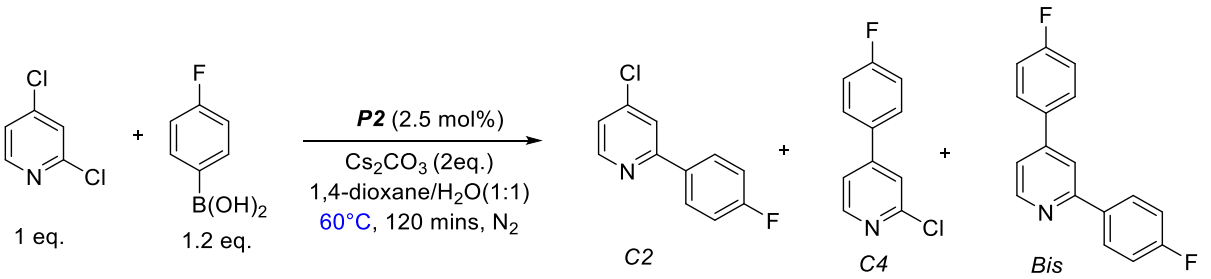


Scheme 22. Catalytic reaction of 2,4-dichloropyridine and *p*-fluorophenylboronic acid at 60, 50 and 40 ℃ for 2 hours.

Compare to the above reaction which is using same condition with 80 ℃, similar trend was seen in the reaction at 60℃ (Scheme 22), with the mono-arylated products reaching their highest point within the first 10 minutes and then decreasing, and the highest yield of 2,4-Ar product was reached at the 30 minutes (Graph 5). Although the yield was lower than when the reaction was run at 80 degrees, it had similar tendency in the graph.

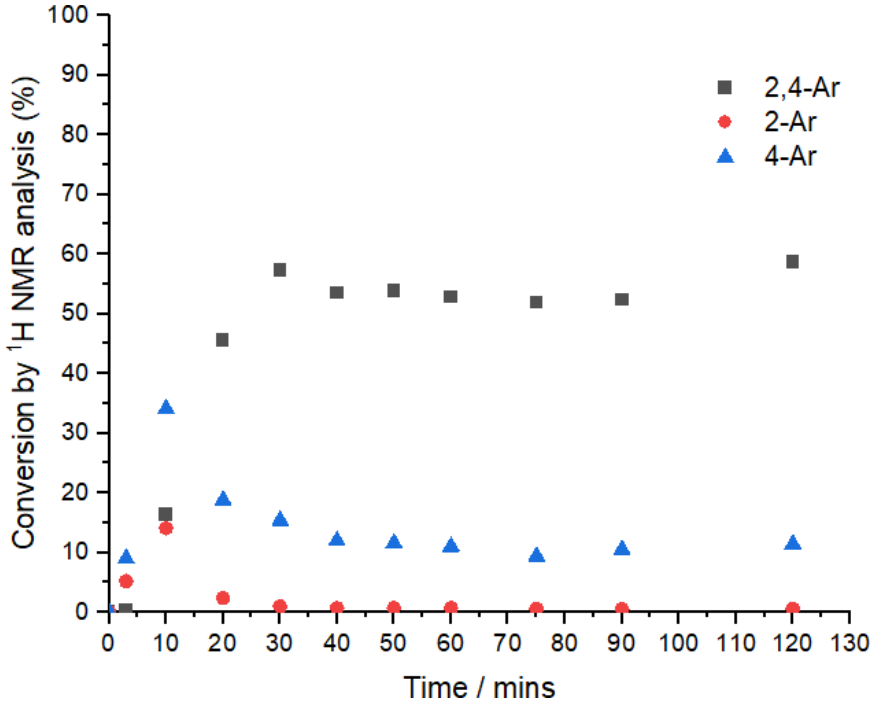


Graph 5. Time-course data showing product yields of 2,4-Ar, 2-Ar and 4-Ar using 2,4-dichloropyridine and *p*-fluorophenylboronic acid with ***P2*** in the SMCC reaction at 60℃.

To compare lower temperature in the reaction (Scheme 22), the reaction was run at 50 ℃, it took theform of a curve for the conversions that decreased slightly after 60 minutes and then gradually increased again (Graph 6). Single products were first generated rapidly and then decreased, with the 2,4-Ar product showing the highest reactivity afterwards. From this result, it can be inferred that the singlet products were first produced and then consumed for the 2,4-Ar product due to hyperarylation. In addition, when the temperature was lowered, the reaction rate was found to be slower than previous reactions. Therefore, it assumed that temperature effects onthe reaction, and reactivity and selectivity also can be changed.

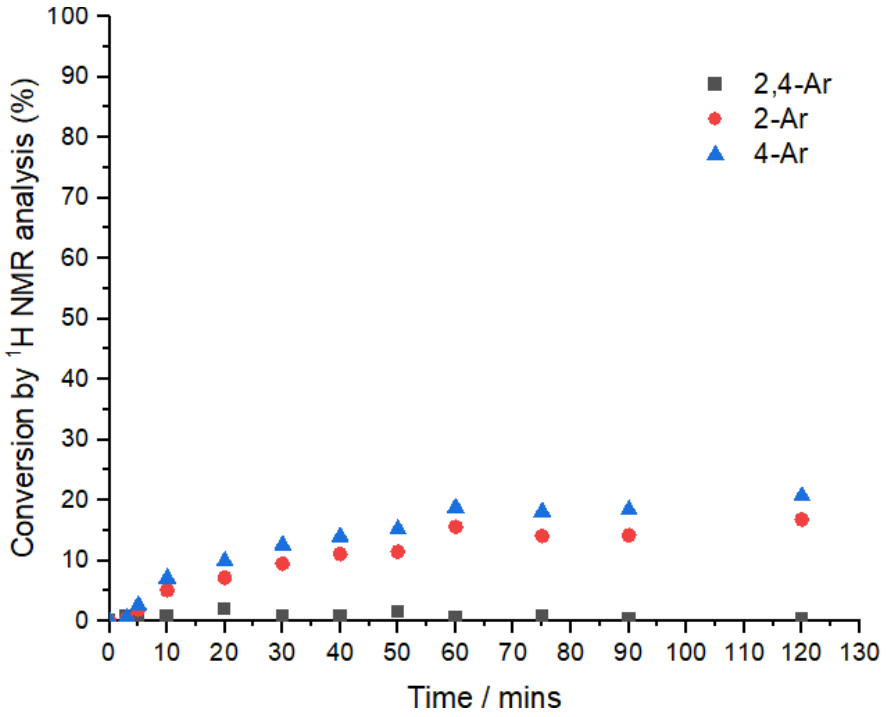


Graph 6.Time-course data showing product yields of 2,4-Ar, 2-Ar and 4-Ar using 2,4-dichloropyridine and *p*-fluorophenylboronic acid with ***P2*** in the SMCC reaction at 50℃.

As expected, lowering the temperature further to 40℃ resulted showed much lower yield (Graph 7). It can be assumed when using PEPPSI catalyst in the SMCC reactions, high temperature lead to better yields due to the best catalytic activation. In this case, C*4* selectivity was observed, but total conversion should be closed to 100 %. The results showed such a low yield that errors must be taken into consideration such as other activation species because in the NMR spectroscopy results confirmed that the starting materials not remained.

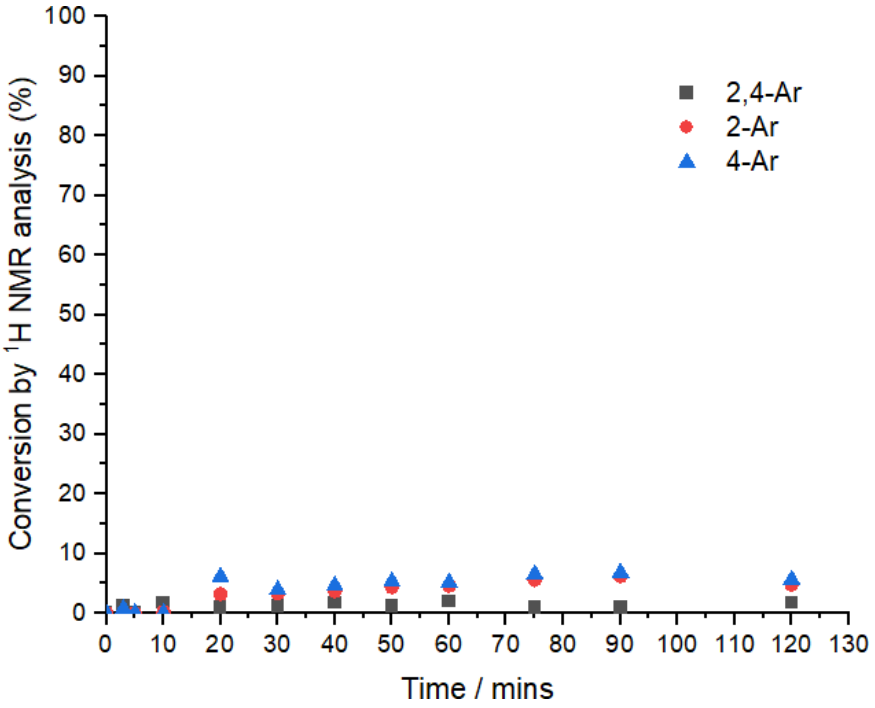


Graph 7. Time-course data showing product yields of 2,4-Ar, 2-Ar and 4-Ar using 2,4-dichloropyridine and *p*-fluorophenylboronic acid with ***P2*** in the SMCC reaction at 40℃.

## 2.8 Related Pd-catalyst systems in the SMCC reaction.

According to the literature, Fairlamb *et al.* found that when using a $Pd(OAc)_2/PPh_3$ (1:2) catalyst in the SMCC of 2,4-dibromopyridine and *p*-fluorophenylboronic acid showed great C*4* selectivity.[57] In addition, when increased the catalyst ratio they showed C*2* selectivity. Followed this, they rationalised as different site selectivity was observed depending upon the Pd and ligand ratio.

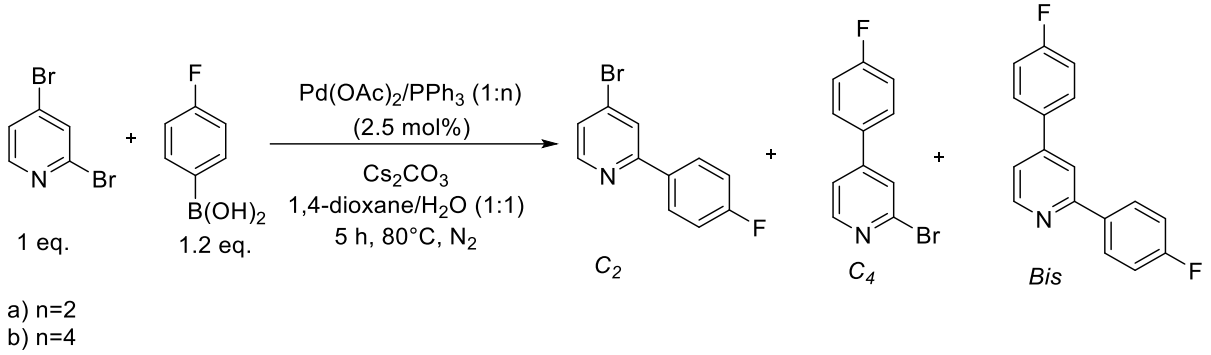


a) n=2
b) n=4

Scheme 23. Catalytic reaction of 2,4-dibromopyridine and *p*-fluorophenylboronic acid with $Pd(OAc)_2/PPh_3$ (1:2 or 1:4).

When using $Pd(OAc)_2/PPh_3$ (1:2) catalyst system in the SMCC, it showed good C*2* selectivity and other products were produced (Scheme 23). When increased the ligand ratio (1:4) in the same reaction, it showed greater C*2* selectivity and the other products yields were lower than 1:2 ratio (Graph 8). As a result, it assumed that when using $Pd(OAc)_2/PPh_3$ catalyst with Willans condition, it gives C*2* selectivity and when increased the ligand ratio it showed greater C*2* selectivity clearly in the SMCCs.

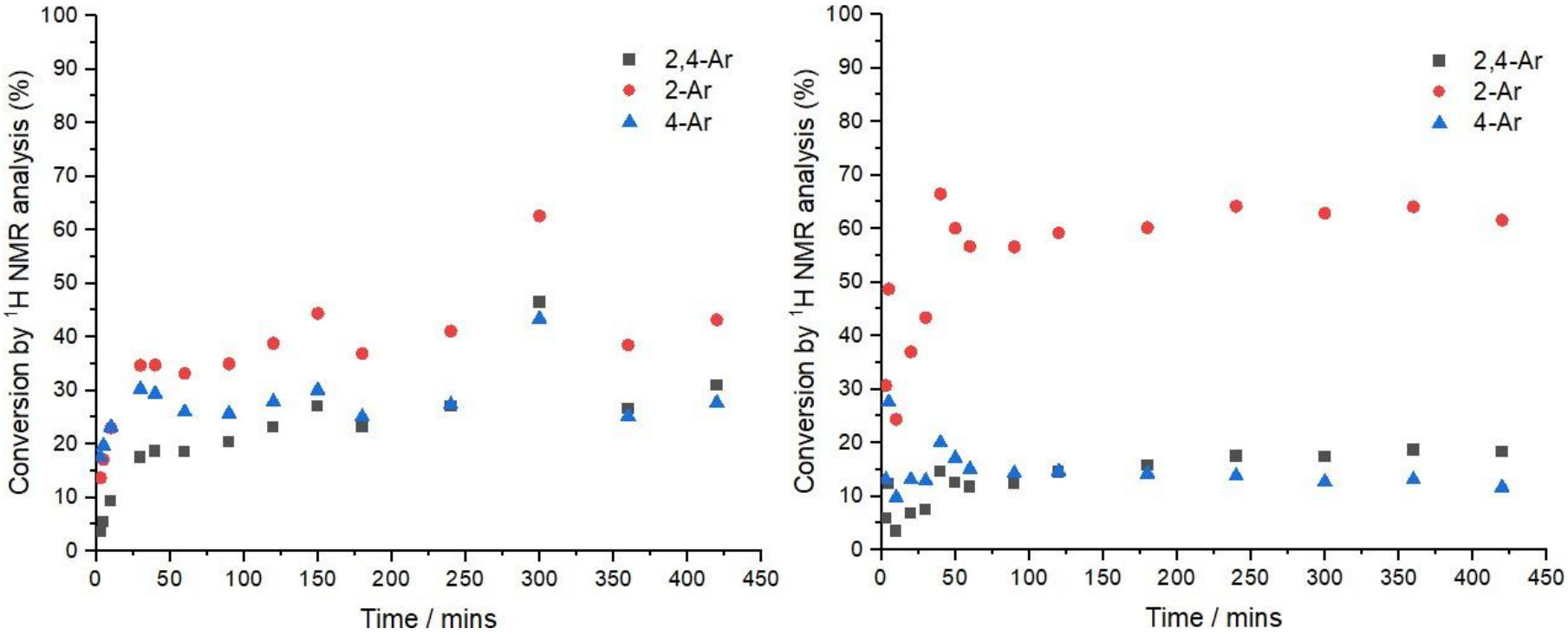


Graph 8. Left) Time-course data showing product yields of 2,4-Ar, 2-Ar and 4-Ar using 2,4-dibromopyridine and *p*-fluorophenylboronic acid with $Pd(OAc)_2/PPh_3$ (1:2) in the SMCC reaction. Right) Time-course data showing product yields of 2,4-Ar, 2-Ar and 4-Ar using 2,4-dibromopyridine and *p*-fluorophenylboronic acid with $Pd(OAc)_2/PPh_3$ (1:4) in the SMCC reaction.

To compare substrate, using 2,4-dichloropyridine to expect better reactivity in the SMCC. However, an important issue was that led to experimental error by adding different amount of 2,4-dichloropyridine: the substrate, 2,4-dichloropyridine was liquid and a disposable syringe was used to inject the reagent into the reaction vial. The disposable syringe was calibrated to 1.0 equivalent, the actual used substrate amount in the experiment was 1.55 equivalent (0.1ml→ 0.155 ml). Due to the wrong adding reagent amount, limiting reagent is changed to *p*-fluorophenylboronic acid and limiting yield was changed up to 120%. However, the main purpose of this section is to understand reactivity and selectivity by various Pd catalysts, this shouldn't cause problems for this experiment purpose and no issues for the reproducibility.

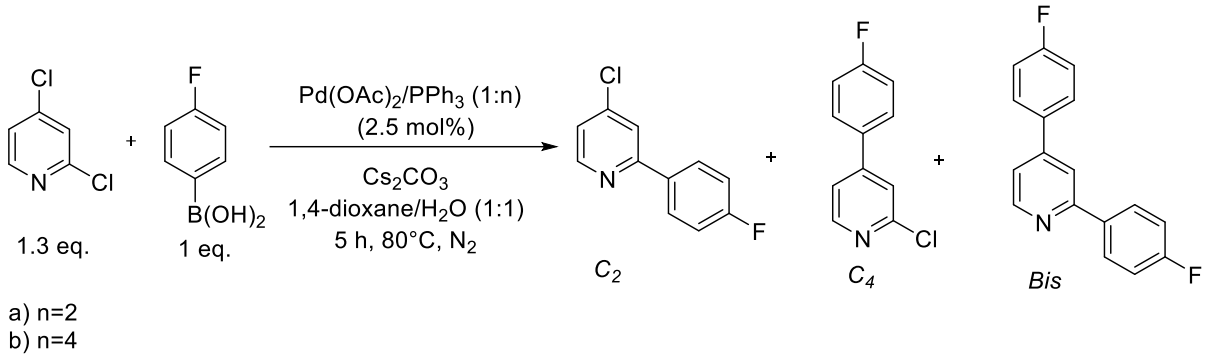


Scheme 24. Catalytic reaction of 2,4-dichloropyridine and *p*-fluorophenylboronic acid with $Pd(OAc)_2/PPh_3$ (1:2 or 1:4) in the SMCC.

The same reaction using $Pd(OAc)_2/PPh_3$ (1:2 or 1:4) were repeated using 2,4-dichloropyridine as the substrate (Scheme 24). When using $Pd(OAc)_2/PPh_3$ (1:2) ratio, it showed C*2* selectivity and 4-Ar and 2,4-Ar products were not produced (Graph 9). Reaction rate was faster than the same condition reaction with 2,4-dibromopyridine substrate by formation of those three products. Same as above reaction, when increased the ligand ratio, it showed greater C*2* selectivity and reaction rate was faster than lower ratio of catalyst. Followed this, when using $Pd(OAc)_2/PPh_3$ catalyst in the SMCC reaction, ligand ratio is important role for reactivity and when rising the ligand ratio it gives great reactivity of product.

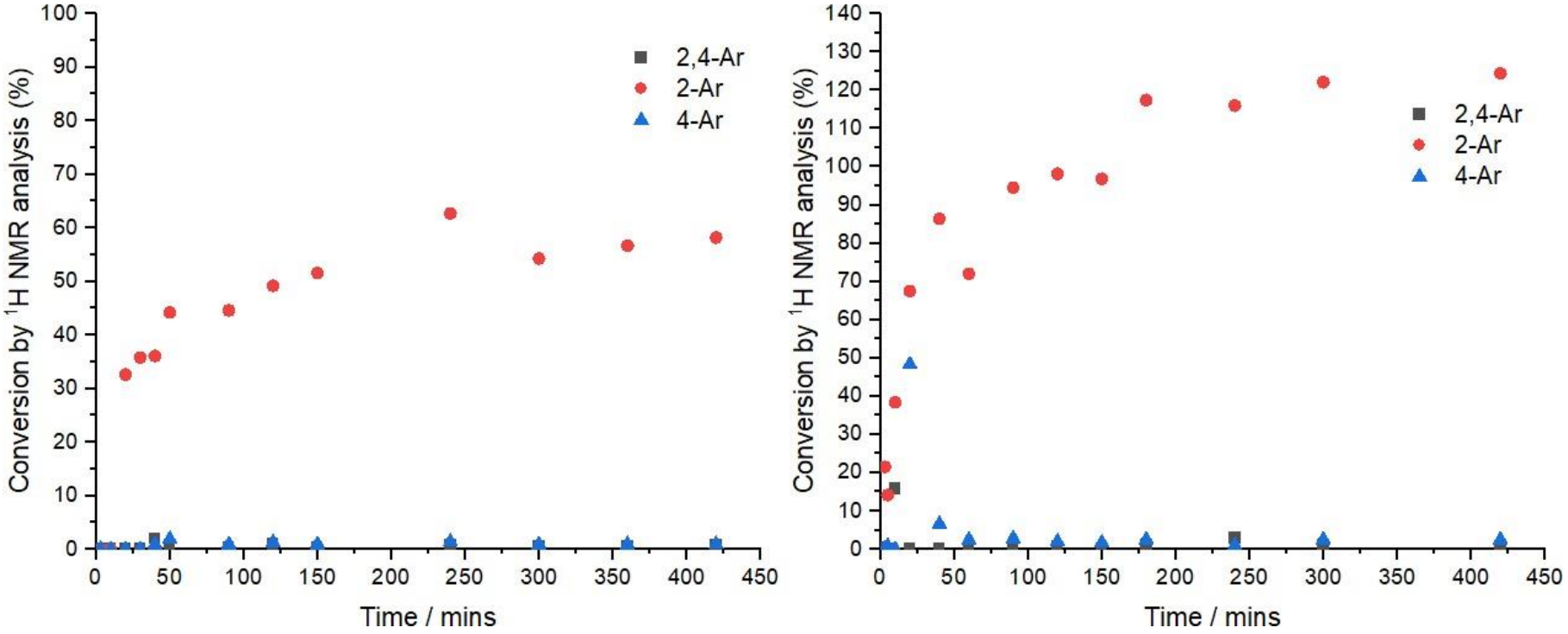


Graph 9. Left) Time-course data showing product yields of 2,4-Ar, 2-Ar and 4-Ar using 2,4-dichloropyridine and *p*-fluorophenylboronic acid with $Pd(OAc)_2/PPh_3$ (1:2) in the SMCC reaction. Right) Time-course data showing product yields of 2,4-Ar, 2-Ar and 4-Ar using 2,4-dichloropyridine and *p*-fluorophenylboronic acid with $Pd(OAc)_2/PPh_3$ (1:4) in the SMCC reaction.

To compare the selectivity and reactivity of the following Pd species, used $PdCl_2$ with $PPh_3$, which are commonly used Pd catalyst species in the experiments and the ratios of $PdCl_2$ and $PPh_3$ (1:2 or 1:4) were used in the experiments to investigate whether the reactivity depends on the ratio or the selectivity depends on the species differentiation (Scheme 25).

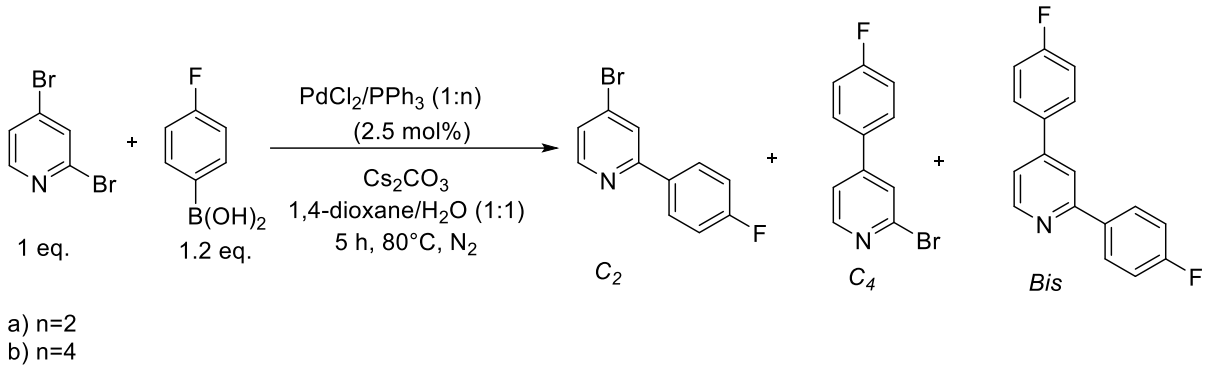


a) n=2
b) n=4

Scheme 25. Catalytic reaction of 2,4-dibromopyridine and *p*-fluorophenylboronic acid with $PdCl_2/PPh_3$ (1:2 or 1:4) in the SMCC. $PdCl_2/PPh_3$ was used as a pre-catalyst with a loading of 2.5 mol% in both reactions.

Same as previously, it showed C*2* selectivity when using $PdCl_2/PPh_3$ catalyst in the SMCC (Graph 10). Interestingly, the results showed that unlike other Pd catalyst systems, the reaction rate was observed to slow down as the proportion of $PPh_3$ ligand increased (Scheme 25) and yields ofall products were lower than 1:2 ratio. It showed slightly lower reactivity and lower yields assumed that the $PdCl_2$ and ligand pre-catalyst system was due to the effect of the ligand onthe reaction. However, when took $^1H$ NMR spectrometry it showed error at the first 60 minutes samples although multiple trial to get right NMR spectra.

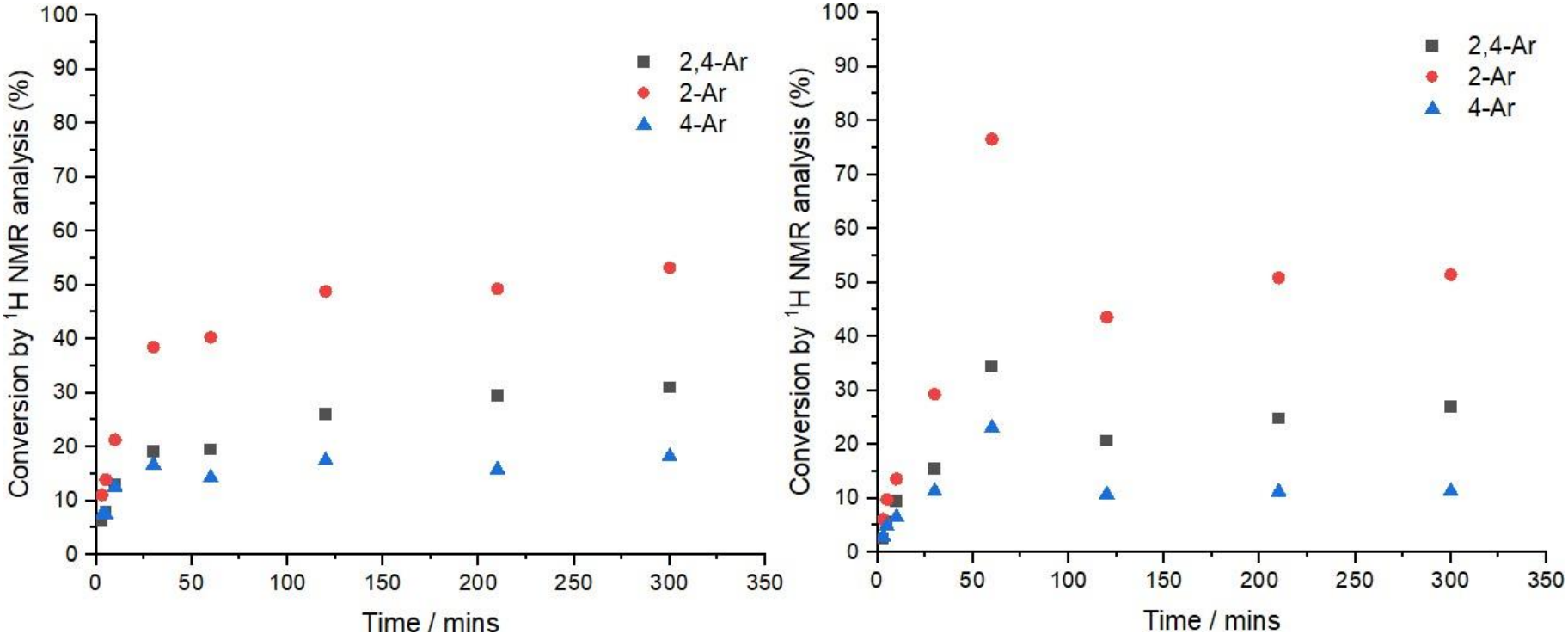


Graph 10. Left) Time-course data showing product yields of 2,4-Ar, 2-Ar and 4-Ar using 2,4-dibromopyridine and *p*-fluorophenylboronic acid with $PdCl_2/PPh_3$ (1:2) in the SMCC reaction. Right) Time-course data showing product yields of 2,4-Ar, 2-Ar and 4-Ar using 2,4-dibromopyridine and *p*-fluorophenylboronic acid with $PdCl_2/PPh_3$ (1:4) in the SMCC reaction.

The $PdCl_2/PPh_3$ reactions were carried out using 2,4-dichloropyridine as the substrate (Scheme 26).

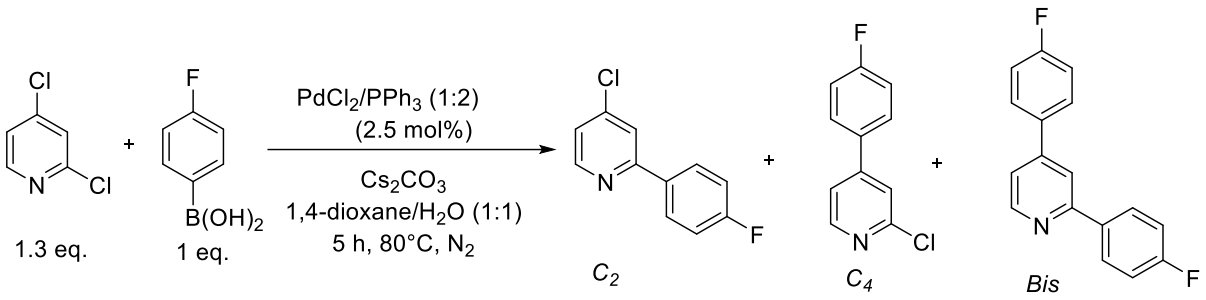


Scheme 26. Catalytic reaction of 2,4-dichloropyridine and *p*-fluorophenylboronic acid with $PdCl_2/PPh_3$ (1:2) in the SMCC.

Despite to use same benchmark reaction condition, when using $PdCl_2/PPh_3$ (1:2) as catalytic reagents showed clear C*2*-selectivity compare to other Pd catalytic reagents in this research. The reaction with 2,4-dichloropyridine was much more reactive with higher yields and greater C*2*-selectivity, despite the addition of more substrate (Graph 11). In this case, maximum conversion should be 120%, the error of adding excess substrate resulted in a peak of approximately 110% and no reproducibility issues in confirming experimental results. However, it showed clear C*2*-selectivity and it would be better to repeated for accuracy.

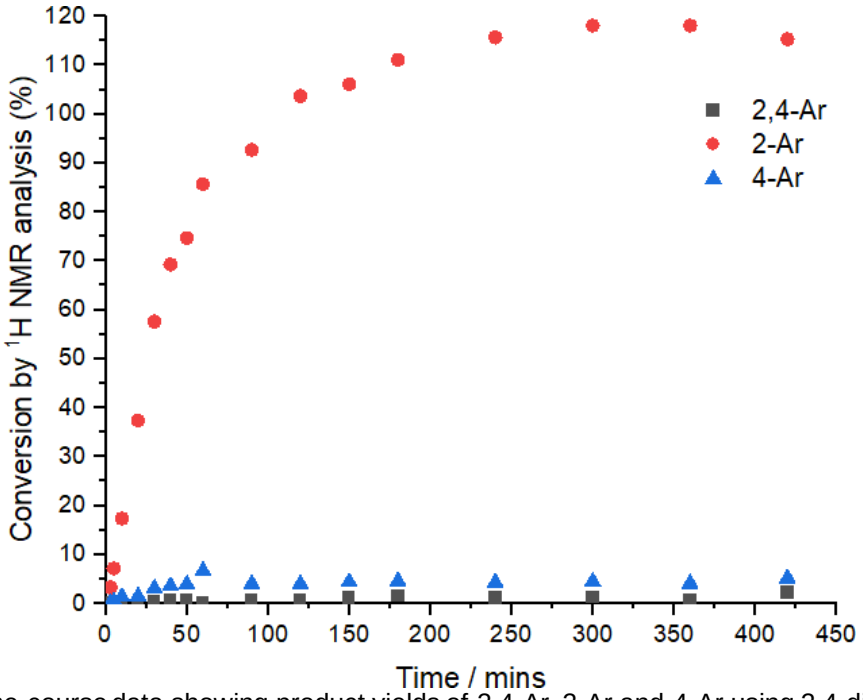


Graph 11. Time-course data showing product yields of 2,4-Ar, 2-Ar and 4-Ar using 2,4-dichloropyridine and *p*-fluorophenylboronic acid with $PdCl_2/PPh_3$ (1:2) on the SMCC reaction.

## 2.9 Site-selective SMCC reaction using BAC as the ligand.

In Section 2.9, to compare the reactivity and selectivity in the SMCC using new class of ligand BAC was used in the reaction. In addition, for comparison the selectivity using Fairlamb condition in the SMCC with 2,4-dibromopyridine, *p*-fluoroboronic acid, *n*-$Bu_4OH$ in THF. In order, $Pd(OAc)_2$/BAC (1:1), BAC, Coulson cluster/BAC (1:1), Coulson cluster, ***P2***, Coulson cluster/***I1*** (1:1) were used as catalysts for the SMCC reaction, respectively (Scheme 27).

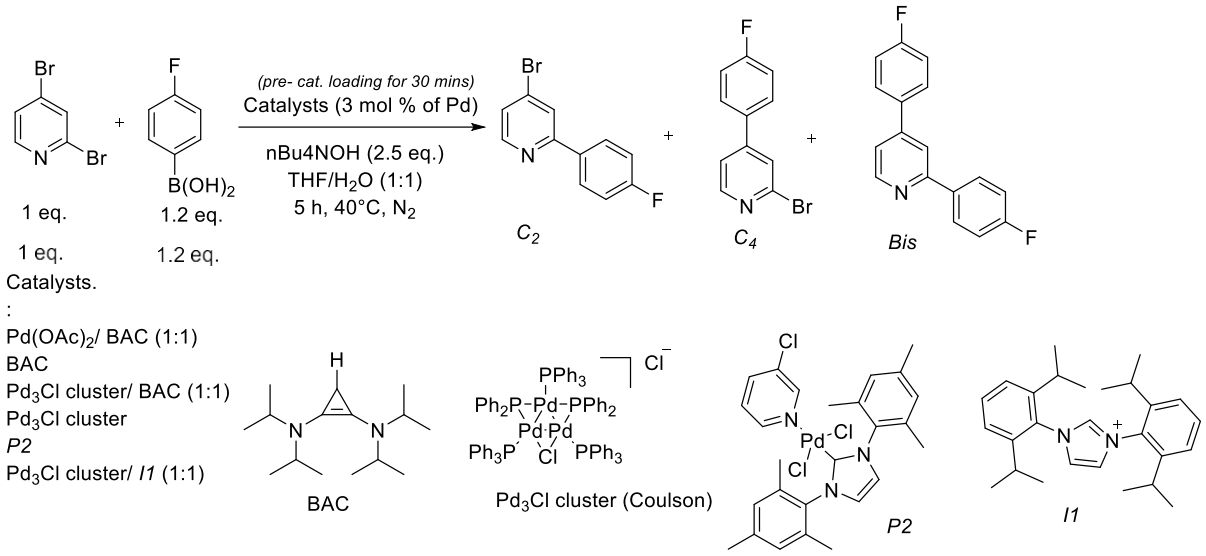


Scheme 27. Catalytic reaction of 2,4-dibromopyridine and *p*-fluorophenylboronic acid with various pre-catalysts using Fairlamb condition and pre-catalyst with a loading of 3 mol% in the reactions. In order, using $Pd(OAc)_2$/BAC, BAC, Coulson cluster/BAC, Coulson cluster, ***P2***, Coulson cluster/***I1*** used as catalysts in the SMCCs.

Using Fairlamb conditions, BAC was found to have little effect as a ligand with the Pd species. Therefore, BAC is not that effective in these SMCC reactions. Coulson clusters showed strong C*4* selectivity, and when used with ligands also showed C*4* selectivity. However, when usingCoulson cluster with ligand it showed that decreased reactivity. Using ***P2*** reaction showed themain product is that 2,4-arylated and the limiting reagent is boronic acid, is also highly reactive, but less so than the Coulson cluster (Graph 12). The results show that the NHC ligand effectis not significant, but it is clearly changing the activity of the Coulson cluster.

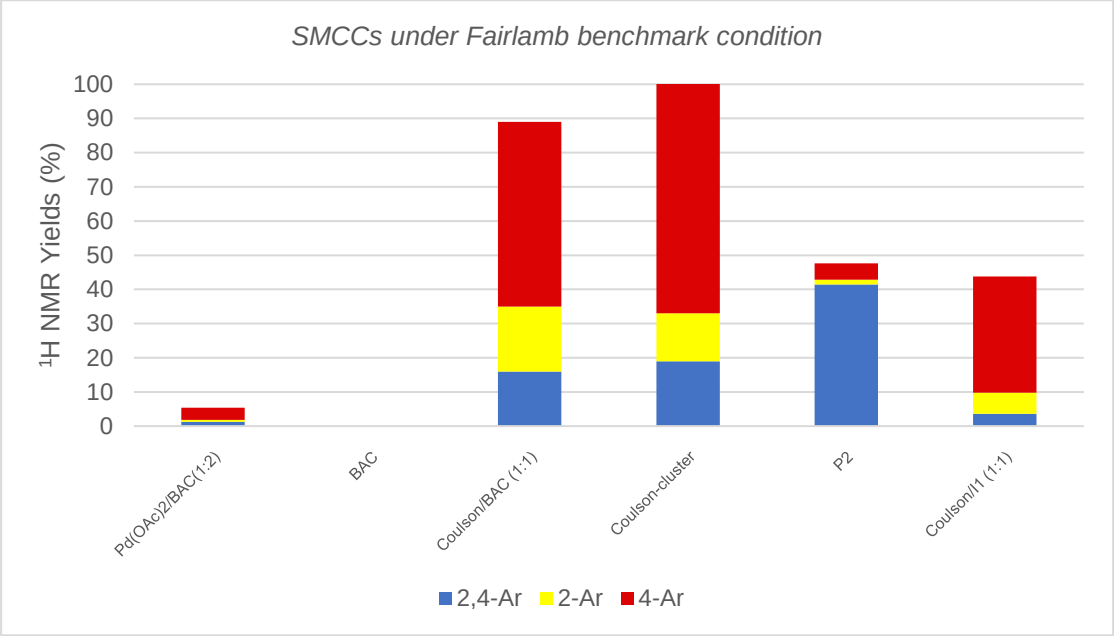


Graph 12. Pd-catalysed SMCCs reactions using 2,4-dibromopyridine, *p*-fluorophenylboronic acid and *n*-$Bu_4NOH$ in THF with various Pd-catalyst system and BAC. Graph showed catalyst effects on the SMCC reaction of selectivity and reactivity.

The reactivity and selectivity of the various Pd-catalysts in the SMCC reactions, under Willans' conditions were compared. As for the above reaction, $Pd(OAc)_2$/BAC (1:1), BAC, Coulson cluster/BAC (1:1), Coulson cluster, ***P2***, Coulson cluster/***I1*** (1:1) were used as catalysts for theSMCC reaction, respectively (Scheme 28). According to the literature, the reaction was carried out after 30 min of catalytic loading.

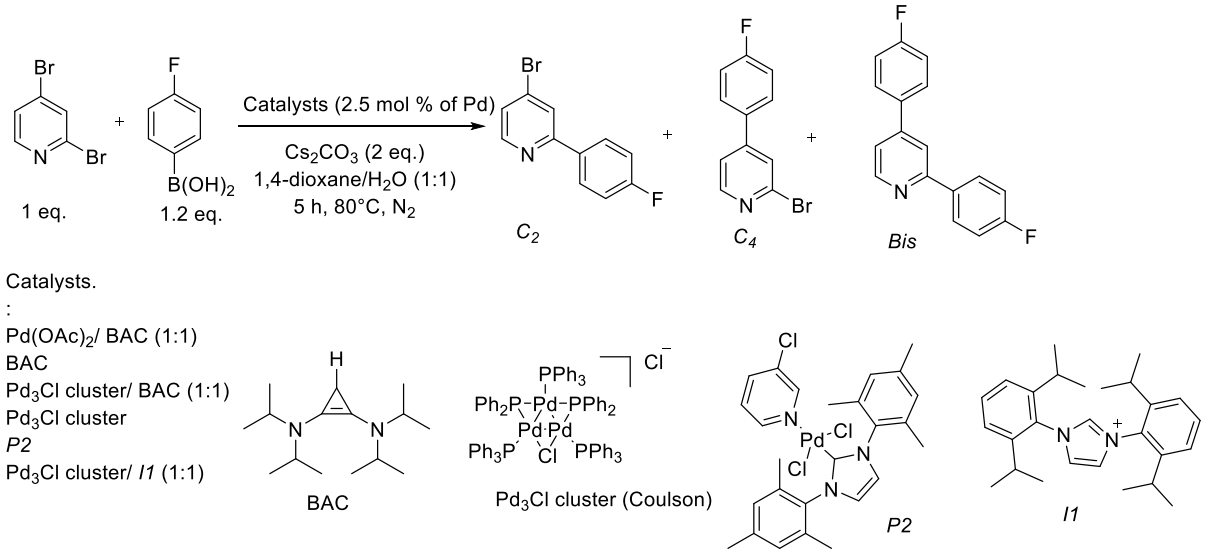


Scheme 28. Catalytic reaction of 2,4-dibromopyridine and *p*-fluorophenylboronic acid with various pre-catalysts using Willans conditions and pre-catalyst with a loading of 2.5 mol% in the reactions. Catalysts were used $Pd(OAc)_2$/BAC, BAC, Coulson/BAC, Coulson cluster, ***P2***, Coulson/***I1*** used for thecatalysts in the SMCCs.

BAC does not influence the catalysis to any great extent (Graph 13). In contrast, the Coulsoncluster was less strongly C*2*-selective, with all products showing weak selectivity of almost 1:1:1, and a 20% drop in conversion compared to Fairlamb's conditions. Furthermore, the useof the Coulson cluster with ligands resulted in lower yields than the Coulson cluster alone, *i.e.* displacement of the phosphine by the NHC ligands leads to a slight loss in site-selectivity. The results using the ***P2*** complex were the same as those above, with the highest conversion almost up to the maximum considering that the main product was the 2,4-arylated product and the limiting reagent was arylboronic acid.

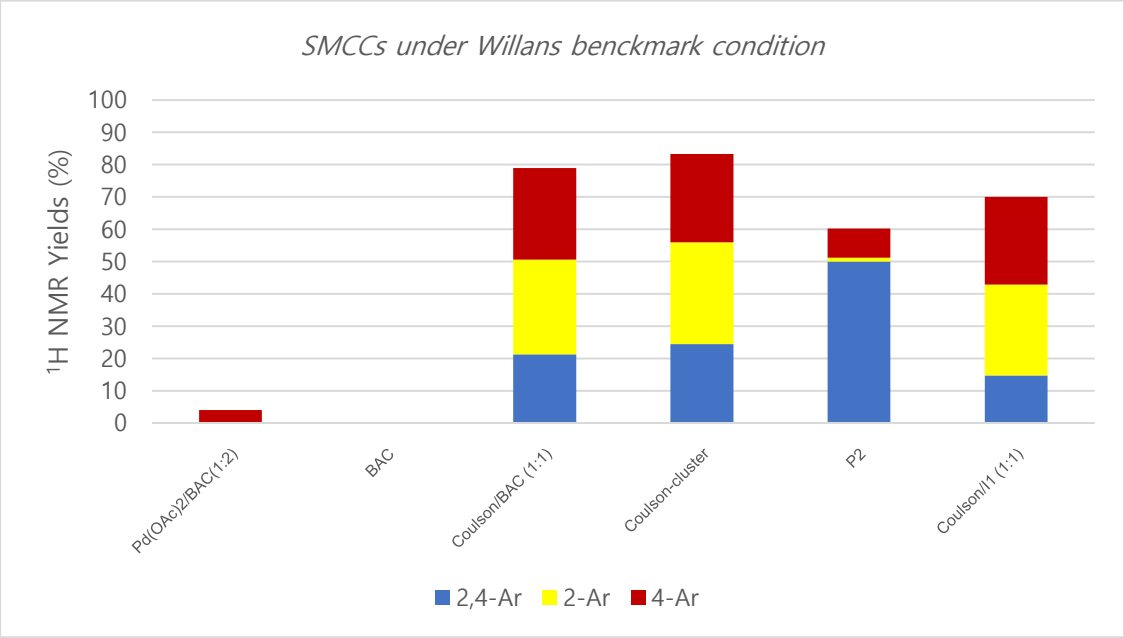


Graph 13. Pd-catalysed SMCCs reactions using 2,4-dibromopyridine, *p*-fluorophenylboronic acid and $Cs_2CO_3$ in 1,4-Dioxane with various Pd-catalyst system and BAC. Graph showed catalyst effects on the reaction of selectivity and reactivity.

Therefore, the results of SMCC reactions with two conditions (Fairlamb and Willans) demonstrate that base, solvent, and temperature in the reaction effects the reactivity and site-selectivity. While the catalyst structure clearly influences the efficacy of the SMCC reactions,these general reaction conditions play an important overall role.

## 2.10 Conclusions

The SMCC reactions of 2,4-dibromopyridine and 2,4-dichloropyridine with *p*-fluorophenylboronic acid was examined using the PEPPSI complexes as pre-catalysts. The PEPPSI complexes with bulky ligands exhibit high catalyst activity. For 2,4-dibromopyridine, the major product was formed by diarylation (2,4-Ar). The result suggests that the mono- arylated product does not dissociate form the Pd(0)L species quick enough prior to the second oxidative addition event. Indeed, the mono-arylated product might be more reactive than 2,4-dibromopyridine.

In order to compare the activation of the Pd catalysts depending on the temperature changing, the temperature was lowered from the benchmark condition of 80 degrees, and it was observed that lower the temperature lead to decrease the reactivity. However, selectivity towards the C*4*-Ar product did increase at lower temperatures.

To compare the substrates were used 2,4-dibromopyridine or 2,4-dichloropyridine in the same reaction, respectively. Under the same reaction conditions, 2,4-dichloropyridine surprisingly exhibited higher reactivity. Reaction rates were faster than when employing the 2,4-dibromopyridine substrate. In addition, other Pd pre-catalysts, $Pd(OAc)_2/PPh_3$ and $PdCl_2/PPh_3$ were tested. For the later, high C*2* site-selectivity was seen. Generally, 2,4-dichloropyridine ismore reactive than 2,4-dibromopyridine, despite the C-Br bonds being weaker than the C-Br bonds.

Furthermore, to examine the selectivity and reactivity, Fairlamb's conditions and Willans' conditions were compared. Interestingly, when changing the reaction condition with the samepre-catalyst it showed quite different results. When using Fairlamb's conditions, the Coulson cluster showed greater C*4* selectivity and high reactivity. In contrast, using Willans's conditions,the bulkier PEPPSI complex (***P1, P2***) showed greater formation of the 2,4-Ar product. Use of the Coulson cluster showed lower site-selectivity than for Fairlamb's conditions. Lastly, thenew class of ligand, BAC, showed some interesting effects in the SMCC reactions, under both Fairlamb's and Willans' conditions.

# Chapter 3- Understanding the reactivity of PEPPSI complexes through identification of intermediate species in the regioselective SMCC reaction

## 3.1 Introduction

Recent studies have developed on Pd-catalysed cross-coupling reactions with atypical site selectivity and various research groups have reported that site selectivity can be controlled by ligand choice.[44,49,58] In addition, different studies have shown that yield and regioselectivity can be modified depending on the substrate in addition to other factors such as base or reagent equivalents.[49]

Neufeldt *et al*. reported that the greatest selectivity towards the abnormal C*4* position with highest yields were obtained when bulky NHC ligands (***I1***, ***I2***) were used in the SMCC reaction with 2,4-dichloropyridine and *p*-fluorophenylboronic acid (Scheme 29).[28,49] Results showed that ***I1,*** a bulky ligand provides the best compromise between high C*4* over C*2* selectivity and low diarylation over monoarylation, maximising the yield of C*4*-monoarylation products. A proposed mechanism was supported by DFT calculations.[58]

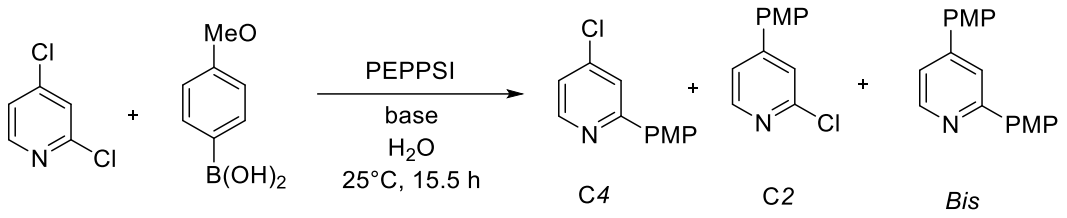


Scheme 29. Neufeldt *et al*. showed Pd-NHC catalysed SMCC reaction led to C*4*-selectivity.[58]

To help understand the catalytic data presented in Chapter 2, which shows over arylation to form the bis-arylated products or abnormal C*4* site-selectivity when using PEPPSI with bulky N-substituents of NHC ligand in the SMCCs. Mass spectrometry was used to examine in-situformed Pd species. The effect of the size of the NHC N-substituent on the in-situ formed Pd species has been explored, using bulky (***I1***) and non-bulky (***I3***) substituted NHC ligands. Additionally, the effect of substrate examined using 2,4-dibromopyridine and 2,4-dichloropyridine. This chapter is an extension of Chapter 2 and each SMCC reaction was re-run in an identical manner and analysed through mass spectrometry (MS) to prove the abovekinetic graph data.

## 3.2 Mass Spectrometry techniques

Mass spectrometry (MS) is used to analyse chemical compounds or complexes, by measuring the mass-to-charge ratio of ions. It is used to determine the mass of a molecule or reveal thechemical properties or structure of a compound. In mass spectrometry, the structure of a molecule (solid or liquid) can be determined through soft ionization. This process imparts little residual energy to the molecules of interest and thus causes little fragmentation. Two frequently used techniques are matrix-assisted laser desorption/ionization (MALDI)[59] and electrospray ionization (ESI)[60] and one of the examples of illustration showing how different between MALDI and ESI to analyse peptide (Figure 14).

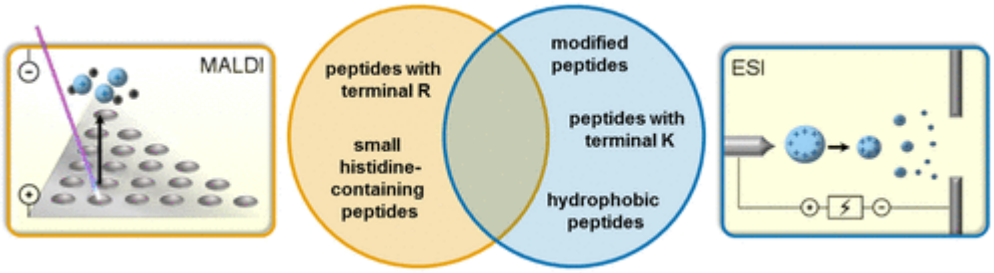


Figure 14. Optimal one of example showed differences between two mass spectrometry methods(ESI, MALDI) presented in peptide identification by Rösli *et al.*[61]

One of the key differences between the two methods is the way in which the sample is introduced to the ion source: ESI uses a solvated sample injected into the instrument, while MALDI uses a solid-state sample.[62] Both measurement methods have their advantages and disadvantages. ESI-MS can observe molecules (M) in their protonated form $[M + H]^+$, but in some cases it is not possible to detect intact molecular ions.[62] This drawback can be overcome through softer MALDI, which allows the detection of intact molecular ions, hence MALDI-MS was selected in this study with the aim of observing intact metal species.

## 3.3 Sample collection and analysis methods

Samples were collected at different time points during the experiment with 0.1 µL of samplebeing quenched in 10 ml of DCM, which prevents the reaction from proceeding further and obtains a suitable concentration for the mass spectrometer. Filtration was performed through celite plug to ensure only solution state species for analysis. A drop of a matrix solution suitable for MALDI-MS was dropped onto the solid phase and dried. Then, the prepared sample was dropped onto the matrix and dried before being placed in the MALDI-MS spectrometer.

## 3.4 Potential mechanism for C*4*-selectivity

A recent publication by Neufeldt *et al.* reported unusual C*4*-selectivity in the SMCC reaction of 2,4-dichloropyridine and arylboronic acid when using Pd complexes bearing ***I1*** and ***I2*** which are considered bulky NHC ligands. (Scheme 30)[28,49,58] The oxidative addition step of the reaction determines product selectivity, and the Neufeldt group used DFT calculations to determine potential intermediates of the reaction help explain the mechanistic aspects of C*4*-selectivity.[28,49,58] Through substrate comparison, they found that the highest yield and greatest C*4*-selectivity were achieved when 2,4-dichloropyridine was used as the substrate over 2,4- dibromopyridine. They have also shown that mono-ligated Pd(0) ('*PdL*') and bis-ligated Pd(0)('$PdL_2$') allow oxidative addition at different sites of the substrate due to their respective HOMO symmetries.

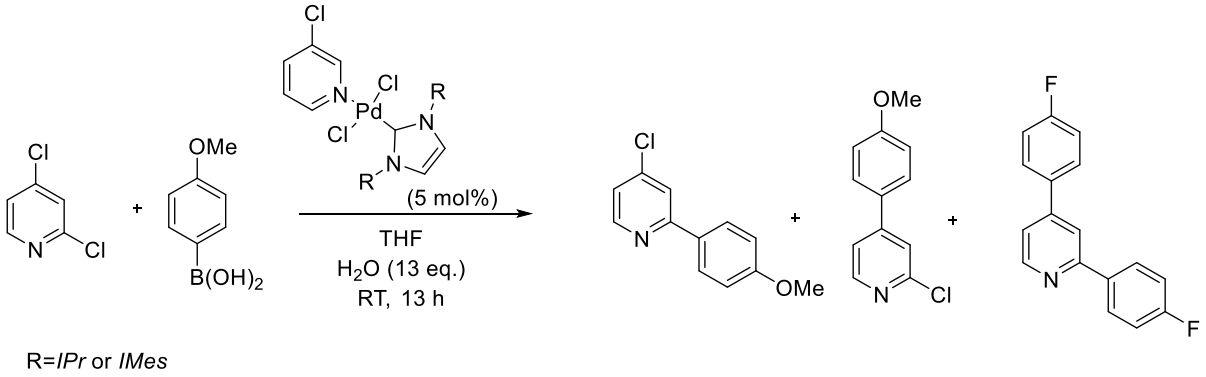


R=*IPr* or *IMes*

Scheme 30. Catalytic reaction between 2,4-dichloropyridine and *p*-methoxyphenylboronic acid with Pd-$Cl_2$(3-Cl-pyridine)(NHC) pre-catalyst, bulky NHC ligand used ***I1*** and ***I2*** as a non-bulky NHC ligand used by Neufeldt *et al*.[28,49,58]

When the NHC ligand with diisopropylphenyl N-substituents (***I1***) was used, the oxidative addition of the C*4*-position was energetically favourable compared to the C*2*-position. Thoseconditions favour a three-centred mechanism with the *PdL* active species. On the other hand,the *PdL*$_2$ system preferred the oxidative addition of the C*2*-position, but still this pathway was higher in energy than the *PdL* co-oxidative addition pathway, corroborating the experimentally observed C*4*-selectivity.[28] According to the Neufeldt's group DFT calculations using Pd/***I1*** showed that in the reaction is favoured at a C*4*-position by 1.7 kcal/mol (C*4*:C*2* = 18:1) over C*2*, which leads to the strong C*4*-selectivity.[28,49,58]

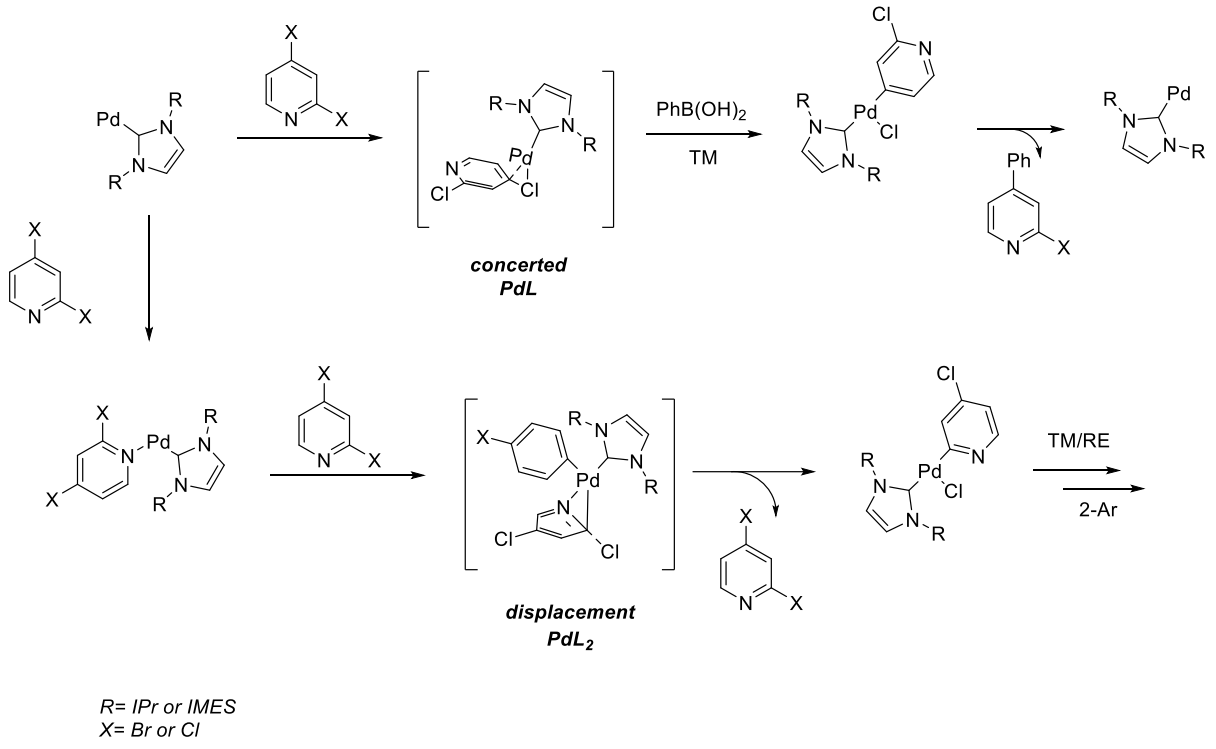


Scheme 31. Proposed mechanism for C*2*-arylated and C*4*-arylated selectivity with PEPPSIs in the SMCCs by Neufeldt *et al.*[28]

According to Willans and co-workers, when bulky NHC ligand are used with 2,4-dibromopyrdine as the substrate, it lead to C*4*-selectivity and significant amounts of bis-arylated product.[44] Willans group applied Neufeldt's SMCC conditions using 2,4-dibromopyridine with arylboronic acids and demonstrated a similar abnormal highest C*4* yields using a bulky PEPPSI catalyst (Scheme 31). However, it could not determine clear mono-arylated selectivity. According to the James research, he showed highest yields of bis arylated products in the catalytic reactions with bulky NHC ligands with same condition by over arylation.[63]

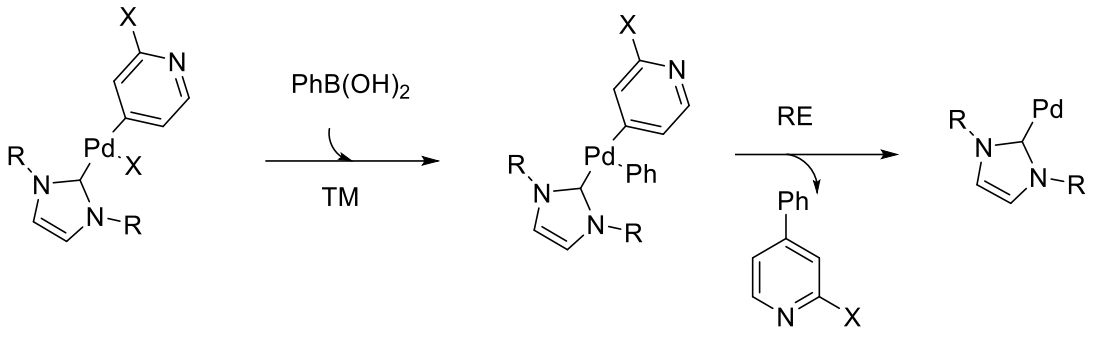


X= Cl or Br
R= *IPr*, *IMES*

Scheme 32. Proposed steps for mono-arylated products (C*4*-arylated and C*2*-arylated) with bulky PEPPSIs in the SMCCs by James Williams.[44]

However, James studies showed a double oxidative addition reaction can proceed from the mono-arylated oxidation addition, which leads to hyper-diarylation and forms almost exclusively 2,4-Ar products (Scheme 32). In metal catalysed cross-coupling reactions, steric clashes can occur between the bulky and ligand and the coordinated phenyl group, which reduces the rate of metal exchange. It is assumed that monoaryl products remain on the L- PEPPSI complexes after the formation of monoaryl products and it tends to form diarylation products (Scheme 33). By MS data and catalytic time course kinetic graphs in Chapter 2 helped to understand this phenomenon. This phenomenon increases the tendency for a second oxidative addition step, as observed experimentally in complexes 2,4-Ar is formed more easily.[64]

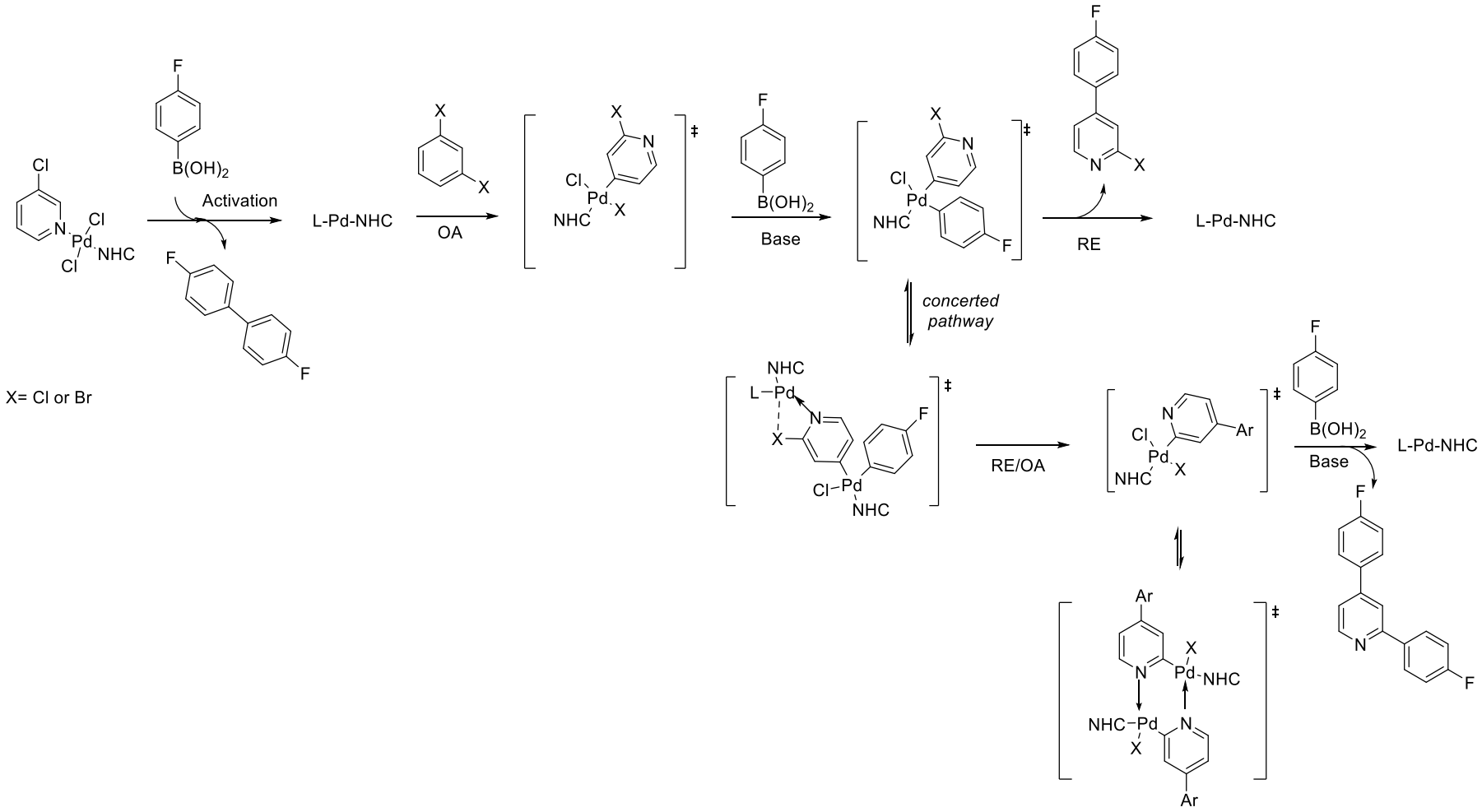


Scheme 33. Proposed mechanism of Pd-catalysed reaction for mono-arylated and bis-arylated products on the SMCC reaction by Wiliams.

## 3.5 Mechanistic understanding of the reactivity with *P1* pre-catalyst (which is a [$PdCl_2$($NHC_{IPr}$)(3-Cl-Py)] complex) on SMCC reactions.

To understand how the selectivity of the SMCC reaction is affected by substrate and by NHCsteric bulk, reactions need to be performed under identical conditions so that data is directly comparable. This chapter uses MALDI-MS to capture Pd species formed under catalytic conditions, with the aim of further understanding the mechanism that leads to different products. However, when analysing complex samples with a mass spectrometer, there are limitations to ionising all compounds. In addition, reaction intermediates that are not known products have been identified by matching isotope patterns rather than something as specific as a structural x-ray, so their exact structures are somewhat difficult to determine. Therefore, the reaction intermediates identified in this chapter are a reference for mechanistic studies to understand the selectivity of SMCC reactions.

### 3.5.1. MALDI-MS analysis of a SMCC reaction of 2,4-dibromopyridine with *p*-fluorophenylboronic acid and *P1* complex in the SMCC

The reaction showed in Scheme 34 was carried out with samples being collected over time (10 minutes, 30 minutes, 1 hour, 5 hour and 24 hours point) and analysed by MALDI-MS.

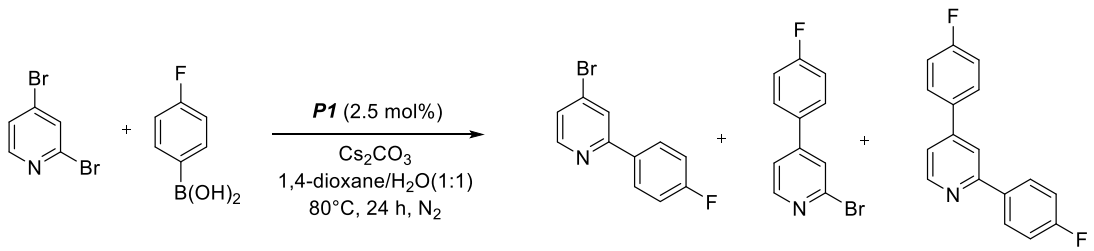


Scheme 34. Catalytic reaction of 2,4-dibromopyridine with *p*-fluorophenylboronic acid using benchmark conditions. ***P1*** was used as a bulky pre-catalyst with a loading of 2.5 mol%.

The data collected by mass spectrometry were complex and various peaks of Pd complex species were present. Unfortunately, only few species have been successfully identified (Figure 15).

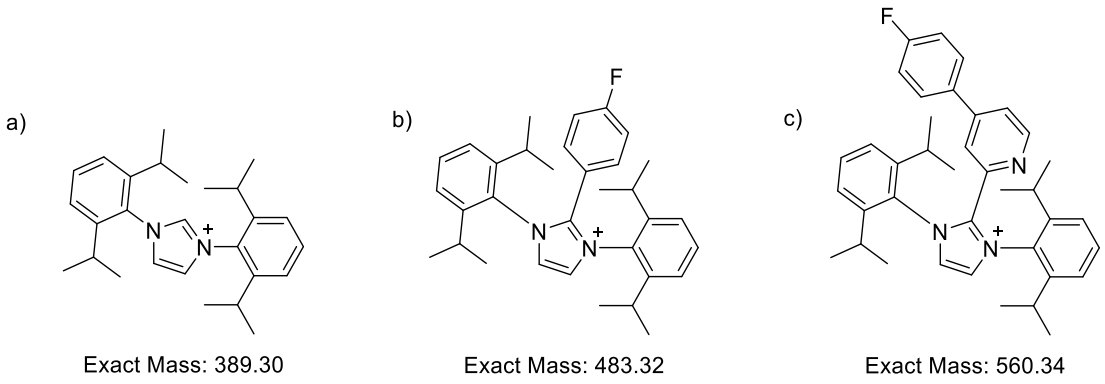


Figure 15. Imidazolium species identified by MALDI-MS during the reaction of 2,4-dibromopyridine with *p*-fluorophenylboronic acid catalysed by ***P1*** complex.

After the reaction was started, the signal for imidazolium salts signal a) (Figure 15) was present in all of the multiple samples from the time course reaction in Scheme 34. The *p*-fluorophenyl-imidazolium b) is formed from thereductive elimination of the NHC and an aryl group following transmetalation of *p*-fluorophenylon the Pd. The signal for b) appeared during the first 5 hours and had disappeared after 24 hours. Imidazolium c) is formed from the reductive elimination of the NHC and arylated pyridinyl, with arylation being in either the C*4*-position or the C*2*-position. The signals were revealed during the first 5 hours of the reaction had disappeared after 24 hours.

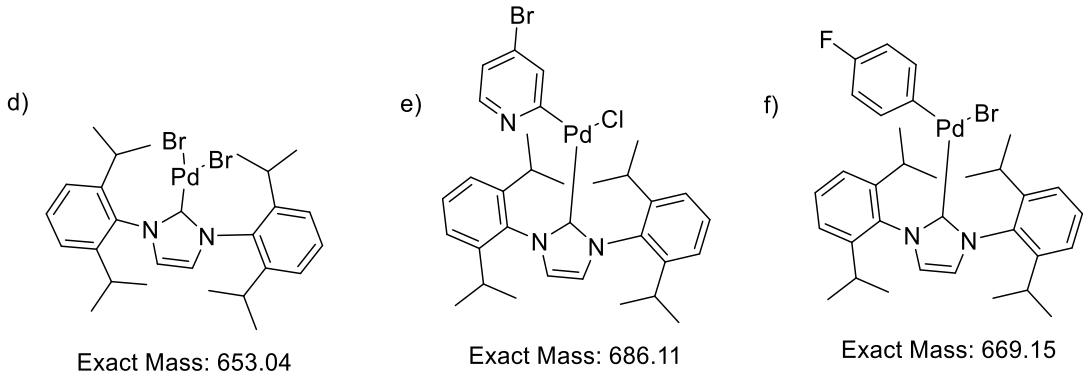


Figure 16. Pd species identified by MALDI-MS during the reaction of 2,4-dibromopyridine with *p*-fluorophenylboronic acid catalysed *P1* pre-catalyst.

In Figure 16 signals for Pd species were also observed in the MS data (Figure 17). All three complexes shown in Figure 16 were seen in samples collected first 5 hours and had disappeared after 24 hours. Complex d possibly forms from a double oxidative addition of 2,4-

dibromopyridine, with subsequent reductive elimination of a bipyridine. Complex e forms from oxidative addition at one of the C-Br bonds in 2,4-dibromopyridine, with halide scrambling possibly being responsible for the presence of Cl from the starting Pd complex. Complex f may be a product of transmetalation of the arylboronic acid reagent with complex d.

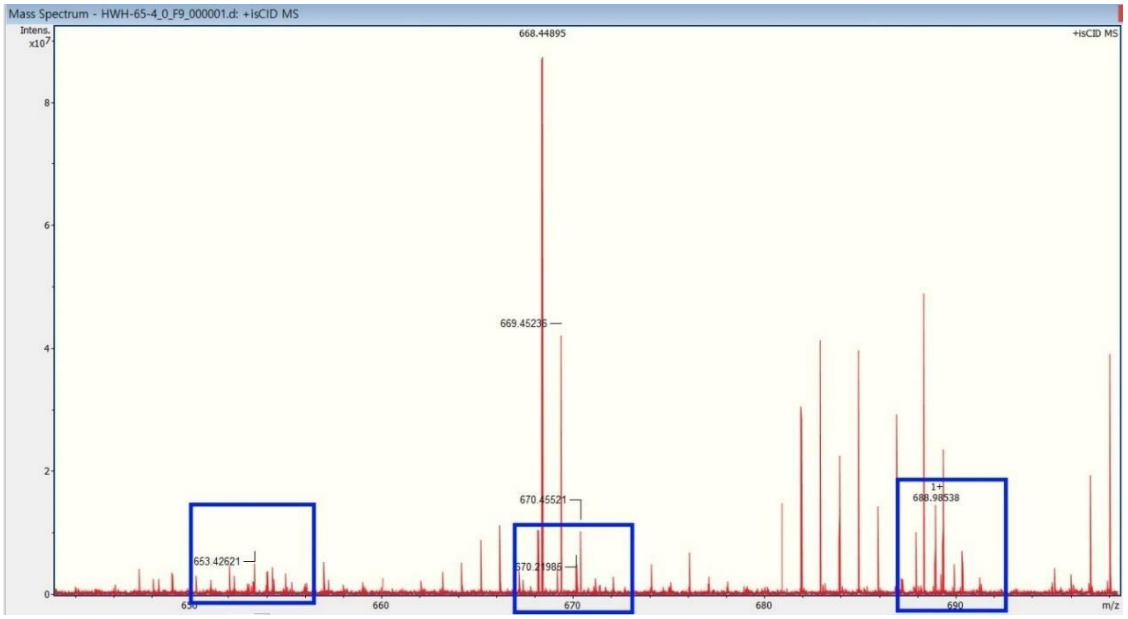


Figure 17. Pd species observed in the MALDI-MS following the reaction of 2,4-dibromopyridine with *p*-fluorophenylboronic acid catalysed by ***P1*** at the first 5 hours match the species in figure 16.

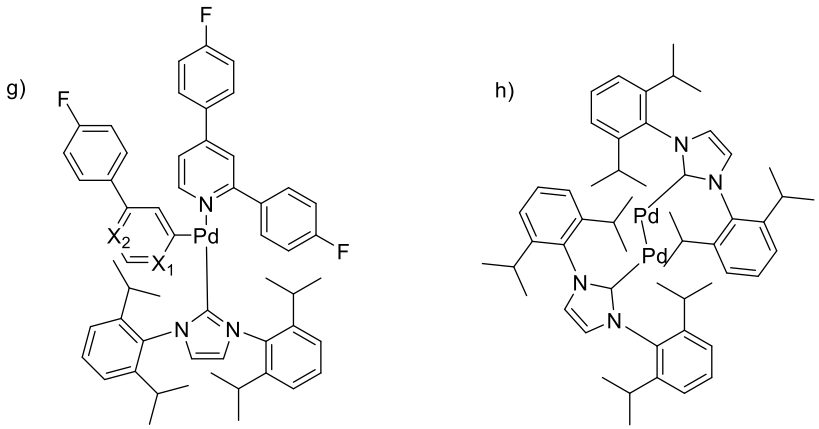


Figure 18. Pd species identified by MALDI-MS during the reaction of 2,4-dibromopyridine with *p*-fluorophenylboronic acid catalysed by ***P1*** pre-catalyst.

Complex g shows coordination of bis-arylated pyridine, in addition to a mono-arylated pyridine (Figure 18). In Figure 19, the signal appears 10 minutes after the start of the reaction, which explains the rapid formation of 2,4-Ar product observed in the kinetic data. It also indicates that arylated pyridine does not readily leave the Pd centre, and mono-arylated product may remain bound to Pd for a second arylation, rather than leaving and coming back on. The signal for h) indicates aggregation of Pd(0) species, which is formed after 1 hour and is still presentat 5 hours, hence may be a resting state prior to oxidative addition.

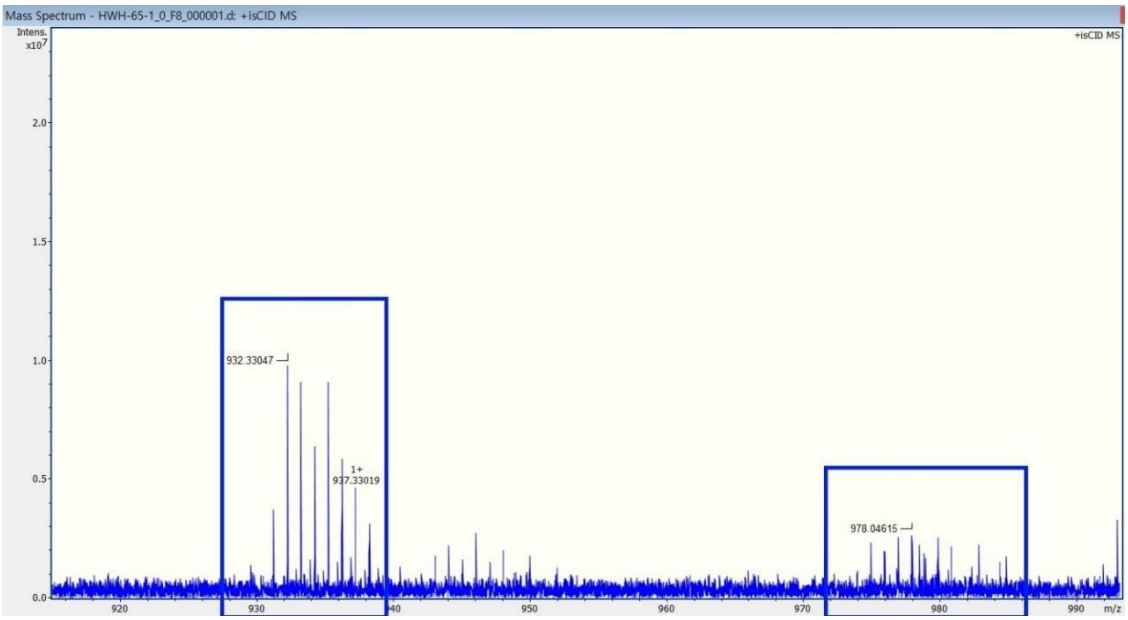


Figure 19. g) a nitrogen bound 2,4-Ar and either 2-arylpyridine-4-yl or 4-arylpyridine-2-yl complex; h) a combination complex of two activated Pd(0)-NHC species

### 3.5.2 MALDI-MS analysis of a SMCC reaction of 2,4-dichloropyridine with *p*-fluorophenylboronic acid and *P1* complex in the SMCC.

The same reaction was performed using 2,4-dichloropyridine in place of 2,4-dibromopyridinewith samples being collected after 10 minutes, 30 minutes, 1 hour, 5 hours, and 24 hours for MALDI-MS analysis (Scheme 35).

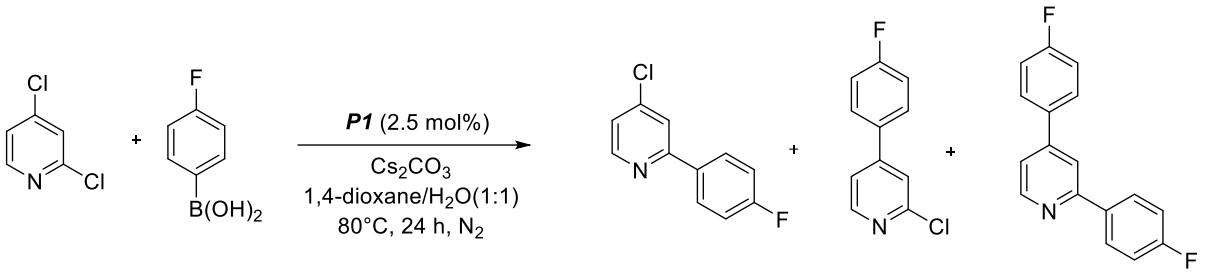


Scheme 35. Catalytic reaction of 2,4-dichloropyridine with *p*-fluorophenylboronic acid usingbenchmark conditions. ***P1*** was used as a bulky pre-catalyst with a loading of 2.5 mol%.

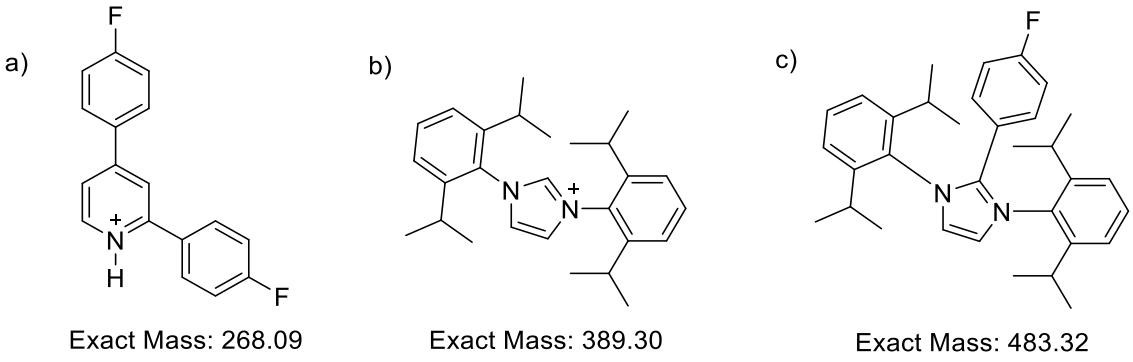


Figure 20. Imidazolium species and bis-arylated species identified by MALDI-MS during the reaction of 2,4-dichloropyridine with *p*-fluorophenylboronic acid catalysed by ***P1*** pre-catalyst.

As previously, signals for imidazolium were observed, in addition to the di-arylated product as a pyridinium (Figure 20). The bis-arylated product shows a peak from 10 minutes after the reaction until the end of the reaction, showing that the bis-arylated product is produced quickly in the reaction. This was proven to be the same phenomenon as the Neufeldt group's study, which showed that C-Cl is more active than C-Br. Both the protonated imidazolium b) and the arylated imidazolium c) are observed in all samples throughout the reaction.

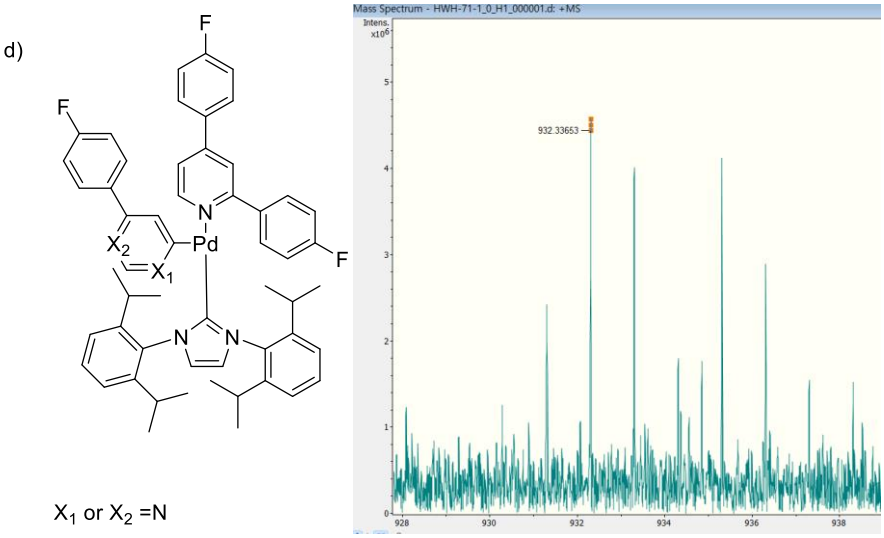


Figure 21. Pd species identified by MALDI-MS during the reaction of 2,4-dichloropyridine with *p*-fluorophenylboronic acid catalysed by ***P1*** pre-catalyst.

The same Pd complex bearing two arylated pyridines seen in the previous reaction was alsoobserved in this reaction (Figure 21). This complex was observed 10 minutes after the start ofthe reaction and had disappeared after 24 hours which is in line with the fast reaction kinetics. The position of *p*-fluorophenyl in the mono-arylated pyridine can be in either the C*2* or C*4* position, given the selectivity of the reaction discussed in Chapter 2, it is estimated that it is more likely bound to the C*4* position.

## 3.6 Mechanistic understanding of the reactivity with *P3* pre-catalyst (which is a [$PdCl_2$($NHC_{n\text{-}propyl}$)(3-Cl-Py)] complex) on SMCC reactions.

In this study, selectivity and reactivity were compared using N-substituents ***I3*** on the PEPPSIcomplex that were clearly smaller than bulky NHC ligands (***I1***). In this section, using ***P3*** as a non-bulky ligand complex was used to invested in identifying intermediates that may exist in the oxidative addition step complex to understand the mechanism.

### 3.6.1 MALDI-MS analysis of a SMCC reaction of 2,4-dibromopyridine with *p*-fluorophenylboronic acid and *P3* complex in the SMCC.

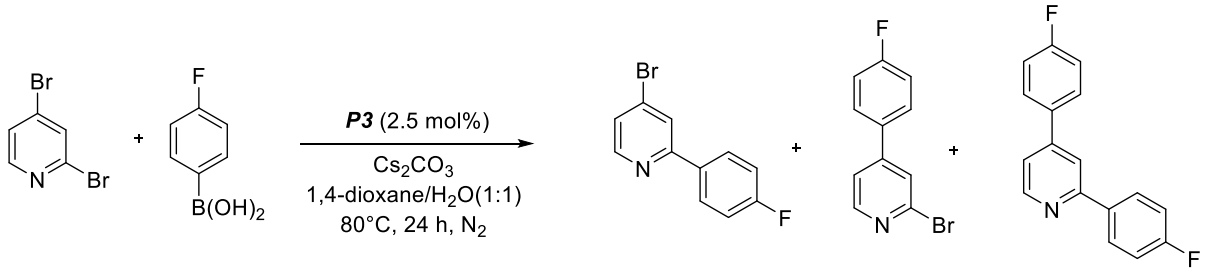


Scheme 36. Catalytic reaction of 2,4-dibromopyridine with *p*-fluorophenylboronic acid using benchmark conditions. ***P3*** [$PdCl_2$($NHC_{n\text{-}propyl}$)(3-Cl-Pyr)] was used as a non-bulky pre-catalyst with a loading of 2.5 mol%.

As previously, reactions were run and samples were collected after 10 minutes, 30 minutes, 1hour, 5 hours, and 24 hours (Scheme 36).

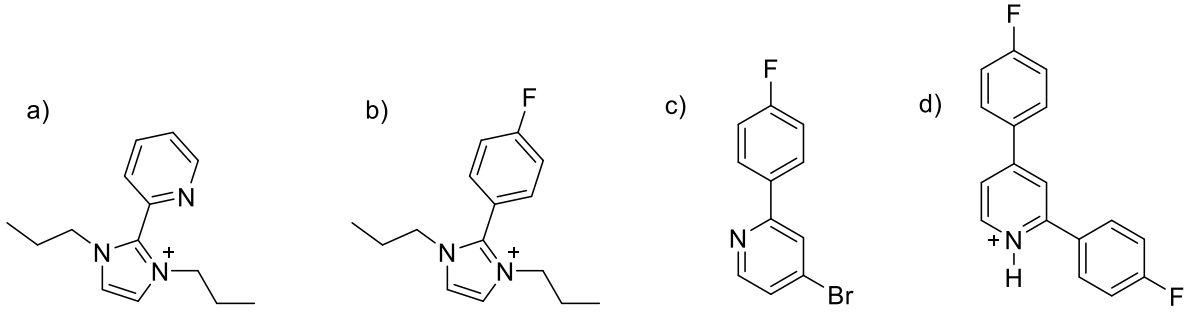


Exact Mass: 230.17 Exact Mass: 247.16 Exact Mass: 250.97 Exact Mass: 268.09

Figure 22. Imidazolium complex and arylated product species identified by MALDI-MS during the reaction of 2,4-dibromopyridine with *p*-fluorophenylboronic acid catalysed by ***P3*** pre-catalyst.

After the reaction was started, the signal for complex a) (Figure 22) is formed from the reductive elimination of the NHC ligand with the pyridine which was originally isolated from the Pd centre after the oxidative addition of 3-chloropyridine on the PEPPSI complex. Complex c is assumed 2-arylated products and 4-arylated product both, but it could not determine by MALDI-MS. The complex c was observed at the first 5 hours and had disappeared.

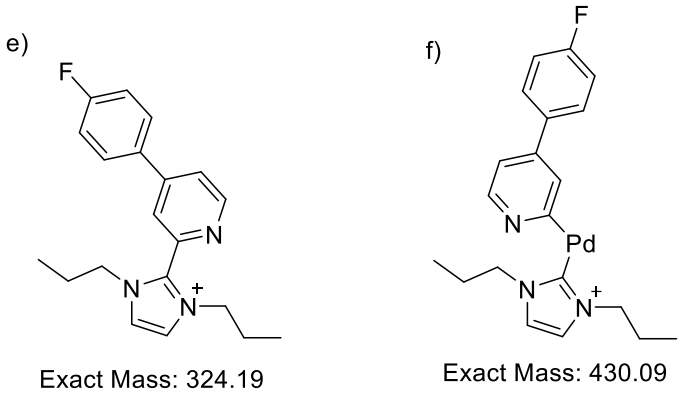


Figure 23. Imidazolium species and Pd species identified by MALDI-MS during the reaction of 2,4-dichloropyridine with *p*-fluorophenylboronic acid catalysed by ***P3*** pre-catalyst.

Complex f (Figure 23) is formed from the second oxidative addition of the 2 or 4 arylated complex on the Pd centre with isolated NHC ligand. This complex is not clear which position of arylated but following the kinetics it assumed for C*4* position and signal showed in Figure 24.

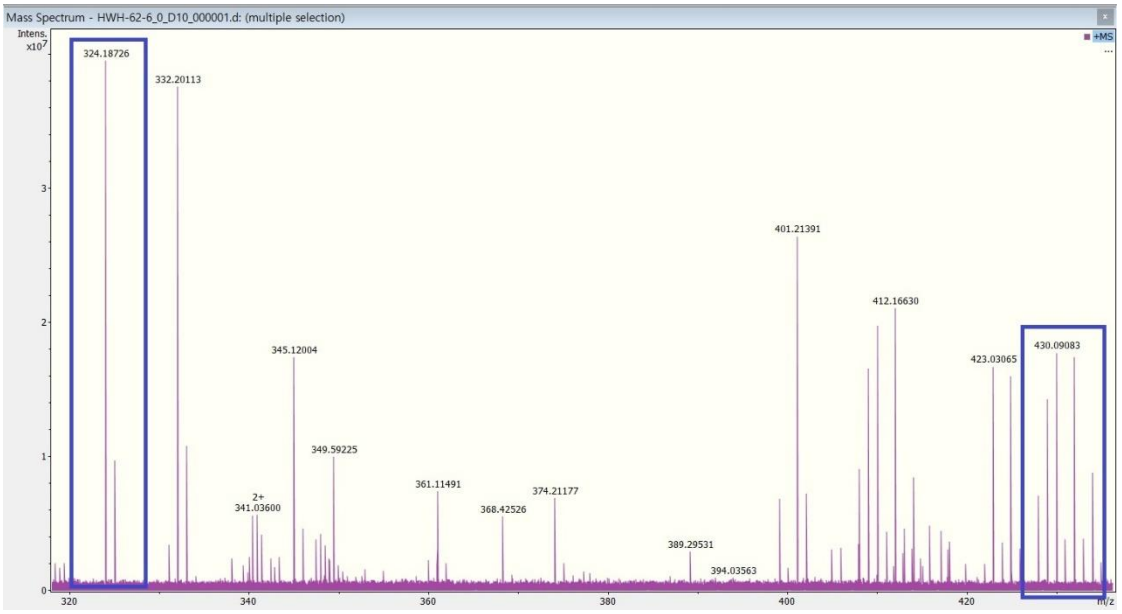


Figure 24. Pd species signal peaks for e) NHC-Arylated complex after reductive elimination; f) mono-arylated-Pd-NHC complex identified by MALDI-MS during the reaction of 2,4-dibromopyridine with *p*-fluorophenylboronic acid catalysed by ***P3*** pre-catalyst.

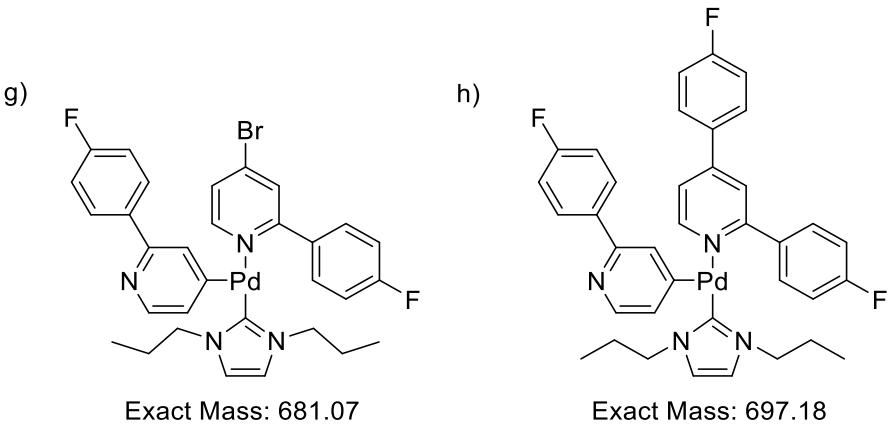


Exact Mass: 681.07 Exact Mass: 697.18

Figure 25. Pd species identified by MALDI-MS during the reaction of 2,4-dichloropyridine with *p*-fluorophenylboronic acid catalysed by ***P3*** pre-catalyst.

Both complex g and h (Figure 25) were observed for the first 5 h during the reaction and haddisappeared after 24 hours and signals showed in Figure 26.

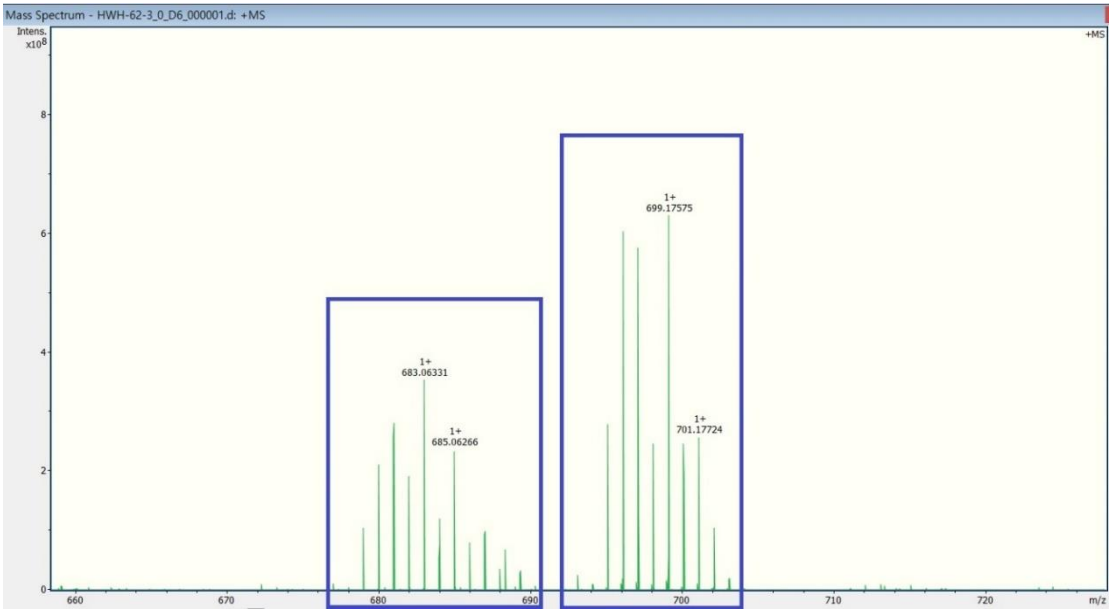


Figure 26. Pd species identified by MALDI-MS during the reaction of 2,4-dichloropyridine with *p*-fluorophenylboronic acid catalysed by ***P3*** pre-catalyst. Left) Pd species signal peaks of nitrogen bound bromo-2 or 4-arylpyridine and either arylpyridine-4-yl or 4-arylpyridine-2-yl respectively; Right) Pd species signal peaks of a nitrogen bound 2,4-Ar and either 2-arylpyridine-4-yl or 4-arylpyridine-2-yl respectively.

### 3.6.2 MALDI-MS analysis of a SMCC reaction of 2,4-dichloropyridine with *p*-fluorophenylboronic acid and *P3* complex in the SMCC.

As previously, reactions were run and samples were collected after 10 minutes, 30 minutes, 1hour, 5 hours and 24 hours (Scheme 37).

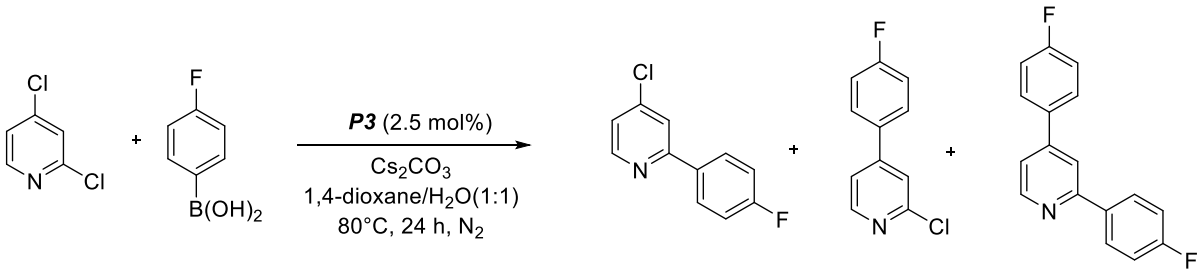


Scheme 37. Catalytic reaction of 2,4-dichloropyridine with *p*-fluorophenylboronic acid using benchmark conditions. ***P3*** [$PdCl_2(NHC_{n\text{-}propyl})$(3-Cl-Pyr)] was used as a non-bulky pre-catalyst with a loading of 2.5 mol%.

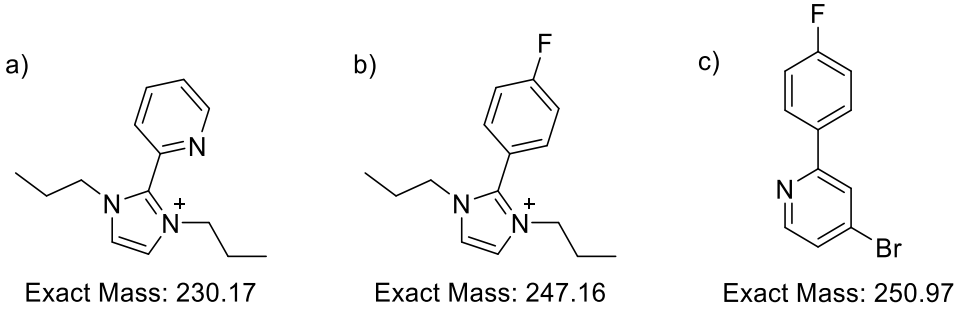


Figure 27. Imidazolium species and mono-arylated species identified by MALDI-MS during the reaction of 2,4-dichloropyridine with *p*-fluorophenylboronic acid catalysed by ***P3*** complex.

Imidazolium species and 2 or 4 arylated species (Figure 27) signal peaks were observed for1 hour and had disappeared after that.

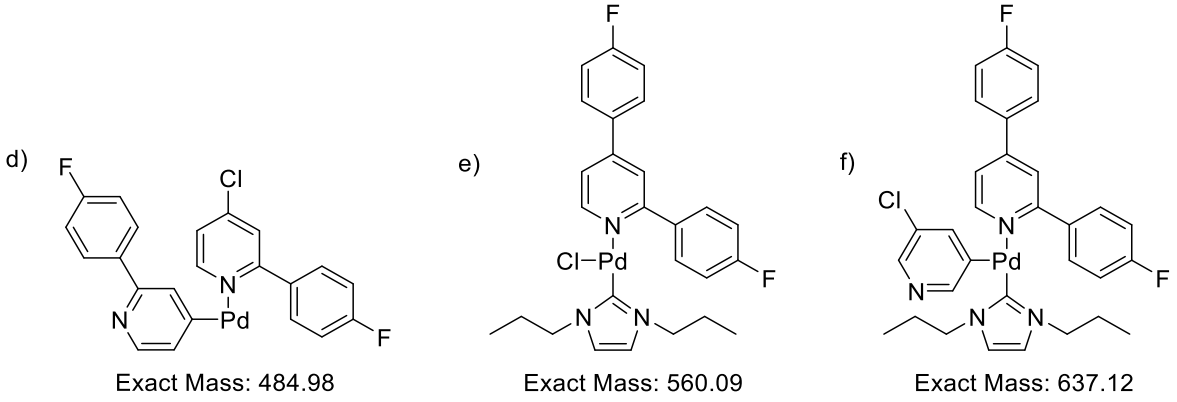


Figure 28. Pd species identified by MALDI-MS during the reaction of 2,4-dichloropyridine with *p*-fluorophenylboronic acid catalysed by ***P3*** complex.

As previously, complex d shows coordination of two mono-arylated pyridine on the Pd species was observed, this was captured during the reaction (Figure 28, d). Complex e shows indicateto form from reductive elimination before produce bis-arylated product. It shows at the first 5 hours and had disappeared after 24 hours (Figure 29).

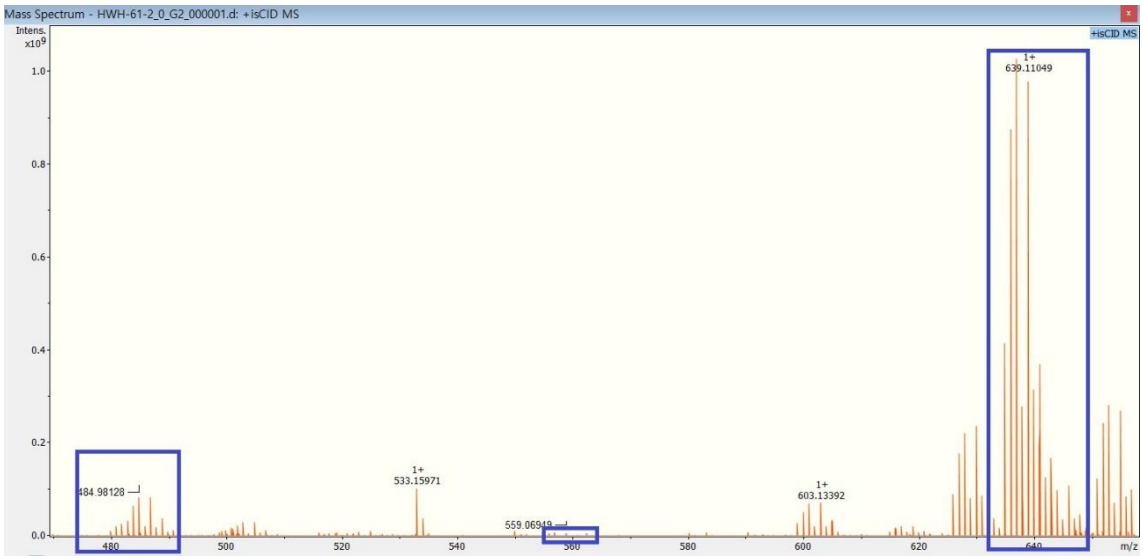


Figure 29. Pd species identified by MALDI-MS during the reaction of 2,4-dichloropyridine with *p*-fluorophenylboronic acid catalysed by ***P3*** complex.

## 3.7 Synthesis of a dimeric palladium complex that is proposed as a potential intermediate in catalysis.

Following C*2*-oxidative addition of 2,4-dihalopyridine to Pd, the geometry is such that a Pd dimer may form through pyridine coordination to a second Pd centre followed the above MS data. An attempt was made to synthesise this dimer, with the aim to examine the pre-activated species in catalysis (Scheme 38).

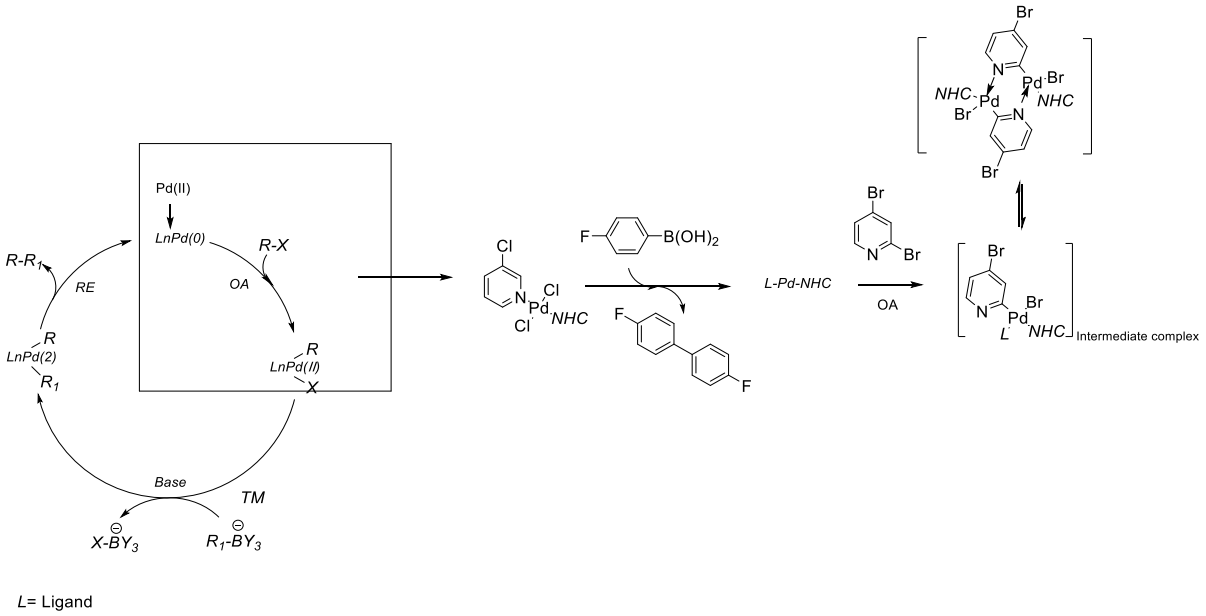


Scheme 38. General mechanism of SMCC reaction and the Pd(II) halide complex formed during oxidative addition step.

Synthesis of the dimer was attempted by reacting ***P2*** with 2,4-dibromopyridine in the presence of 2 equivalents of aryl boronic acid (Scheme 39). However, the expected product was not obtained. After the reaction was completed, I attempted to obtain the structure of the chemical from a single crystal obtained by NMR, MS, and recrystallisation to determine the success ofthe reaction. The results of NMR and MS were unclear, and it was not possible to determine if a product was obtained. Also, recrystallisation was attempted using various reagents as solvents, but a single crystal could not be obtained.

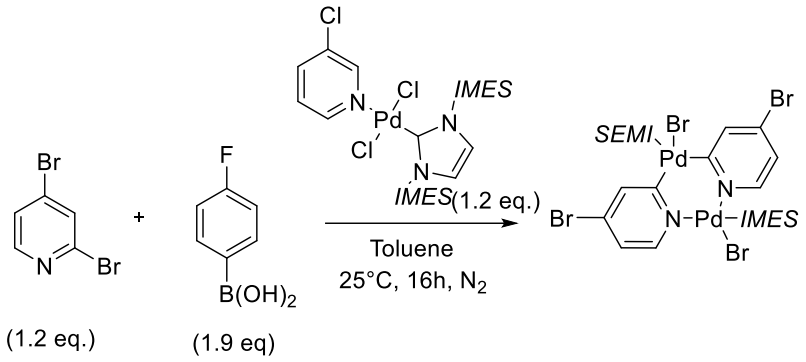


Scheme 39. Attempted synthesis of a Pd dimer.

The reaction was repeated with the addition of cesium carbonate to activate the *P2* complex, and THF was used as a solvent due to a higher solubility of the reagents (Scheme 40). After16 hours, a sample was collected and analysed using MS (Figure 30). The mass of the expected product was 1291.94 m/z when observed via MS, but the mass of the compound predicted to be the actual product was 1108.14014 m/z, suggesting either the loss of severalhalides Br or the loss of an N-substituent, ***I2***, in the NHC ligands analysed by MALDI-MS. Furthermore, the mass spectra was analysed the isotopic patterns to identify which by-products or unexpected products were produced, but were unable to identify a matching compound with the isotope patterns.

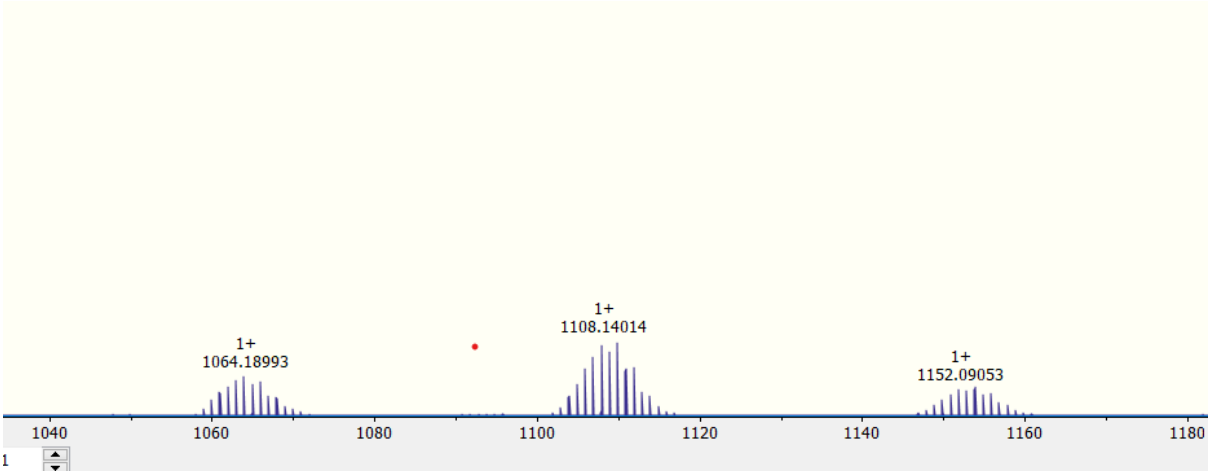


Figure 30. After the reaction, unexpected compounds were observed by MALDI-MS.

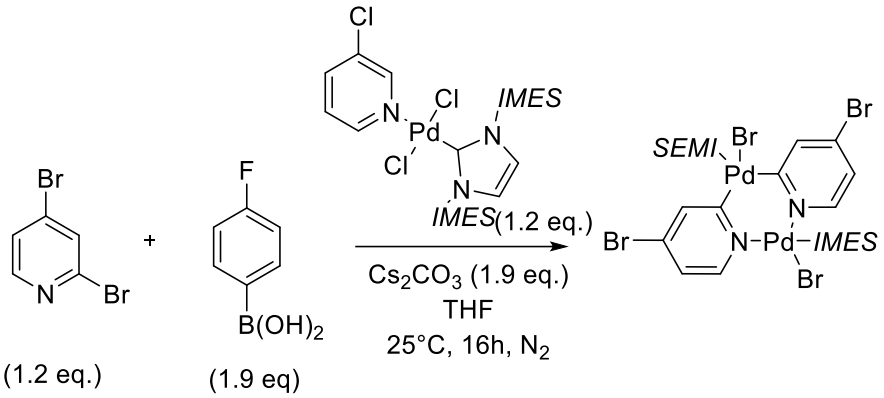


Scheme 40. Attempted synthesis of a Pd dimer in the presence of a base.

## 3.8 Conclusions

In this chapter, extend of Chapter 2, the focus was on the comparison of the reactivity and selectivity of 2,4-dibromopyridine and 2,4-dichloropyridine in the SMCC reaction by understanding the mechanism with the intermediate complexes through mass spectrometry analysis. The results were followed the Neufeldt's studies, the bond dissociation energy of C-Cl was higher than that of C-Br, so the rate of 2,4-dichloropyridine and Neufeldt's results was supported by this study.

In addition, the impact in the SMCC reactions of an NHC ligand with an ***I1*** N-substitute strong electron donation and a ***I3*** NHC ligand with a non-bulk and a weak electron donation were compared. After the examination of the structures of the intermediates found in the cross-coupling reaction, more complex signal peaks were observed in the reaction of 2,4-dibromopyridine, which was harder to determine various complex and it showed the slower reaction rate than the reaction with 2,4-dichloropyridine by MS data. It those study, the 2,4-Arcomplex was major product and supported Willan's study. It has been shown in the MS data that after the formation of the mono-arylated product, a second-catalytic cycle is performed onit form the 2,4-arylated product.

Furthermore, MALDI-MS is used to detect reaction intermediates to better understand the mechanism of the Pd-catalysed cross-coupling reaction. In the case of reactions using bulky ligands (***I1***), complexes presumed to be in the oxidative addition and reductive elimination stages of bis-arylated intermediates for diarylation were mostly found. On the other hand, the intermediates in the reaction using a non-bulky ligand (***I3***) were presumed to be complexes to form mono-arylation compound. Theintermediates were formed and identified by mass spectrometry and the reaction rate was slower than when a bulky ligand (***I1***) was used. The phenomenon is supported Willans study and Neufeldt's results.[28] Unfortunately, it was challenged to identify all signals shown in the mass spectrum and unusually, signal peaks of complexes containing two or more palladium atoms were identified and it is suggesting the possibility of a catalyst speciation reported by Fairlamb *et al.*[57].

# Chapter 4 – Studies using alternative Pd-catalysts: [$PdCl_2$($BAC_{Ipr}$)(3-Cl-Py)] (*P4*) and $Pd_3$(μ-Cl)(μ-$PPh_2$)($PPh_3$)$_3$][Cl] (Coulson clusters)

## 4.1 Introduction

Previous chapters have discussed the use of NHC ligands on Pd. Cyclopropenylidenes are another class of carbenes which bind strongly to metals through nucleophilic (σ-donating) and electrophilic (π-accepting) interactions and can act as very robust catalysts.[65] Among the reported monocyclic carbenes, cyclopropenylidene ($C_3H_2$) was first reported in radio astronomy in 1985.[66] However, cyclopropenylidene was not preferred because it was unstable and posed challenges to isolate.[67–69] Since then, a stable derivative of cyclopropenylidene has been isolated with the addition of a π-electron donor amino group attached to the triangular skeleton.[70] Although the NHC ligand has proven to be highly efficient with ligand diversity, Bertrand and co-workers reported bis(diisopropylamino)cyclopropenylidene (BAC) as a future alternative to NHCs (Scheme 41).[71,72] The authors reported that due to the presence of a strong π-donor amino group, BAC acts as a strong σ-donor ligand similar to NHC. Moreover, the σ-donating power of certain BAC ligands is superior to that of NHC ligands, which was explained by binding constant calculations and their experimental analysis. In addition, single-crystal X-ray analysis suggested that the length of the bond between the metal centre and carbene was shorter in BAC than that of NHC, making it more stable.[19]

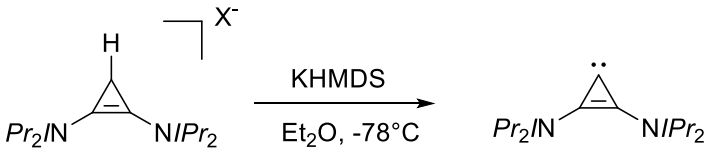


$X_1$= $BPh_4^-$
$X_2$= $BF_4^-$

Scheme 41. The first isolated cyclopropenylidenes by Bertrand *et al*.[71]

The amino group at the 1,2 positions of BAC confers increased stability at the carbenoid carbon via charge delocalisation. These cyclopropenylidenes are reported to be readily available in large quantities, thermally stable and easy to handle. In this chapter, BAC is examined as an alternative ligand to NHC in the PEPPSI complex pre-catalyst for applicationin the SMCC reaction (Figure 31).

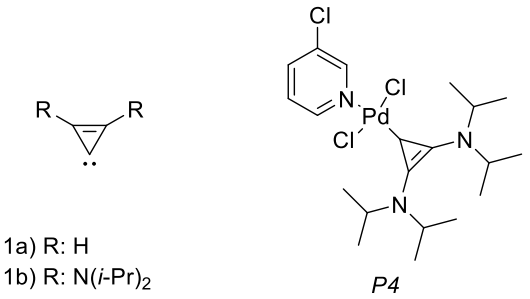


Figure 31. 1a) The first reported cyclopropenylidene and BAC 1a,1b.[66,68,71] ***P4*** was synthesized as novel Pd-BAC PEPPSI catalyst in this chapter.

Fairlamb *et al*. has investigated the role played by catalytically competent aggregated Pd clusters and nanoparticles as an efficient Pd catalysts.[57,73–75] Recently, they reported that mononuclear Pd species thought to be the dominant catalytically active species in the SMCC, can aggregate to form higher-order Pd nanoparticles that can mediate further substrate conversion.[57] This catalytic speciation is supported by experimental evidence which shows that selectivity changes can be linked to the change from mononuclear Pd species to Pd nanoparticles (PdNPs). They reported that Pd clusters and PdNPs were derived through the $Pd(OAc)_2/nPPh_3$ pre-catalyst system under specific reaction conditions – termed 'Fairlamb conditions' throughout this thesis (Scheme 42).

In addition, Li *et al.* reported that the $[Pd_3(\mu\text{- Cl})(\mu\text{-PPh2})_2(PPh_3)_3]+$ complex is an active Pd catalyst for SMCC and an efficient catalyst for reversing the order of the oxidative addition and transmetalation steps. Extending this study, Fairlamb *et al.* showed experimental evidence that $[Pd_3(\mu\text{-Cl})(\mu\text{-}PPh_2)_2(PPh_3)_3]X$ cluster (Coulson cluster) species are generated from $Pd_3(OAc)_6/6PPh_3$ pre-catalysts by the reaction of organohalides.[57] They reported on the basis of Pd-catalysed speciation in the presence of stabilising salt additives, providing a potential bridge from mononuclear $Pd^1$ species to Pd nanoparticles and the Pd nanoparticles and showed that the Pd nanoparticles offer greater C*4* selectivity in cross-coupling reactions.

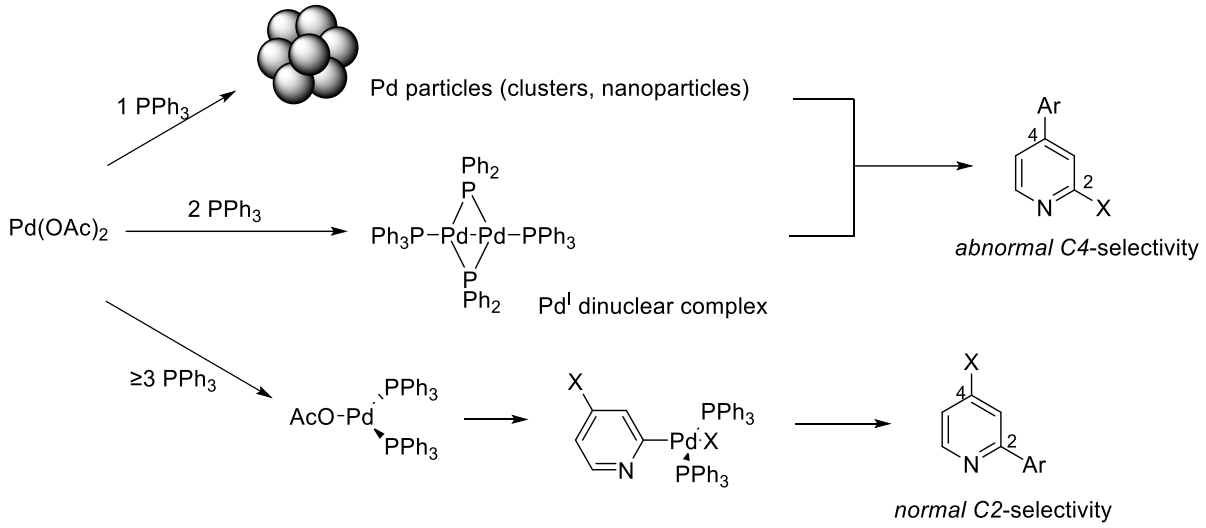


Scheme 42. Different Pd species arising from varying ratios of $Pd(OAc)_2$/n$PPh_3$ resulting in different cross-coupling selectivity in the SMCC reactions using Fairlamb condition.[57]

Li *et al.* demonstrated that the Coulson cluster is not only an active Pd catalyst for SMCC, butalso reverses the order of the oxidative addition and transmetalation steps within the catalyticcycle, providing good selectivity and good reactivity.[42] These Coulson clusters lead to atypical C*4*-selectivity under their benchmark condition with *n*-$Bu_4NOH$ as a specific base for Fairlambcondition. Subsequently, Schoenebeck *et al*. reported a $Pd_3$ cluster catalyst derived from highly active $[Pd(\mu\text{-}Br)(Pt\text{-}Bu_3)]_2$ as a multinuclear catalyst for chemoselective cross-coupling reactions on substrates containing two or more different halide identities, indicating that $Pd_3$ clusters are useful catalysts.[76,77] In this chapter, Coulson-type clusters were tested in the SMCCs and compared using the Fairlamb and Willans conditions. As an increasingly popularalternative to NHC, we invested in the synthesis of pre-catalysts that can be used in cross-coupling reactions by ligand exchange of the phosphine ligand present in the Coulson cluster with the BAC ligand.

## 4.2 Synthesis of novel *P4* [$PdCl_2$($BAC_{Ipr}$) (3-Cl-Py)] complex

A PEPPSI complex was synthesized using BAC in place of an NHC ligand role for use in cross-coupling reactions, using the general synthetic route by Organ et al.[56] The BAC precursor was generated using a new synthetic method reported in an E-Thesis (Scheme 43).[78]

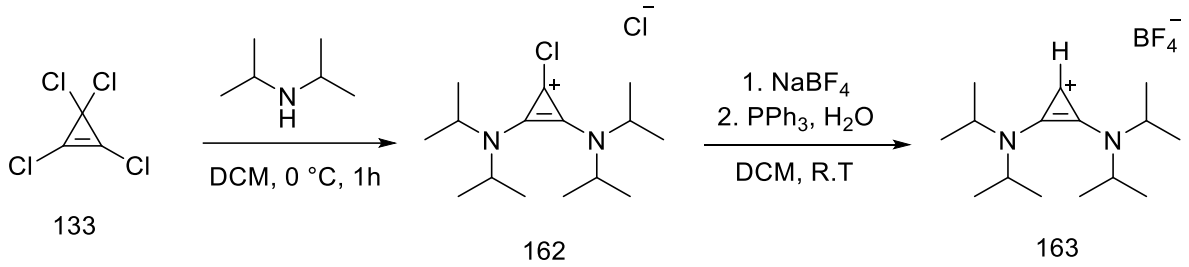


Scheme 43. Synthesis of bis(amino)cyclopropenium salts reported by Tucker in Durham university.[78]

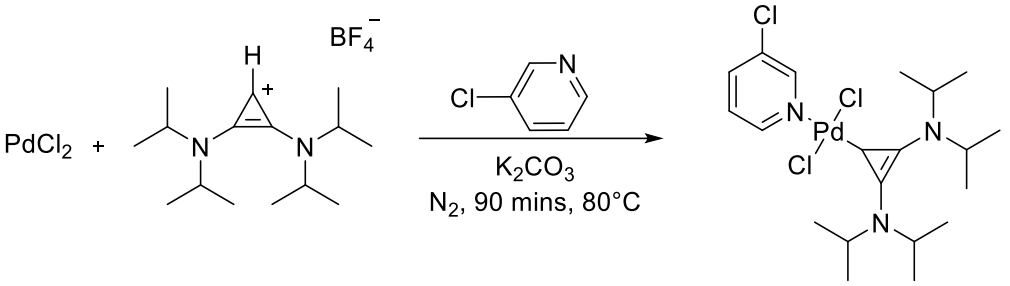


44. Synthesis of novel ***P4*** [$PdCl_2$($BAC_{Ipr}$) (3-Cl-Py)] complex and the yield was 31.7%.[56]

Complex ***P4*** was synthesised in a similar manner to PEPPSI complexes bearing NHCs (Scheme 44).[56] It was analysed by $^1$H NMR spectroscopy which indicated its successful formation (Figure 32). The *IPr* resonances in the N-substitute position are broad due to the protons being freely rotating. Crystallisation was attempted in various ways for single crystal-XRD analysis, but single crystals were not obtained.

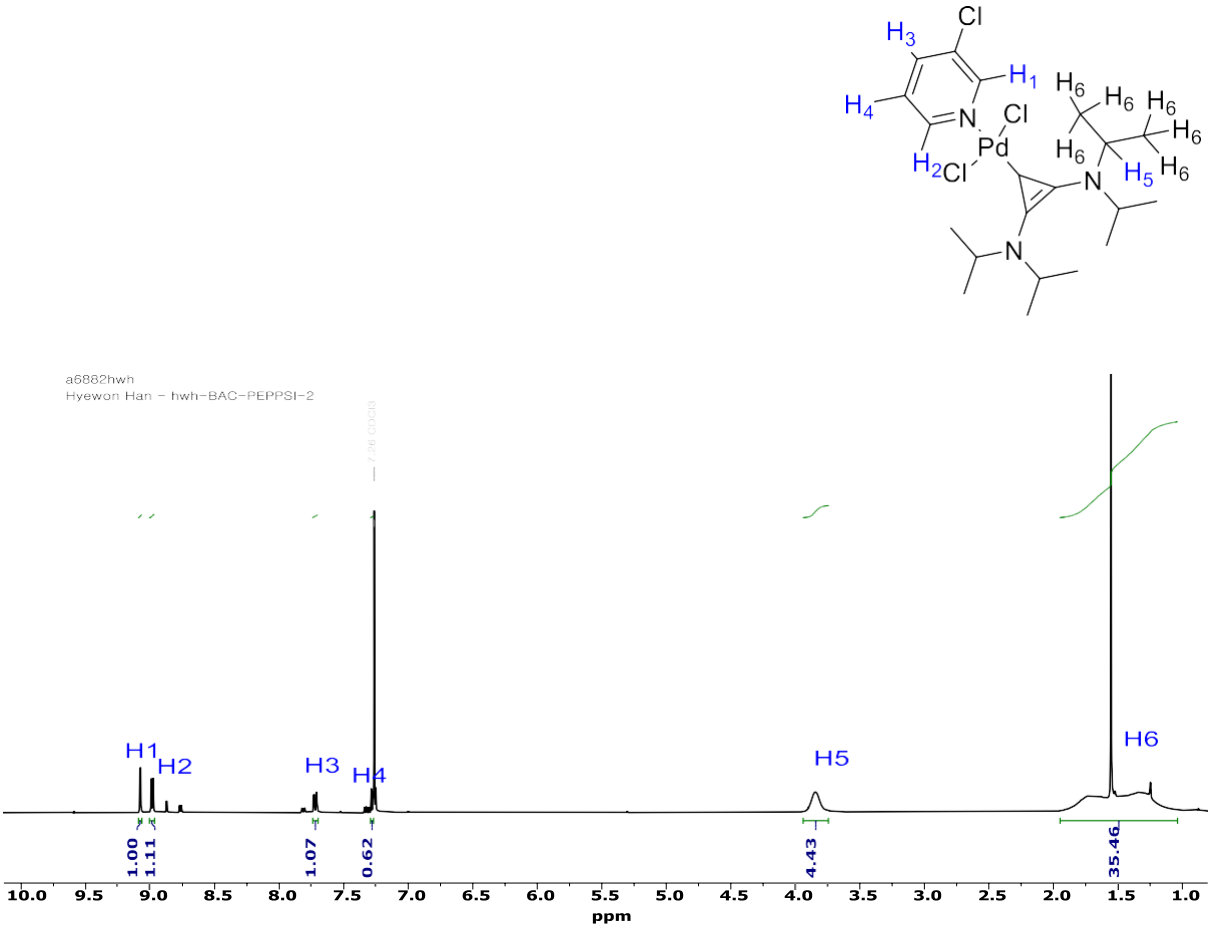


Figure 32. $^{1}$H NMR spectrum (chloroform-d, 400 MHz) of ***P4*** complex.

### 4.2.1 Examination of *P4* complex in the SMCC reaction

A SMCC reaction using Willans conditions was conducted using ***P4*** as a pre-catalyst (Scheme45).

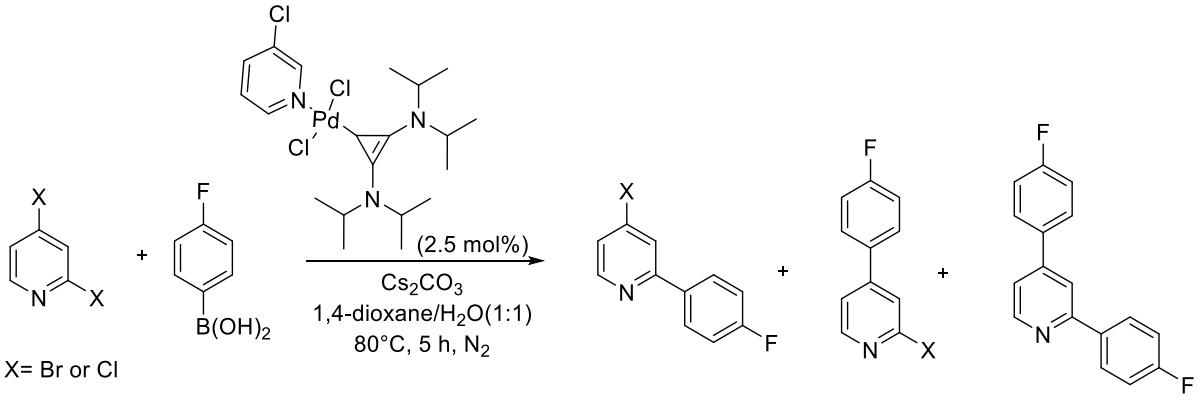


Scheme 45. Pd-catalysed SMCC of 2,4-dibromopyridine and *p*-fluorophenylboronic acid to yield 2-bromo-4-(*p*-fluorophenyl)pyridine (4-Ar), 2-(*p*-fluorophenyl)-4-bromo-pyridine (2-Ar) and 2,4-bis(*p*-fluorophenyl)pyridine (2,4-Ar) under benchmark conditions.

When 2,4-dibromopyridine was used, the main product was 4-Ar. On the other hand, when the substrate 2,4-dichloropyridine was used under the same conditions, C*2*-selectivity was observed, and the reactivity was about 20% higher than with 2,4-dibromopyridine. Samples were taken at 1, 3, and 5 hours from the start of the experiment and analysed by $^{1}$H NMR spectroscopy and the highest conversion points were after 3 hours (Graph 14). Followed the results, the standard reaction time was 3 hours in this reaction.

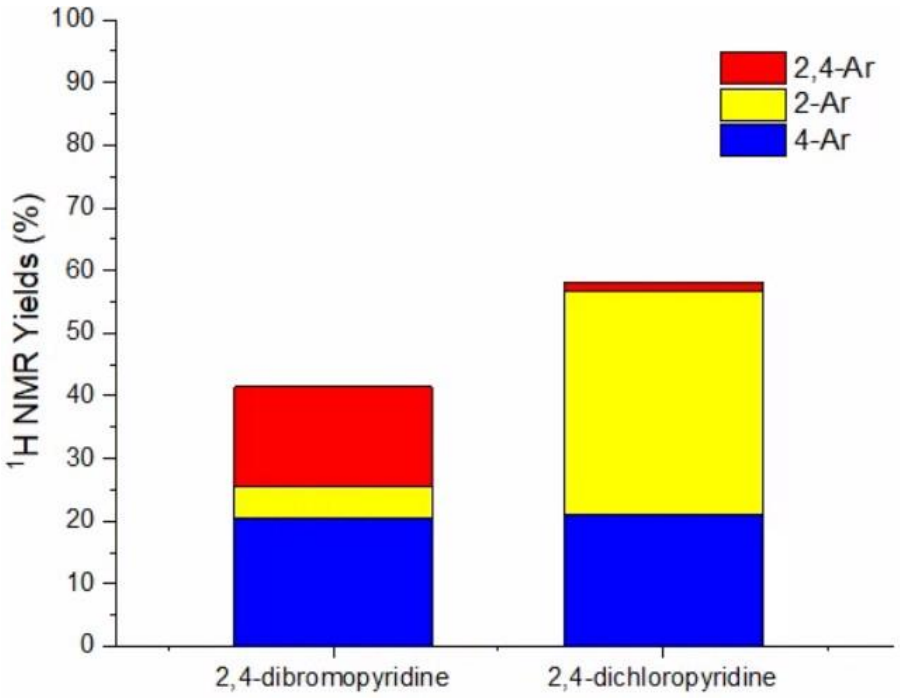


Graph 14. Comparison in selectivity and reactivity two SMCC reactions using ***P4*** complex as a pre-catalyst. Left) 2,4-dibromoprydine and *p*-fluorophenylboronic acid in 1,4-dioxane/$H_2O$ (1:1); Right) 2,4-dichloropyridine and p-fluorophenylboronic acid in 1,4-dioxane/$H_2O$ (1:1). Conversions determined *via* $^1$H NMR spectroscopy at the first 3 hours.

***P4*** is assumed to be less sterically hindered by N-substituents than general PEPPSI complexes (Pd-NHCs). An NHC has a 5-membered ring with N-substituent on the nitrogen net to the carbene centre, whereas the BAC has a nitrogen atom with substituent outside to the 3-membered ring, hence its buried is much smaller than that of the NHC.

According to the literature, BAC has a shorter bond length to metals than NHCs which may lead to better activity due to increased stability.[19] Therefore, BAC is expected to have good reactivity and selectivity as a catalyst, similar to NHCs. To assess this, the reactivity of ***P4*** was explored and compared to that of PEPPSI complexes (Scheme 46).

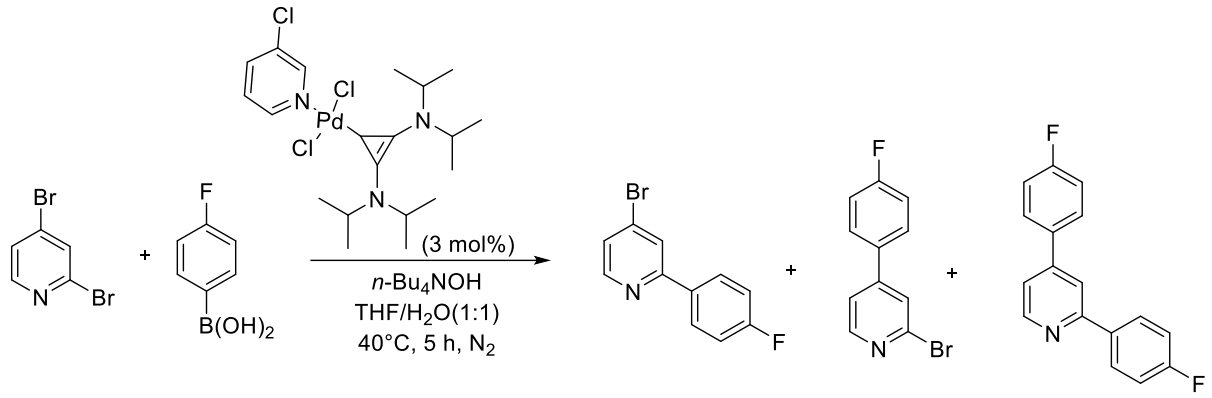


Scheme 46. General reaction of Pd-catalysed SMCC of 2,4-dibromopyridine and *p*-fluorophenylboronic acid to yield 2-bromo-4-(*p*-fluorophenyl)pyridine (4-Ar), 2-(*p*-fluorophenyl)-4-bromo-pyridine (2-Ar) and 2,4-bis(*p*-fluorophenyl)pyridine (2,4-Ar) under Fairlamb conditions.[57]

***P4*** was used in the SMCC reaction using 2,4-dibromopyridine and *p*-fluorophenylboronic acidwith changes in temperature, base, and solvent. Both organic solvents dissolved the reagents well when used in the experiment. When using ***P2*** in these reactions (Chapter 2) a greater yield was observed under the Willans conditions. The preliminary hypothesis was that BACs are more reactive at stronger bases, so it was expected higher yields at stronger base conditions caused by the fact that *n*-$Bu_4NOH$ is a stronger base than $Cs_2CO_3$ which was Fairlamb benchmark reaction. In contrast, the SMCC reaction results were highly reactive in the Willans group's benchmark reaction conditions and going more for 2,4-Ar than mono-Ar products. It can be inferred from the experimental results that the most PEPPSI complexes lead to the high reactivity for 2,4-Ar towards smaller bulk size of ligands and that non-bulky ligands are less reactive than bulky ligands (Graph 15). Regarding selectivity, future research still needs to be done to find a way to remove 2,4-Ar to obtain a yield of only the perfect mono-Ar product for the good selectivity. The PEPPSI catalyst is considered to achieve high reactivity rather than selectivity.

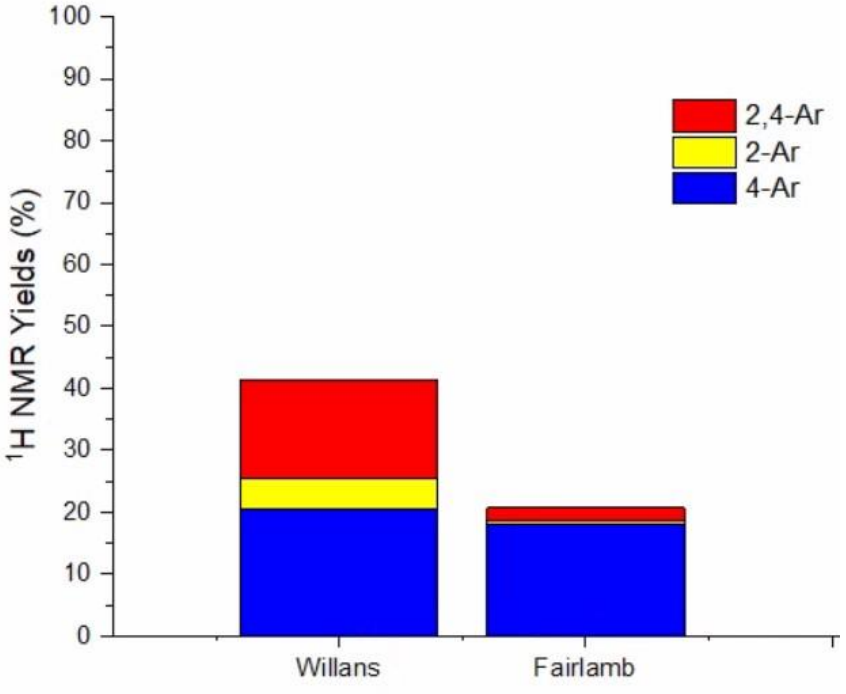


Graph 15. Comparison in selectivity for two SMCC reactions using ***P4*** complex as a pre-catalyst using Willans and Fairlamb conditions. Conversions determined via $^1$H NMR spectroscopy.

## 4.3 Synthesis of $[Pd_3(\mu\text{-}Cl)(\mu\text{-}PPh_2)(PPh_3)_3][Cl]$ cluster – Coulson cluster

The first $[Pd_3(\mu\text{-}Cl)(\mu\text{-}PPh_2)_2(PPh_3)_3]X$ cluster was synthesized by Coulson, who created it through cleavage of P-Ph bonds in triphenylphosphine, and is called the Coulson cluster.[79] The synthetic method reported by Coulson is lengthy, toxic, and extremely complex. Consequently, attempts to develop the synthesis of the Coulson cluster have been reported from the Fairlamb group (Scheme 47).[57] Several attempts were made to synthesise the cluster using $Pd(OAc)_2/nPPh_3$ in $CH_2Cl_2$ and THF with a phosphide peak appearing in the $^{31}$P NMR spectrum, but low yields and the formation of Pd black made the product isolation difficult (Figure 33).

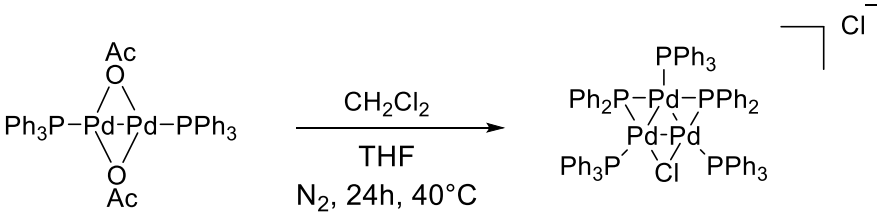


Scheme 47. Attempted synthesis of $[Pd_3(\mu\text{-}Cl)(\mu\text{-}PPh_2)_2(PPh_3)_3]Cl$ cluster (Coulson cluster) from trans-$Pd(OAc)_2/PPh_3$ (1:2) in THF solvent with DCM under $N_2$ by Fairlamb *et al*.[57]

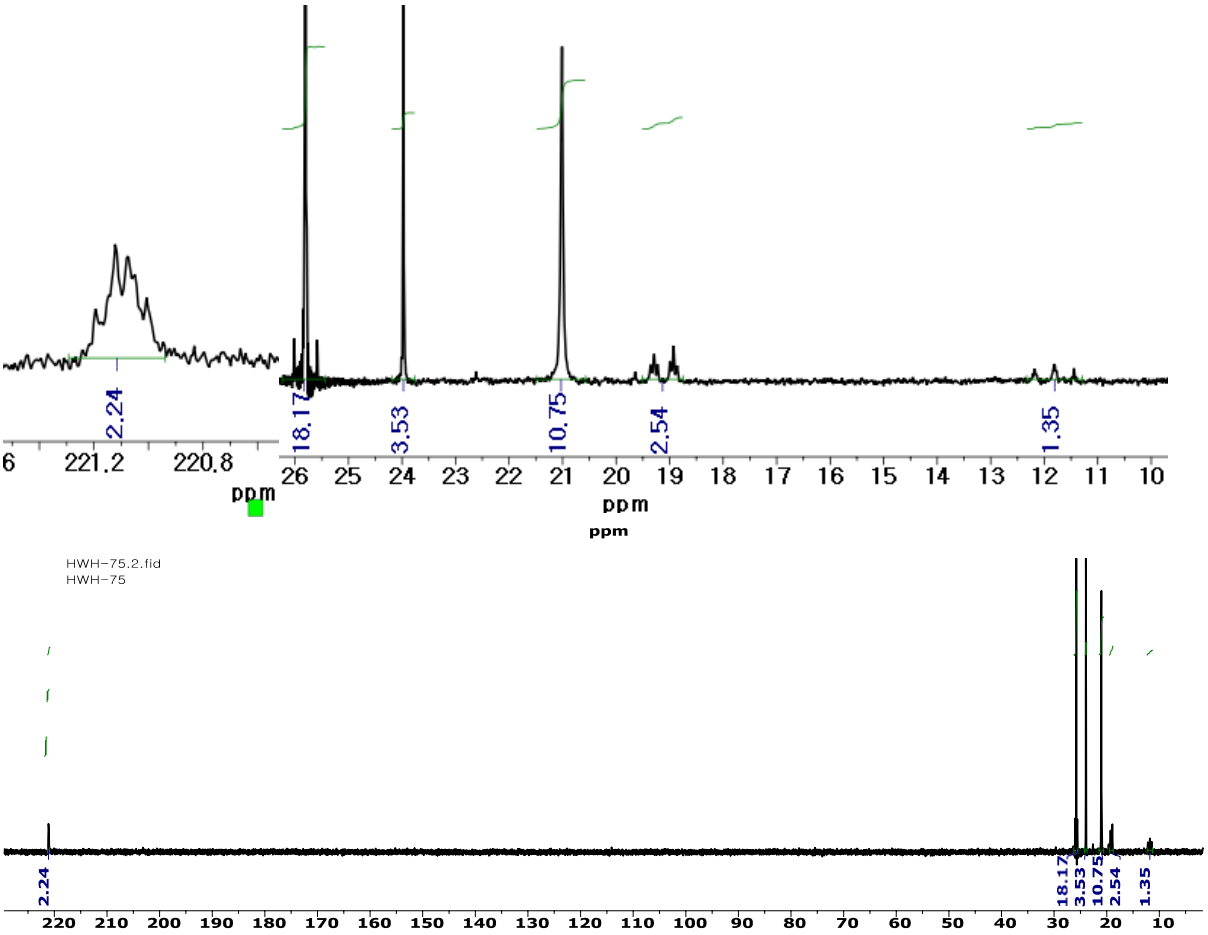


Figure 33. First attempt to synthesis of Coulson cluster using *trans*-$PdCl_2(PPh_3)_2$ in THF solvent under $N_2$; $^{31}P$ NMR (600 MHz, 256 scans, THF) spectrum of $Pd_3Cl_2$ after synthesis and before purification.

Therefore, the Coulson cluster was synthesised using reported methods using $PdCl_2(PPh_3)_2$ in neat aniline under an atmosphere of $H_2$ (Scheme 48). The reaction was found to be very sensitive, giving varying yields and purity.

After purification and drying, the cluster is bench stable as a solid. The synthetic yield was lowwhich decreases further following distillation (Figure 34).

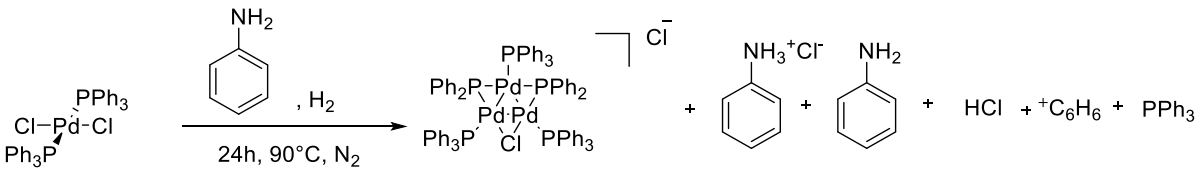


Scheme 48. General procedure for the synthesis of $Pd_3$ clusters from *trans*-$PdCl_2(PPh_3)_2$ in pure aniline solvent under $H_2$ (bottom).

$^{31}$P NMR spectroscopy indicated that the pure Coulson cluster formed before distillation; there was some evidence of degradation following the distillation most likely due to over-heating themixture (Figure 34).

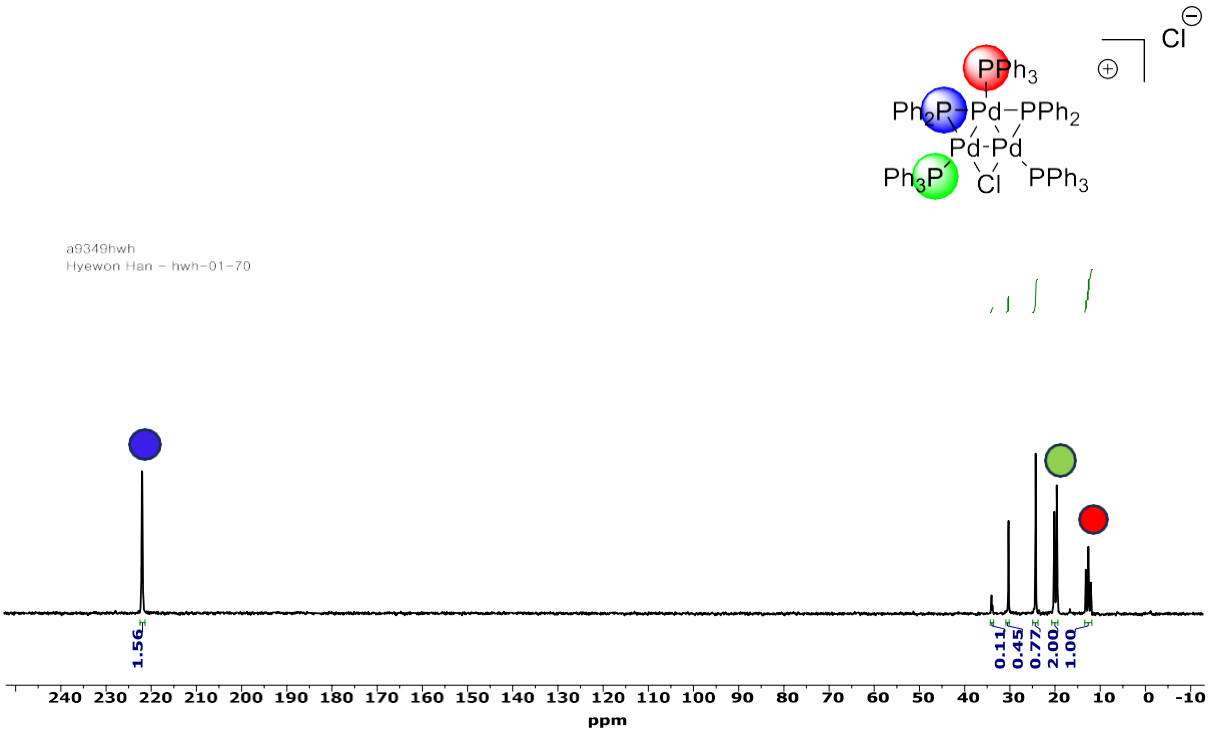


Figure 34. $^{31}$P NMR spectrum ($CD_2Cl_2$, 600 MHz, 256 Scans) of the Coulson cluster.[79] For the other impurities; at the 30 ppm shown triphenylphosphine oxide peak and there are other unknown two components after the synthesise.

### 4.3.1 Examination of the Coulson cluster in the SMCC reaction

In general, SMCC reactions involve a concerted three-step mechanism; Oxidative Addition (OA), Transmetalation (TM) and Reductive Elimination (RE). According to Li *et al.* the Coulson clusters proceed *via* a new SMCC reaction mechanism involving phenylboronic acid reactingfirst to form a $Pd_3Ar$ *via* a boronate i.e. transmetalation first (Scheme 49).[42]

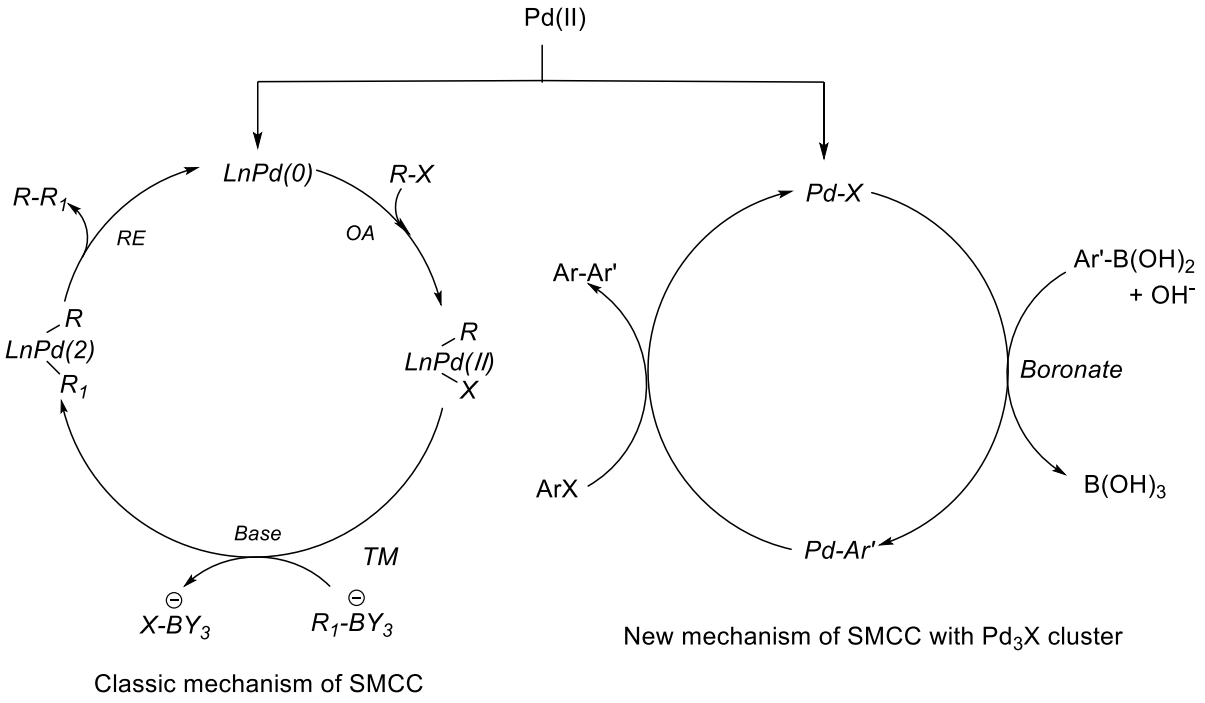


Scheme 49. Comparison between traditional SMCC reaction mechanism and new SMCC mechanism using $Pd_3X$ cluster proposed by Li *et al*.[42]

It has been reported that the $PPh_3$ and $PPh_2$ ligands of Coulson clusters provide bulky protection, making access to the Pd centre by large substrates difficult, slowing down the transmetalation step and providing greater selectivity and also high yields.[42] This is very similar to the principle in PEPPSI complexes, where the bulkier NHC ligands provide selectivity dueto steric hindrance effects.

According to research by Fairlamb *et al*., Coulson clusters exhibit excellent atypical C*4*-selectivity under their reaction conditions.[57] These reactions were repeated (Scheme 50) in the same silicon-capped vials that have been used throughout this thesis, providing even better selectivity. A reaction was also conducted using the Coulson clusters under

Willans conditions for comparison (Scheme 50) and it was found that the Coulson cluster had a normal *C2*-selectivity in the SMCC reaction, and the yield was less than Fairlamb condition (*C2*: *C4*: Bis=31.5: 27.4: 24.4; Graph 16). However, all three products conversions were similar and it is ambiguous that it is a specific selectivity. Therefore, $Pd_3$ cluster used under Fairlamb's condition led to abnormal *C4*-selectivity.

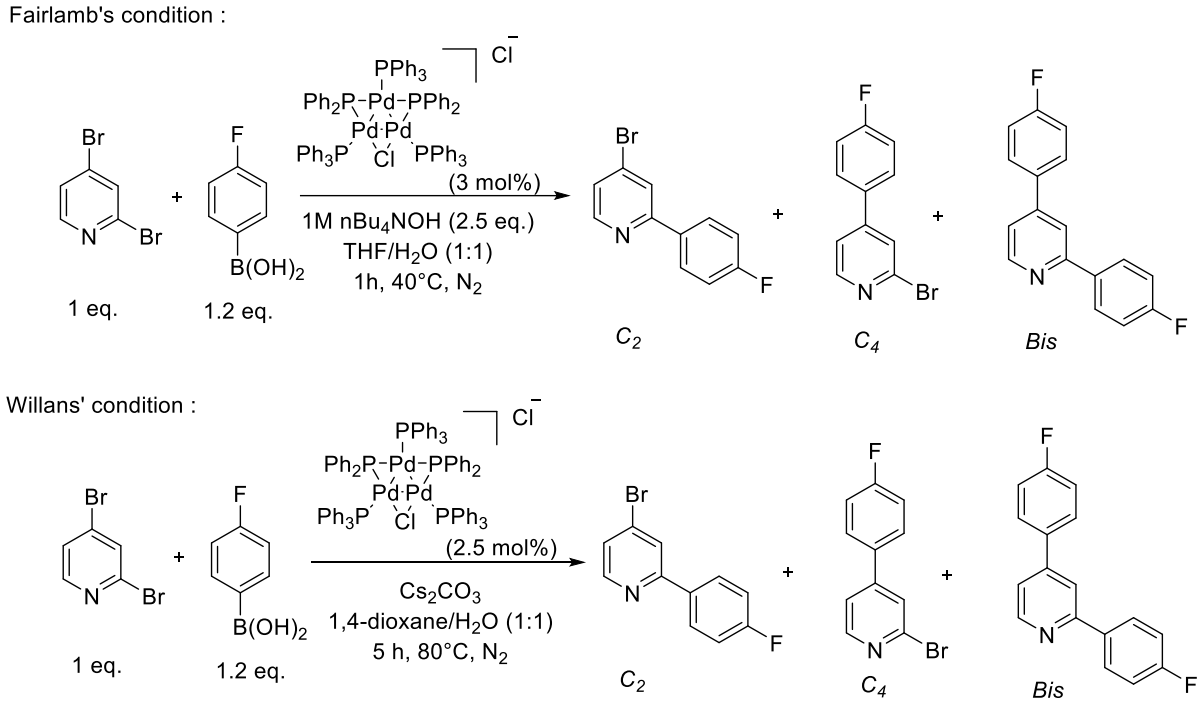


Scheme 50. General reaction for two SMCC reactions using Fairlamb and Willans conditions. Up) SMCC using Coulson clusters and 2,4-dibromopyridine and *p*-fluorophenylboronic acid in THF/$H_2O$(1:1) under Fairlamb's conditions.[57]; Down) SMCC using Coulson clusters and 2,4-dibromopyridine and *p*-fluorophenylboronic acid in 1,4-dioxane/$H_2O$ (1:1) under Willans's conditions.[44]

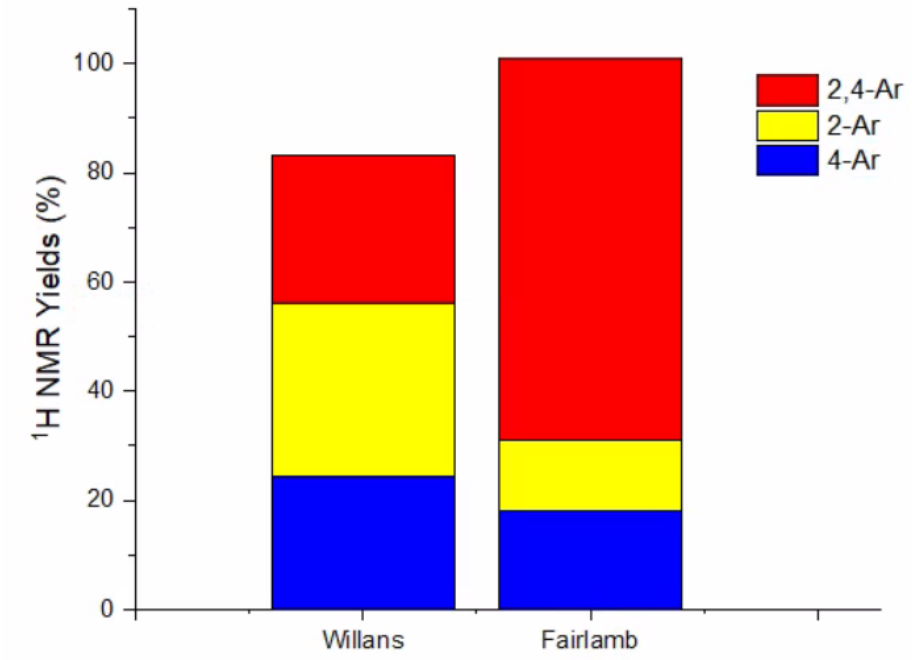


Graph 16. Comparison between two SMCC reactions with Coulson cluster as a pre-catalyst using Willans and Fairlamb conditions. Conversion determined by $^1$H NMR spectroscopy, the Coulson cluster synthesized by Neda Jeddi.

### 4.3.3 Ligand exchange in Coulson cluster

It has been reported in the literature that bulky $PPh_3$ and $PPh_2$ ligands on highly nucleophilic Coulson clusters slow down the rate of transmetalation providing good selectivity and yield.[42,57] Therefore, modification of Coulson clusters via ligand exchange potentially provides control over the desired reactivity and selectivity in a reaction and provides a control for further investigation. Currently, studies on the control of selectivity and reactivity via ligand exchangeof these $Pd_3$ clusters are still limited.[80] Malacria and co-workers used a sulfonate-substituted triphenylphosphine ligand to form a structurally modified $[Pd_3(\mu\text{-}SR')_3(PR_3)_3][X]$ cluster and reported the high catalytic reactivity of this substituted $Pd_3$ cluster (Scheme 51).[80–82] The focusof this study was the modification of the Coulson cluster with a BAC ligand as a strong σ-donor.

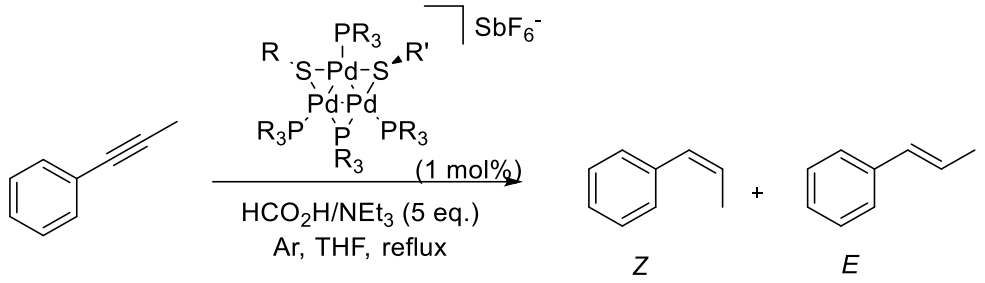


Scheme 51. Proposed hydrogenation reaction of internal 1-phenly propyne promoted by modified Coulson cluster $[Pd_3(\mu\text{-}SR)_3(PR_3)_3][SbF_6]$ in THF with $HCO_2H/NEt_3$ under argon in reflux temperature, cis 1-phenylpropene *Z* as main product and the trans-isomer *E* formed in a side-product by Malacri and co-workers.[80]

Ligand exchange of the Coulson cluster with the BAC precursor was carried out. 1 equivalent of Coulson cluster was reacted with 3.5 equivalents of BAC and 5 equivalents of $Cs_2CO_3$ in THF for 48 hours (Scheme 52, a). Evidence of ligand substitution was provided by mass spectrometry (MS-MALDI).

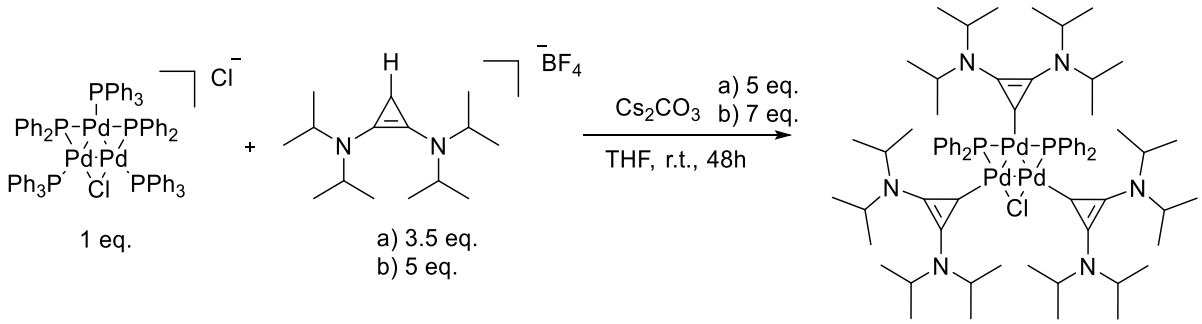


Scheme 52. Ligand exchange of Coulson cluster with BAC ligand precursor. First attempt used BAC 3.5 equivalent with $Cs_2CO_3$ 5 equivalent in THF and second attempt used BAC 5 equivalent with $Cs_2CO_3$ 7 equivalent in THF. Main product was 3-substituted Coulson cluster and side-products were di-substituted and mono-substituted Coulson clusters.

After completing the reaction, the $^{31}P$ NMR spectrum showed the peaks of the main product, 3-substituted Coulson cluster, and the by-products, di-substituted and mono-substituted clusters, in a ratio of approximately 100:37:78. The reaction was repeated with a higher ratio of BAC (5 equivalents) and base (7 equivalents) (Scheme 52, b)). The $^{31}P$ NMR spectrum showed that the proportion of side products had reduced with a ratio of 100:21:19 (Figure 35).

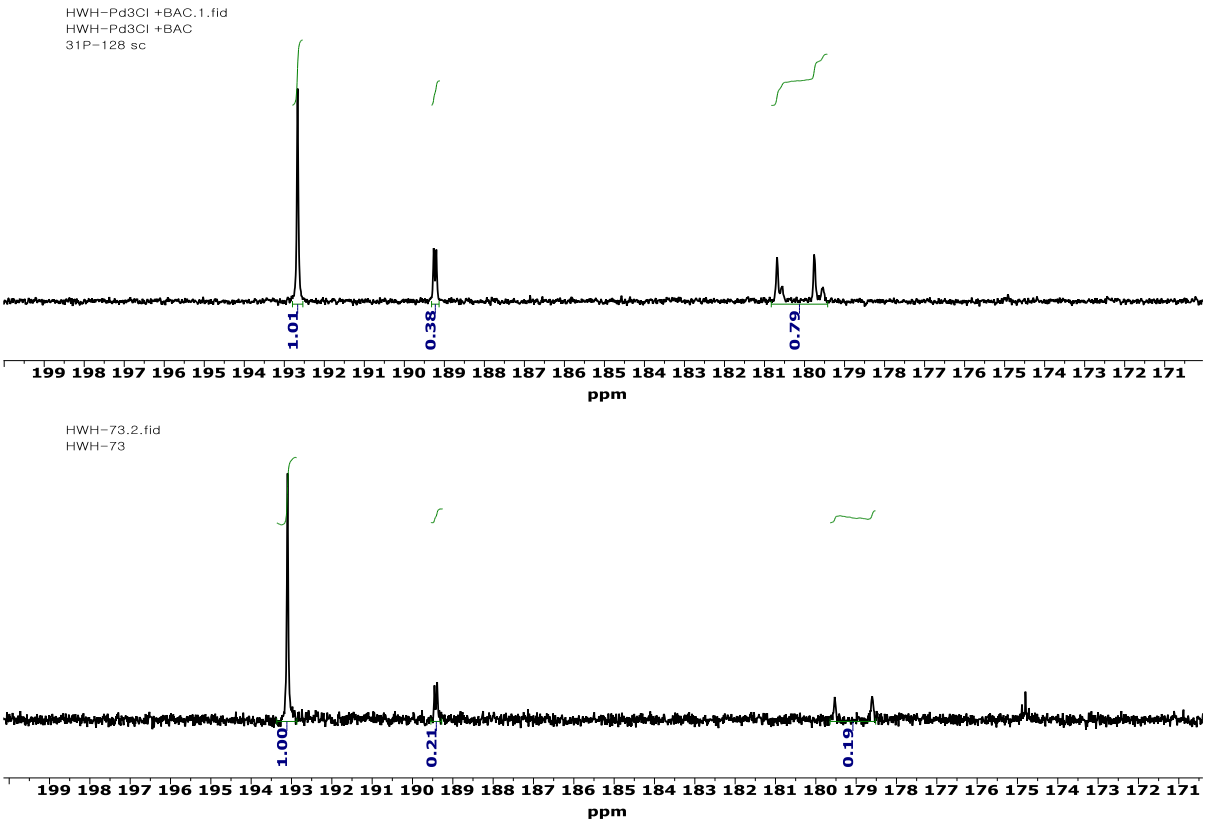


Figure 35. The above $^{31}P$ NMR spectrum (600 MHz, 64 scans, $CD_2Cl_2$) of Coulson cluster (1 eq.) with BAC (3.5 eq.) in $CD_2Cl_2$ at room temperature. The below $^{31}P$ NMR spectrum (600 MHz, 64 scans, $CD_2Cl_2$) of Coulson cluster (1 eq.) with BAC (5 eq.) in $CD_2Cl_2$ at room temperature. Each signal peaks showing formation of 3-substituted Coulson cluster derivative at 193 ppm, di-substituted Coulson derivative at $\delta_P$ 189.5 ppm, mono-substituted Coulson derivative centred at $\delta_P$ 179 and 180-181 ppm.

To confirm the $^{31}P$ NMR spectrum, the sample was cross analysed by MS (Figure 36). MALDI-MS was used to obtain peaks of intact complexes without losing ions or ligands. The results obtained by mass spectrometry were consistent with the $^{31}P$ NMR, the peak of the major product, the 3-substituted Coulson cluster, appeared largest peak, while the minor products, the di-substituted and monosubstituted Coulson cluster peaks appeared smaller, almost in the same proportions as the NMR results. This supported that the ligand exchange reaction wassuccessful.

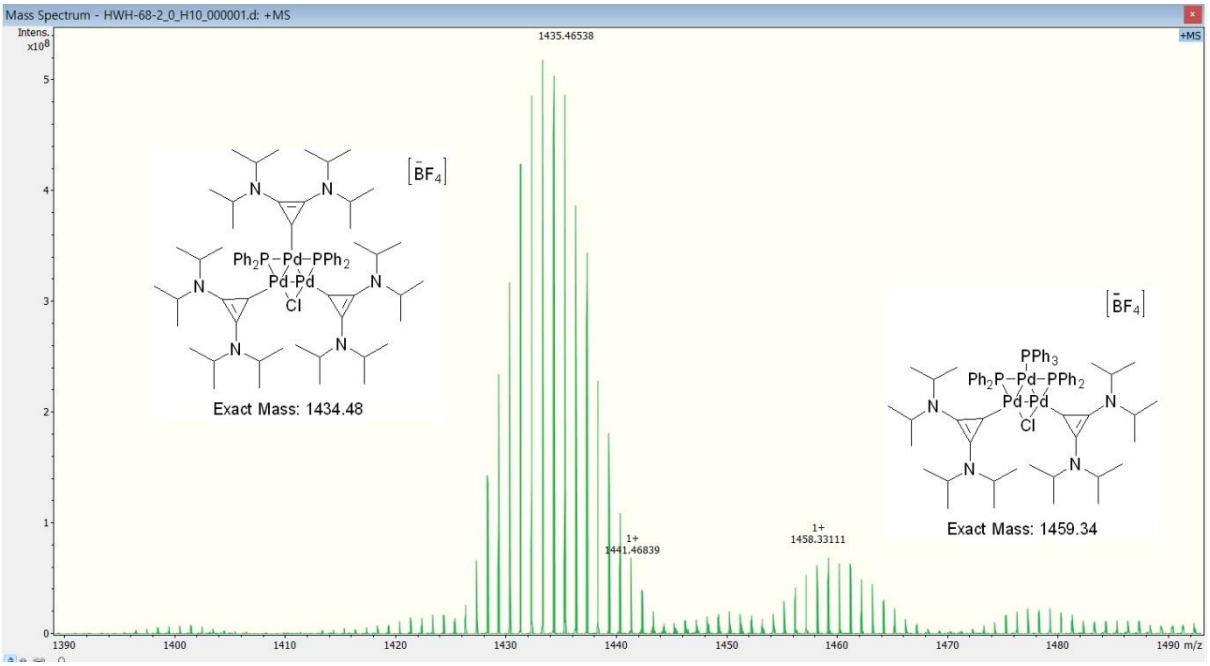


Figure 36. MS spectrum peaks (MALDI-MS) in degassed $CH_2Cl_2$ and low concentration as much as in the small HPLC vial. The 3-substituted Coulson cluster signal was 1435.46538 m/z and the di-substituted and monosubstituted Coulson cluster peaks were 1458.33111 m/z, 1477 m/z.

## 4.4 Conclusions

In this chapter, the potential of BAC as an alternative ligand to NHC was examined, specifically in SMCC reactions. The Willans' reaction conditions were found to be effective usingPEPPSI,[44] but when using ***P4*** was less effective when tested. On the other hand, under the Fairlamb conditions,[57] the PEPPSI complex was not very effective. When the ***P4*** complex wastested as a pre-catalyst, it was almost twice as effective as the equivalent reaction run underWillans' conditions. These results suggested that the use of BAC with a strong base is expected to improve the efficiency of the cross-coupling reaction to get better reactivity and may have slightly different properties than NHC.

Also, attempts to improve the original Coulson cluster synthesis method and applied the Coulson cluster to the SMCC reactions. First this was applied to the original Fairlamb conditions from the literature, alongside Willans' conditions. Interestingly, when using the Fairlamb's conditions, the reactions were stable in inert $N_2$ gas (using silicon-capped vials instead of Schlenk flasks) upon sample removal for analysis. This resulted in slightly better selectivity than the original literature. Whereas the experiment under the Willans' conditions showed much lower yields and reactivity with the Coulson cluster in the SMCC reaction. Therefore, the Coulson cluster proved to be effective in the Fairlamb condition for SMCC reaction.

Lastly, the impact of controlling steric effects was investigated, through ligand exchange on the Coulson clusters, which is still lacking. Using BAC as an alternative ligand for the phosphine, $PPh_3$, the $^{31}P$ NMR spectrum and MALDI-MS showed the ligand exchange experiment to be successful. However, attempts to obtain a single crystal and solve the diffraction pattern were unsuccessful, as a powder was obtained. This ligand exchange was achieved with relative ease under inert gas ($N_2$), suggesting that the ligand control of the Pd cluster possible. The use of Pd clusters as robust and efficient catalysts can be expected to play a positive role in future catalytic applications.

## Conclusion and Future work

This study, focused on the Pd-catalysed cross coupling reactions with various catalytic species to compare selectivity and reactivity. Bulkier PEPPSI provide good reactivity in the SMCC reactions by steric hinderance effect which provide stronger σ donation on the Pd centre and when using less size PEPPSI showed lower reactivities. Using 2,4-dichloropyridine as a substrate gives better reactivities than 2,4-dibromopyridine and it is speculated that the change of reactivity is due to energy differences caused by differences in the different LUMO coefficients of the substrates. In addition, using MALDI-MS to capture the intermediates generated during the reaction to understand the differences in reactivity and reaction rates, it was found that reactions with bulky ligands generated intermediates more rapidly than reactions with less bulky ligands due to 'hyper-arylation'. To compare the selectivity with various Pd catalysts in the benchmark SMCC reactions and despite used the same condition, all the other Pd catalytic species lead to C*2*-selectivity.

To investigated new class of ligand, BAC was used in the SMCC reactions but it still needs to develop to get better reactivity and selectivity. In addition, succeed to synthesis of novel PEPPSI complex which used BAC as a ligand under the same synthetic route. Lastly, $Pd_3$ cluster which called Coulson cluster used in the two conditions of the SMCC (Willans and Fairlamb) to compare selectivity and reactivity and it showed greater C*4*-selectivity and reactivity. It proved that the Coulson cluster performed as a great Pd catalyst in the SMCC to get a specific selectivity.

# Chapter 5- Experimental part

## 5.1 General Considerations

Manipulations were performed under an atmosphere of dry nitrogen, by means of standard Schlenk line. All solvents were degassed with nitrogen. All chemicals were purchased from Sigma Aldrich, Alfa Aesar, Apollo scientific or Fluorochem used without further purification.

NMR spectra were recorded on a 400, 600 spectrometers. $^{1}H$, $^{19}F$ chemical shifts were referenced to the internal standard. Mass spectroscopy was collected on a solariX XR FTMS 9.4T based on ion funnel technology for MALDI and ESI.

## 5.2 General synthesis of NHC ligand precursors.

### *5.2.1 I1*

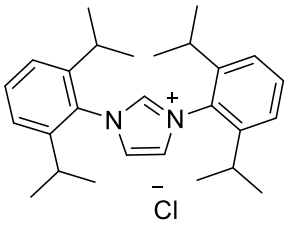


In a round bottomed flask, *N,N*-diisopropylphenyl-1,4-diaza-1,3-butadiene (10 g, 26.6 mol, 1 eq) was dissolved in degassed EtOAc (100 ml). In a separate flask, paraformaldehyde (0.7974 g, 26.6 mmol, 1 eq) was added to 4M HCl in dioxane (12 ml) and stirred for 20 minutes to complete dissolutions. The second mixture was added dropwise (via cannula transfer) to the diaza-butadiene solution at 0 ℃ for 30 minutes and the mixture stirred for overnight. The brown mixture was filtered and washed with EtOAc (50 ml) until clear colour. The off-white solid was dissolved in $CH_2Cl_2$, Calcium chloride was added to absorb any moisture and the mixture was filtered again and DCM was removed in vacuo, allowing collection of a pale-yellow solids. (4.8169 g, 42.65 %) $^{1}H$ NMR (400 MHz, Chloroform-*d*) δ 10.05 (d, 1H), 8.16 (d, 2H), 7.57 (t, *J* = 7.8Hz, 2H), 7.34 (d, *J* = 7.8Hz, 4H), 4.11 (q, 3H), 2.44 (hept, 4H), 2.03 (s, *J* = 13.5, 6.8 Hz, 4H), 1.31 – 1.16 (m, *J* = 18.9, 6.8 Hz, 24H). ESI+ m/z: 389.295

*Lab book reference number*: hwh-01-15

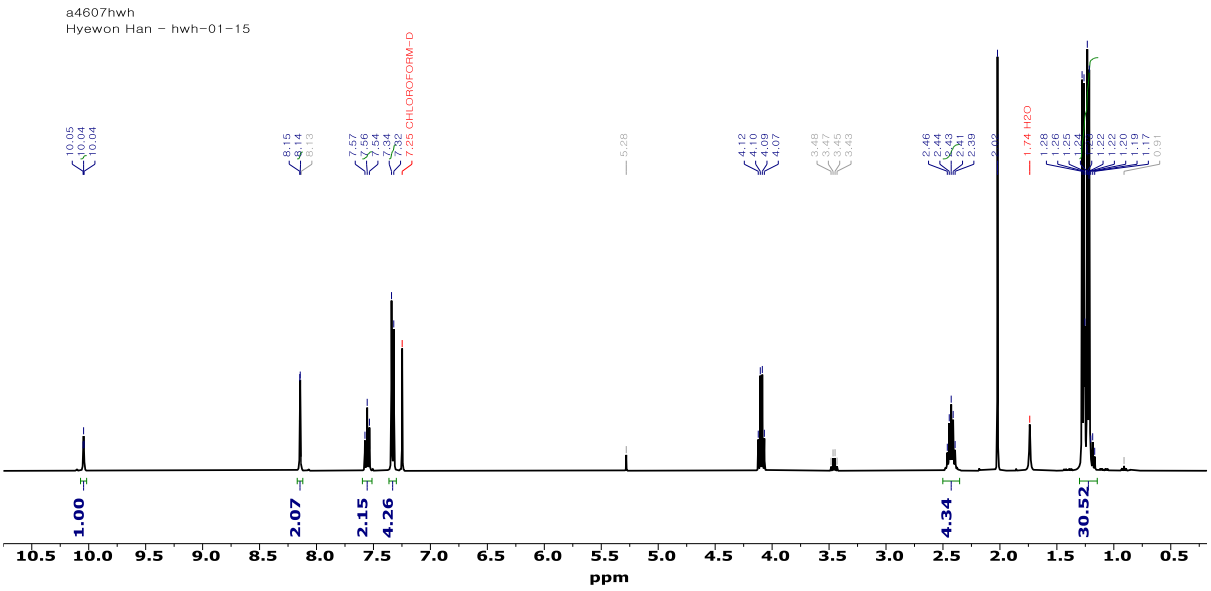


Figure 37. $^{1}$H NMR spectrum (400 MHz, 32 scans, Chloroform-*d*) of ***I1*** and impurity in the sample δ 5.36 ppm showed DCM, 4.12 and 2.07 showed Ethyl Acetate, 3.48 showed rest of paraformaldehyde and 1.74 showed $H_2O$.

### *5.2.2 I2*

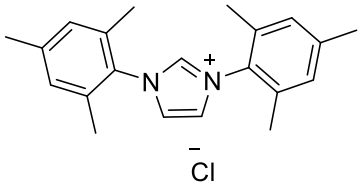


Precursor: *N,N*-dimesityl-1,4-diaza-1,3-butadiene (made by Willans' group) $^{1}$H NMR (400 MHz, chloroform-*d*) δ 10.86 (s, 1H, H1), 7.60 (d, *J* = 1.4 Hz, 2H, H3), 7.03 (s, 4H, H7), 2.34 (s, 6H, H9), 2.18 (s, 12H, H6) ppm. ESI+ m/z: 315.1834

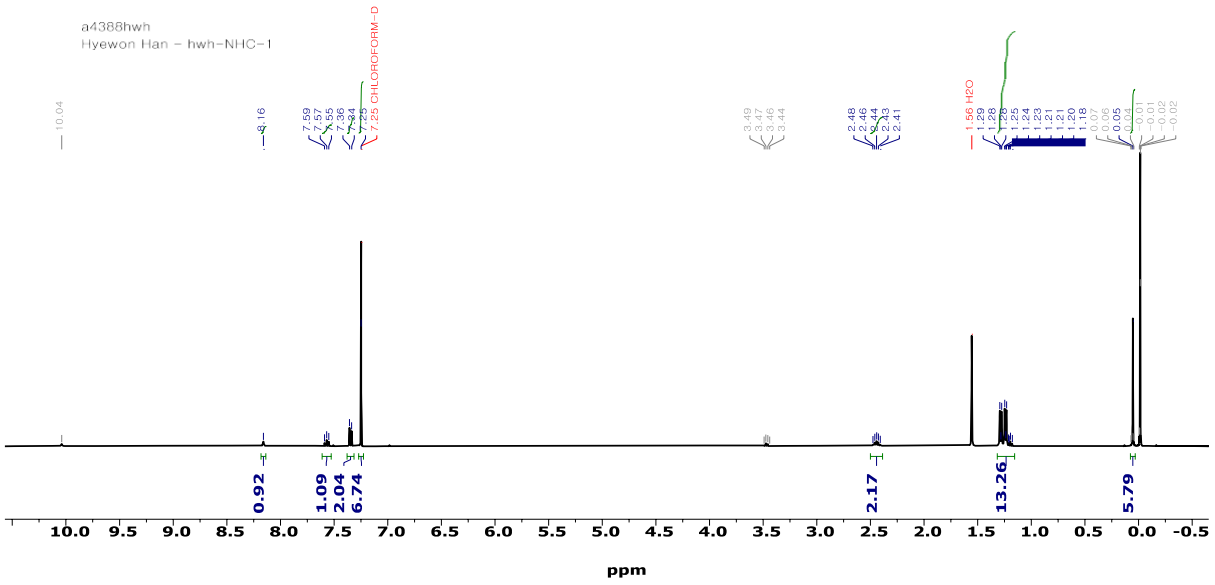


Figure 38. $^{1}$H NMR spectrum (400 MHz, 32 scans, Chloroform-*d*) of ***I2*** and impurities of 3.48 ppm showed rest of paraformaldehyde and 1.74 ppm showed $H_2O$.

### *5.2.3 I3*

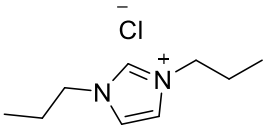


An Schlenk flask was added paraformaldehyde (1.5 g, 50 mmol, 1 eq), n-propylamine (4.2 ml, 51 mmol, 1.02 eq) was evacuated and backfilled*3 with $N_2$ and added degassed toluene (50 ml) with intense stirring for 30 minutes at R.T. After stirring, n-propylamine (4.2 ml, 51 mmol, 1.02 eq) was added dropwise and stirred for 10 minutes at 0℃ and by dropwise added 4M HCl in dioxane (3 ml, 52 mmol, 1.04 eq). The reaction mixture turn to R.T. and added glyoxal (40 % in $H_2O$, 8 ml, 50 mmol, 1 eq) and stirred for overnight under $N_2$. The mixture vac off and washed with diethyl ether (3* 10 ml) and collect the brown oil. The yielded as a sticky brown oil (0.19 g, 1 mmol, 91.5 %)$^{1}$H NMR (400 MHz, Chloroform-d) δ 9.65 (q, 3H), 7.31 (d, *J* = 1.3 Hz, 6H), 3.89 (t, *J* = 7.3 Hz, 12H), 1.56 – 1.44 (m, 12H), 0.50 (td, *J* = 7.4 Hz, 19H) ppm. $^{13}$C NMR (126 MHz, chloroform-*d*) δ136.7 (CH), 122.62(CH), 51.29 ($CH_2$), 23.55 ($CH_2$), 10.66 ($CH_3$) ppm. ESI+ m/z : 153.14

*Lab book reference number*: hwh-01-18, hwh-01-30

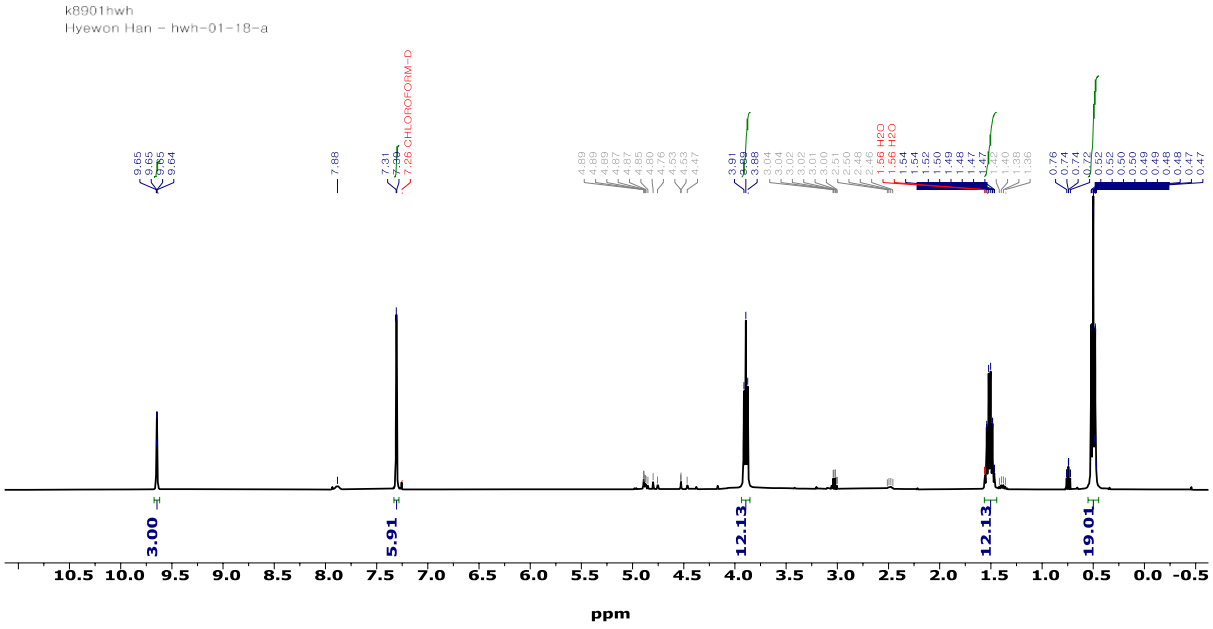


Figure 39. $^{1}$H NMR (400 MHz, 32 scans, Chloroform-*d*) of ***I3*** impurity in the sample δ 5.36 ppm showed DCM, 4.12 and 2.07 showed Ethyl Acetate, 3.48 showed rest of paraformaldehyde and 1.74 showed $H_2O$.

## 5.3 General Synthesis of PEPPSI complexes

An Schlenk flask equipped NHC precursor (0.56 mmol, 1 eq), $PdCl_2$ (100 mg, 0.56 mmol, 1 eq), $K_2CO_3$ (386 mg, 2.5 mmol, 4.46 eq) was evacuated and backfilled *3 under $N_2$ and added 3-chloropyridine (7 ml, 0.06 mmol, 0.11 eq) and stirred at 80℃ for 90 minutes (if the reaction mixture colour to get dark turn off the heating and continue running the sample for purifying). The reaction mixture was transferred to Kugelrohr for 30 minutes and mixture washed through in a short silica plug (10 cm) with DCM and solvent evaporated by rotary evaporator. The crude solid dissolved in Hexane in a round bottom flask. After dissolving, the sample putted in sonicator for 20 minutes and solid crushed out and dried in *vacuo*.

### *5.3.1 P1*

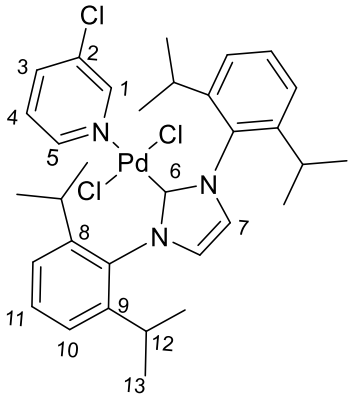


NHC precursor: 1,3-bis(diisopropylphenyl)imidazolium chloride. Pale yellow solid (0.09 g, 25.28 %) $^{1}$H NMR (400 MHz, chloroform-*d*) δ 8.60 (d, *J* = 2.3 Hz, 1H, H1), 8.52 (dd, *J* = 5.5, 1.3 Hz, 1H, H5), 7.55 (ddd, 1H, H3), 7.52 – 7.47 (m, *J* = 7.7 Hz, 2H, H11), 7.35 (d, 4H, H10), 7.14 (s, 2H, H7), 7.07 (dd, *J* = 8.2, 5.6 Hz, 1H, H4), 3.23– 3.06 (m, 4H, H12), 1.48 (d, *J* = 6.6 Hz, 12H, H13), 1.12 (d, *J* = 6.9 Hz, 12H, H13) ppm. ESI+, m/z: 681.1465 (Expect mass: 677.13)

*Lab book reference number*: hwh-01-19, hwh-01-32

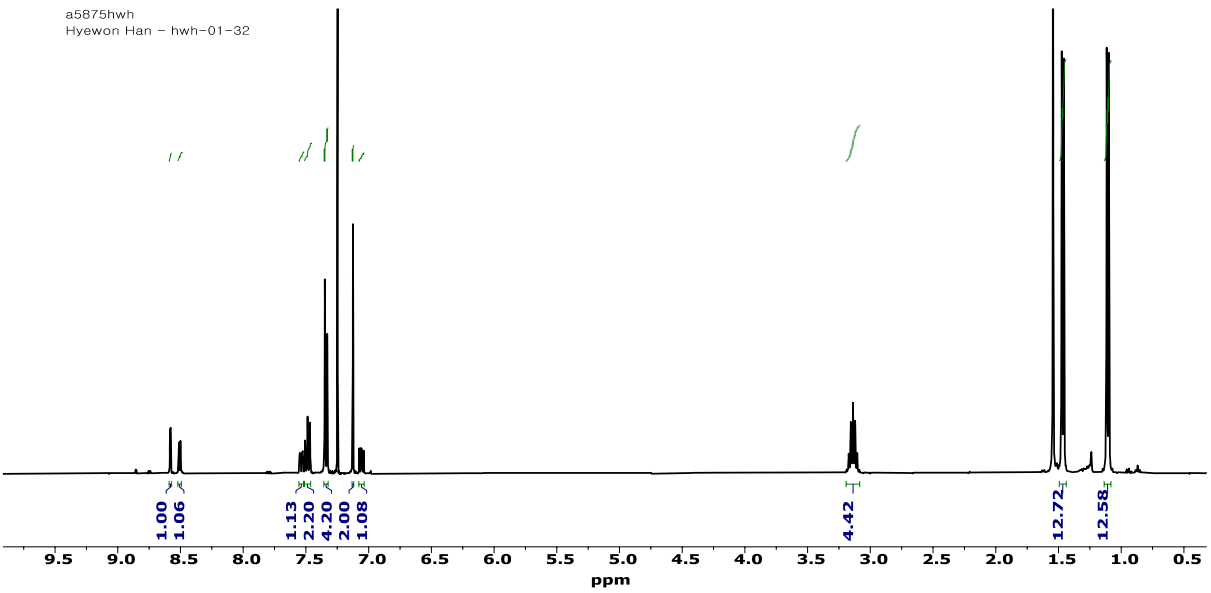


Figure 40. $^{1}$H NMR spectrum (400MHz, 32scans, Chloroform-*d*) of ***P1***

### *5.3.2 P2*

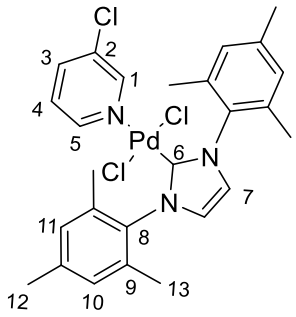


NHC precursor: 1,3-bis(mesityl)imidazolium chloride. Pale yellow solid (0.11 g, 30.86 %)$^{1}$H NMR (400 MHz, chloroform-*d*) δ 8.61– 8.58 (d, *J* = 2.3 Hz, 1H, H1), 8.51 – 8.48 (dd, *J* = 5.5, 1.0 Hz, 1H, H5), 7.59 - 7.54 (ddd, *J* = 8.2, 1.0, 1.4 Hz, 1H, H3), 7.2 - 7.18 (m, 1H, H4), 7.08 (s, 2H, H7) 7.07 (s, 4H, H10), 2.40 – 2.33 (s, 6H,H12), 2.43 – 2.30 (s, 12H, H13) ppm. ESI+ m/z: 597.0525 (Expect mass: 593.04)

*Lab book reference number*: hwh-01-17, hwh-01-34

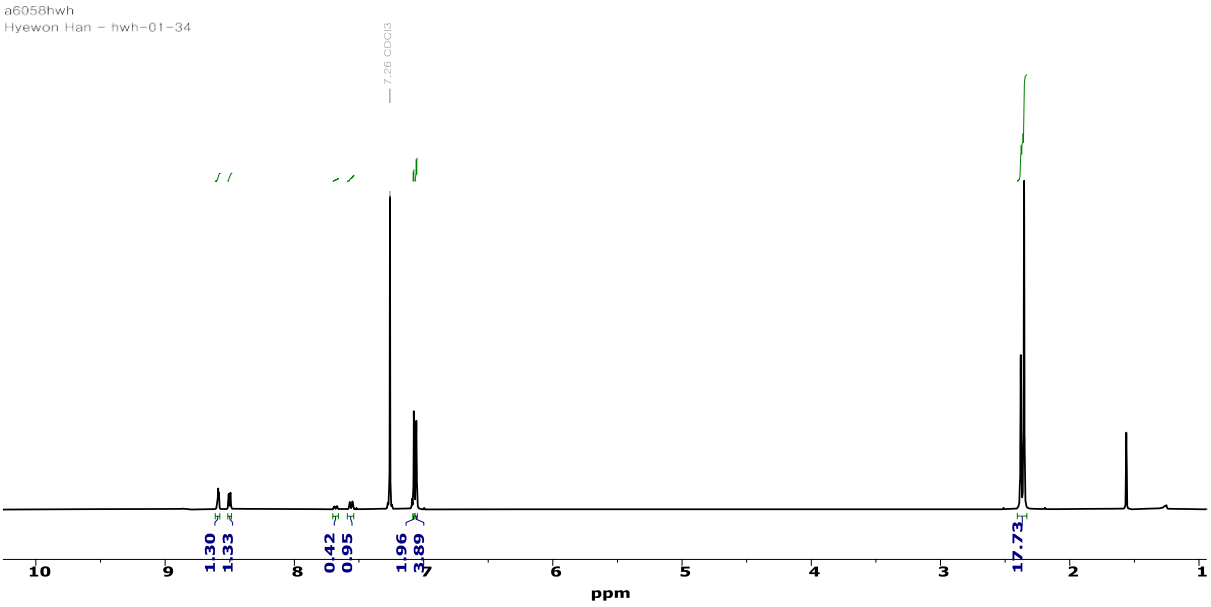


Figure 41. $^{1}$H NMR spectrum (400MHz, 32 scans, Chloroform-*d*) of ***P2*** and 1.56 ppm showed $CDCl_3$.

### *5.3.3 P3*

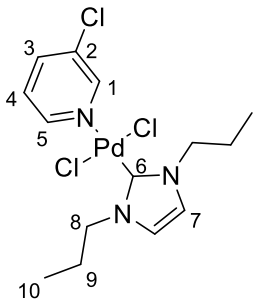


NHC precursor: 1,3-dipropylimidazolium chloride Pale yellow solid (0.041g, 16.6 %) $^{1}$H NMR (400 MHz, chloroform-*d*) δ 9.07 (d, *J* = 2.3 Hz, 1H, H1), 8.97 (dd, *J* = 5.5, 0.9 Hz, 1H, H5), 7.79 – 7.75 (m, 1H, H3), 7.32 (dt, *J* = 10.0, 5.0 Hz, 1H, H4), 6.93 (s, 2H, H7), 4.56 – 4.45 (m, 4H, H8), 2.16 – 2.07 (m, 4H, H9), 1.06 (t, *J* = 7.4 Hz, 6H,H10) ppm. $^{13}$C NMR (126 MHz, chloroform-*d*) δ 136.70 (CH), 122.62 (CH), 104.92 (CH), 99.82
(CCl), 98.86 (CH), 89.12 (CH), 51.29 ($CH_2$), 23.55 ($CH_2$), 10.66 ($CH_3$) ppm. ESI+ m/z: 444.9896 (Expect mass: 440.98)

Lab book reference number: hwh-01-30

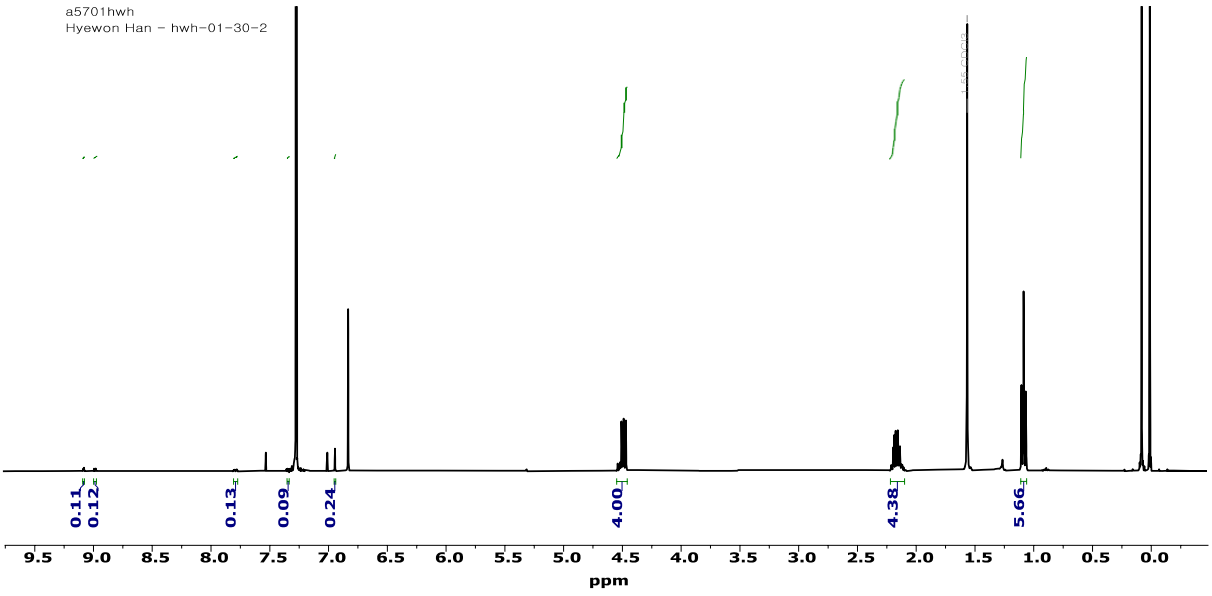


Figure 42. $^{1}$H NMR (400 MHz, 32 scans, Chloroform-*d*) of ***P3*** and unknown chemical impurities in 6.81 ppm and hexane in 0.06 ppm.

### 5.3.4 Synthesis of BAC-PEPPSI complex (*P4*) – novel complex

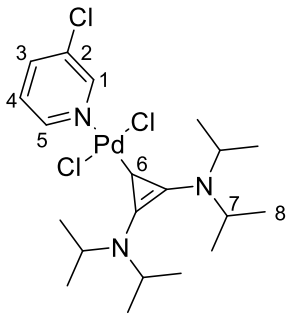


BAC precursor: bis(diisopropylamino)cyclopropenylidene. *Difference*: Washed through silica plug (20 cm) twice until to get yellow liquid. (0.1409g, 31.7 %) $^{1}$H NMR (600 MHz, Chloroform- *d*) δ 9.08 (d, 1H), 9.00 – 8.96 (d, 1H), 8.88 (d, 1H), 8.78 – 8.74 (d, 1H), 7.74 – 7.69 (m, 1H), 7.29 – 7.26 (d, 1H), 3.94 – 3.74 (s, 4H), 1.95 – 1.04 (d, 35H). $^{13}$C NMR (101 MHz, Chloroform- *d*) δ 150.44 (C), 149.44 (CH), 140.11 (CH), 137.70 (C), 132.47 (C), 124.66 (CH), 111.66 (CH), 23.32 - 20.89 ($CH_3$) ESI+ m/z: 529.0836 (Expect mass: 528.28). melting point: 225 ℃

*Lab book reference number*: hwh-01-40

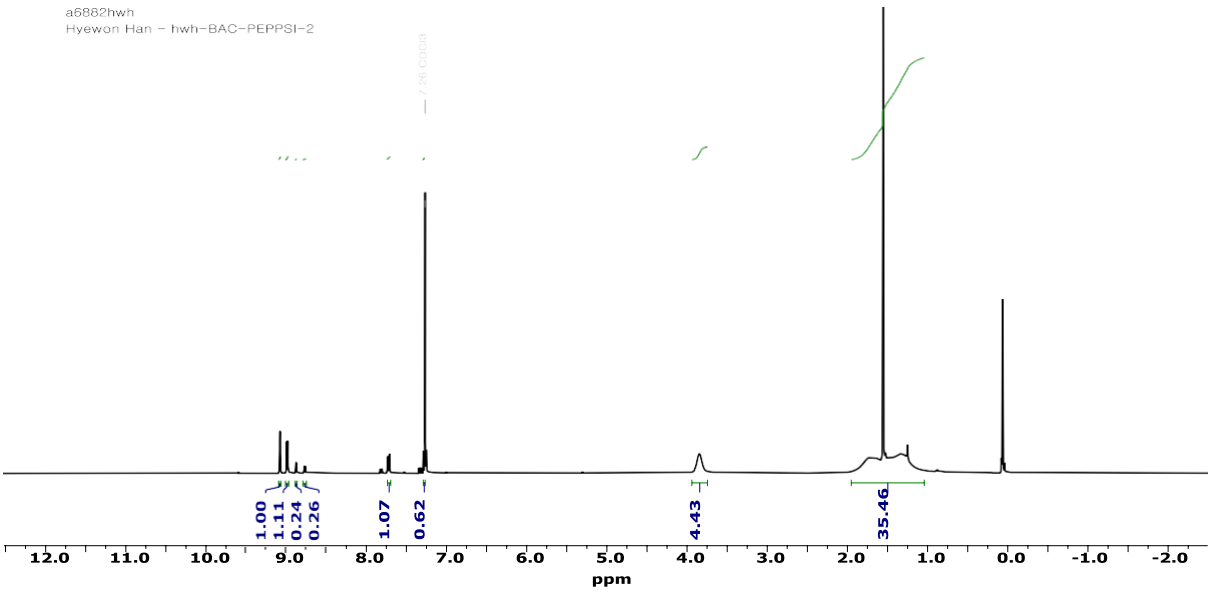


Figure 43. $^{1}$H NMR spectrum (600 MHz, 256 scans, Chloroform-*d*) of ***P4*** and by rotation of isopropyl group signal showed broad and inaccurate peak.

## 5.4 Synthesis of Coulson-cluster

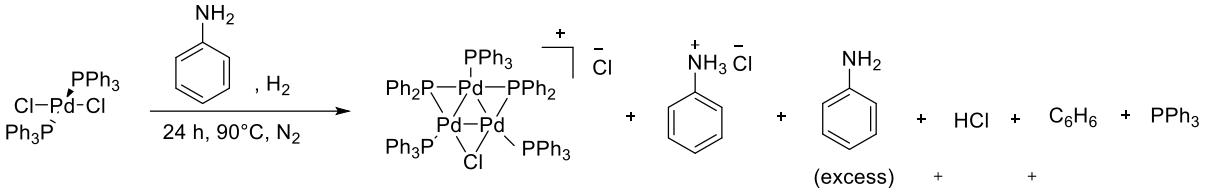


An oven-dried Schlenk flask equipped with *trans*-$PdCl_2(PPh_3)_2$ (1.76 g, 1.78 mol) was added and evacuated and backfilled with $N_2$*3 and colourless pure aniline (35.25 ml) was carefully added to the flask (when handling aniline should wear Marigold gloves!) and heated up to 90℃ over 15 minutes. (Homogenous orange solution) At this point, for exposing the flask with $H_2$ balloons, the headspace of the flask was carefully and quickly evacuated*2 and $H_2$ balloon was inserted into the flask. (colour was changed to dark red solution after 20-30 minutes).

Work up.

: After reaction complete the $H_2$ balloon was removed, and the flask was cooling down to room temperature. Preparing oven-dried distillation glassware and evacuated and backfilled*3 and the mixture was shortly transferred to a vacuum distillation glassware (round bottom flask part). After distillation, the residue of crude red solid washed with (dried, degassed) $Et_2O$ (3*14 ml) under $N_2$ and extracted with (dried and degassed) benzene (4*14 ml) and wait for 20 minutes to see some salts and if its confirmed salts do cannula filteration. After cannula filteration, the residue of benzene liquid was eliminated by vacuum and do recrystallization with $CH_2Cl_2$/Hexane (1:4) (7 ml: 28 ml). Dark red solid (0.178 g, 34.5 %) $^1$H NMR (600 MHz, $CD_2Cl_2$) δ 7.39-7.34 (tt, *J* = 7.4, 6H, *para*-B), 7.33-7.26 (t, 4H, *para*-X), 7.19 – 7.11 (tt, 12H, *ortho*-B), 7.11-6.95 (m, 23H, 12H-*meta*-B, 8H-*ortho*-X, and 3H-para-A), 6.78-6.73 (m, 6H, *ortho*-A), 6.73-6.66 (q, 8H, *meta*-X) 6.58-6.52 (m, 6H, *meta*-A). $^{31}$P NMR (203 MHz, $CD_2Cl_2$: δ 221.7-221.2 (td, $2PPh_2$, 1), 19.1- 18.2 (dt, $2PPh_3$, 2), 12.4-11.2 (tt, $PPh_3$, 3).

*Lab book reference number*: hwh-01-70

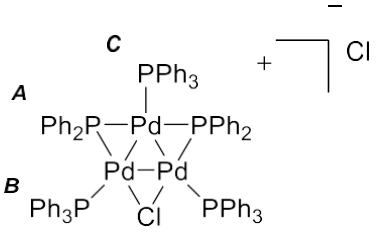

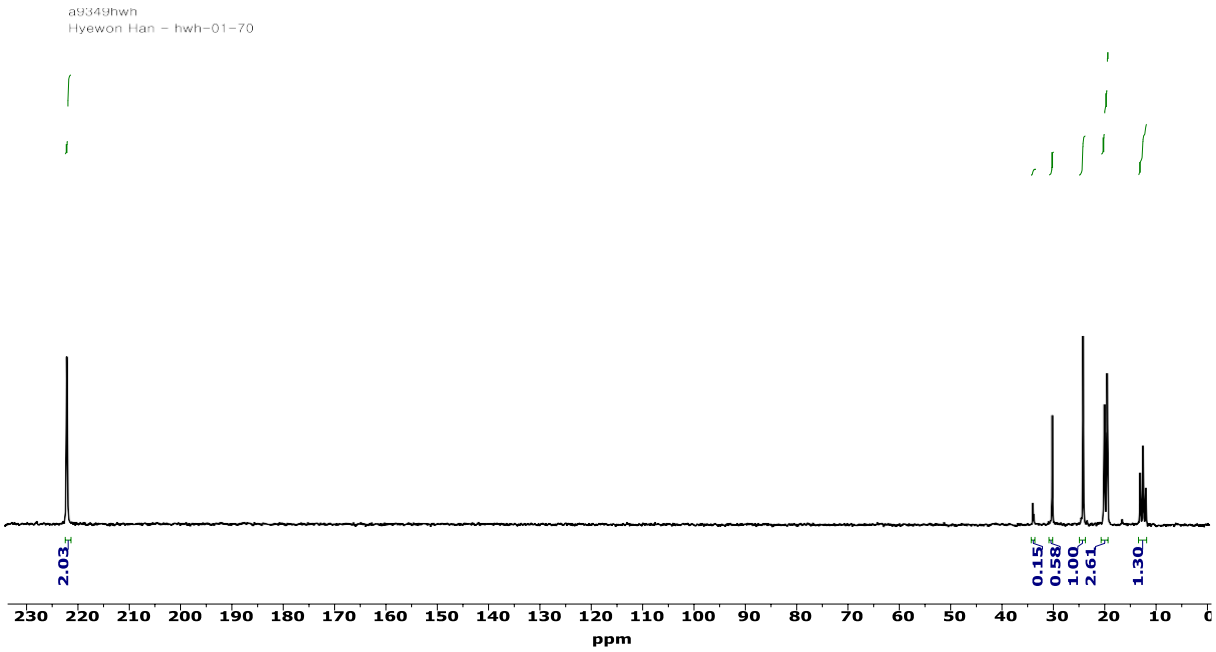


Figure 44. $^{31}P$ NMR spectrum (600 MHz, 256 scans, $CD_2Cl_2$) of Coulson cluster and δ 34, 30.5, 24.5 ppm showed impurities of crude liquid which combined with aniline after filtration.

### 5.4.2 Substitution of Coulson cluster with BAC ligands.

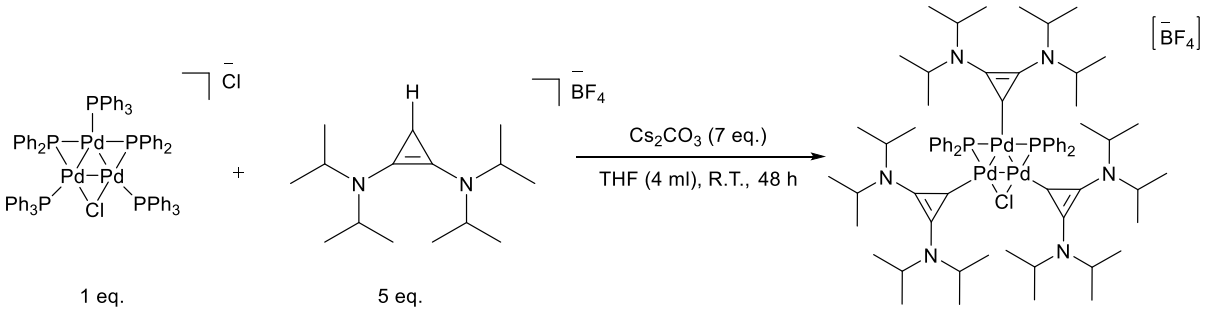


An oven-dried Schlenk flask equipped with Coulsen-cluster (30.95 mg, 0.02 mmol, 1 eq.), BAC (45.53 mg, 0.1 mmol, 5 eq.), $Cs_2CO_3$ (45.62mg, 0.14 mmol, 7 eq.) was evacuated and backfilled *3 under $N_2$ and added THF (degassed, 4 ml) via a syringe and stirred for 16 h at room temperature. After completing the reaction, vac off the solvent and do recrystallization with $CH_2Cl_2$/Hex (1:4 v v). Yielded solid was too small quantity and not measurable. $^{31}P$ NMR (203 MHz, $CD_2Cl_2$: δ 193.36 (td, $2PPh_2$). MALDI m/z: 1435.46538 (Expect mass: 1436.31)

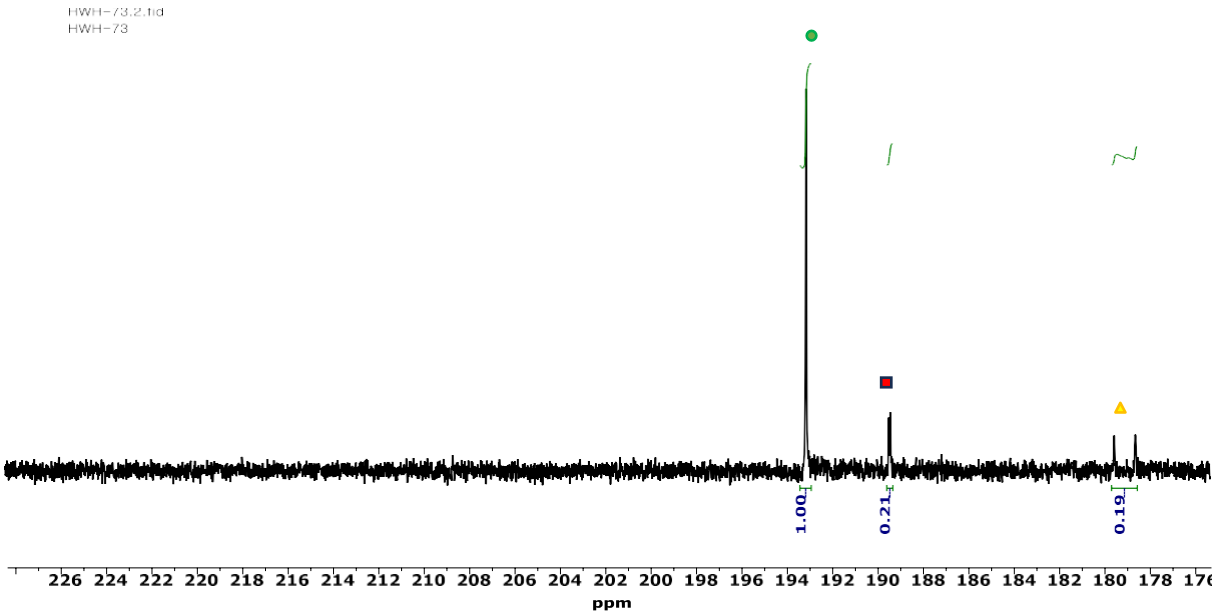


Figure 45. $^{31}P$ NMR (203 MHz, 256 scans, $CD_2Cl_2$) of $[Pd_3(\mu\text{-}Cl)(\mu\text{-}PPh_2)_2(BAC_3)[Cl]$ in $CD_2Cl_2$ and other peaks showed di-substitution of Coulson cluster and mono-substitution of Coulson cluster.

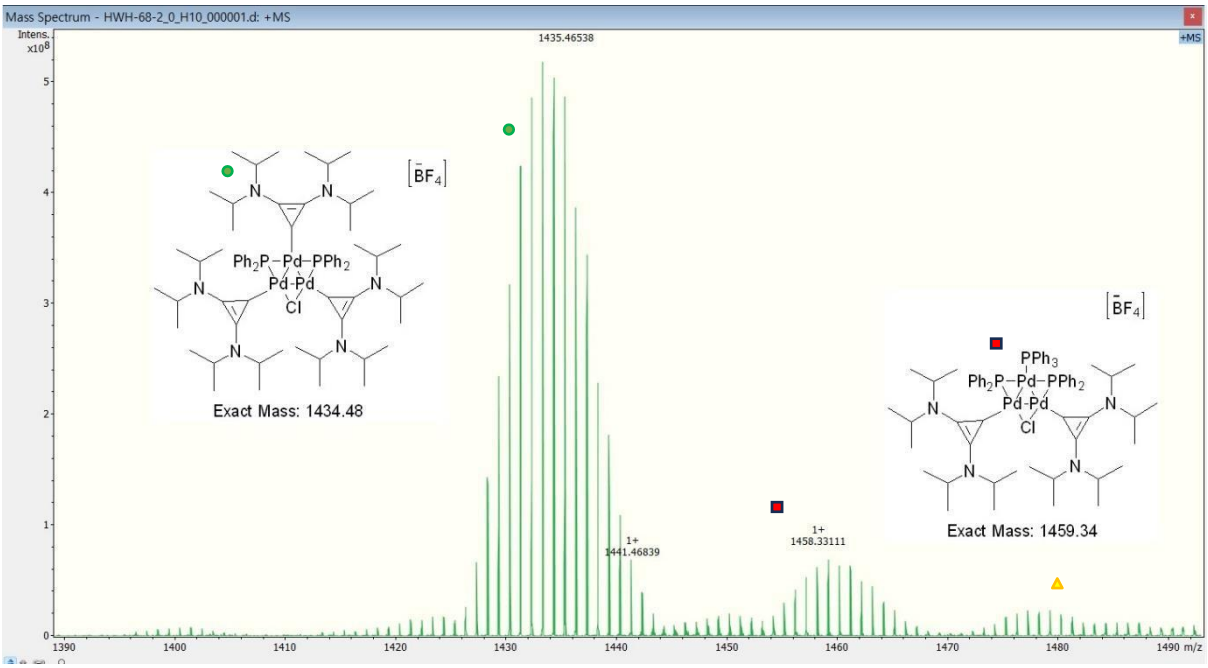


Figure 46. MALDI-MS spectrum showed tri-substitution of Coulson cluster and di-substitution and mono-substitution of Coulson cluster signal peaks.

## 5.5 Synthesis of di-μ-(4-bromo-pyrid-2-yl)-kN:kC*2*-bis[bromomesityl-NHC palladium(II)]

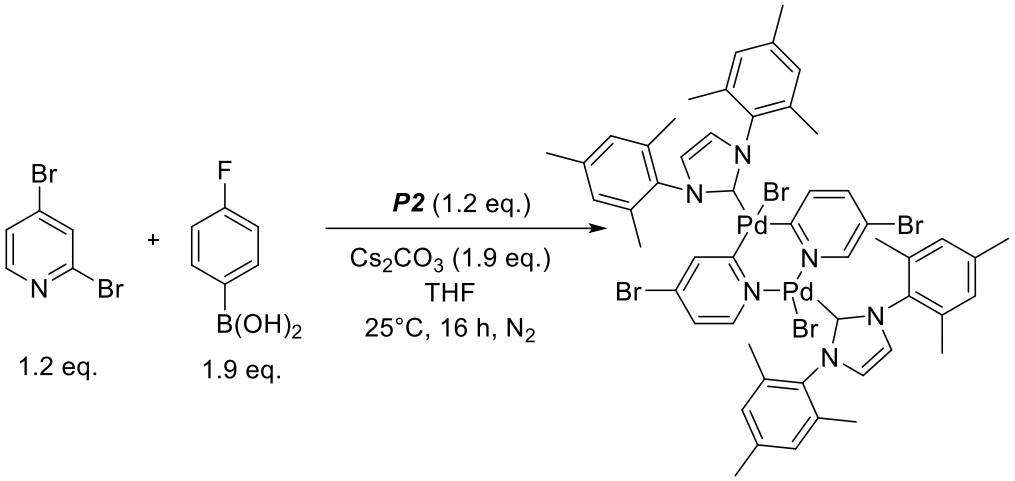


An oven-dried Schlenk flask equipped with ***P2*** (191.82 mg, 0.32 mmol), 2,4-dibromopyridine (76 mg, 0.32 mmol), *p*-flurophenylboronic acid (70.8 mg, 0.51 mmol), $Cs_2CO_3$ (166.17 mg, 0.51 mmol) was evacuated and backfilled*3 with $N_2$. The reaction mixture stirred for overnight at 30 ℃, $N_2$ and check $^1H$, $^{13}C$ NMR and MS. Do crystallization with (degassed) $CH_2Cl_2$/Hexane (1:4). → Failed and $^1H$, $^{13}C$ NMR, MALDI-MS spectrum showed unmatched with the expected structure.

## 5.6 Benchmark (Pd pre-catalyst refined) conditions

In an silicon-capped vial, equipped with magnetic bead was charged with Pd catalyst (0.025 mmol), *p*-fluorophenylboronic acid (167 mg, 1.20 mmol), 2,4-dibromopyridine (236.89, 1.00 mmol) and caesium carbonate (650 mg, 2.00 mmol) and 1,3,5-trimethoxybenzene (168 mg, 1.00 mmol) was evacuated and backfilled with nitrogen (x 3). Degassed 1,4-dioxane/$H_2O$ (1:1, 2.5 ml) was added to the reaction vial. The reaction mixture was stirred at the reaction temperature for 5 hours. Samples (100 μL) were taken at t = 3, 5, 10, 20, 30, 40, 50, 60, 90, 120, 150, 180, 240, 300, 420 mins. Each sample was quenched in $CH_2Cl_2$ (2 ml) then passed over a Celite® plug (~1 cm). The solvent was removed under reduced pressure and the residue dissolved in chloroform-*d* and analysed by $^1H$ and $^{19}F$ NMR spectroscopy.

### 5.6.1 General procedure for time course reactions using 2,4-dichloropyridine

In an silicon-capped vial, equipped with magnetic bead was charged with Pd catalyst (0.025 mmol), *p*-fluorophenylboronic acid (167 mg, 1.20 mmol), and caesium carbonate (650 mg, 2.00 mmol) and 1,3,5-trimethoxybenzene (168 mg, 1.00 mmol) was evacuated and backfilled with nitrogen (x 3). Degassed 1,4-dioxane/$H_2O$ (1:1, 2.5 ml) and 2,4-dichloropyridine (0. 11 ml, 1.00 mmol) were added to the reaction vial. The reaction mixture was stirred at the reaction temperature for 5 hours. Samples (100 µL) were taken at t = 3, 5, 10, 20, 30, 40, 50, 60, 90, 120, 150, 180, 240, 300, 420 mins. Each sample was quenched in $CH_2Cl_2$ (2 ml) then passed over a Celite® plug (~1 cm). The solvent was removed under reduced pressure and the residue dissolved in chloroform-*d* and analysed by $^{1}H$ and $^{19}F$ NMR spectroscopy.

### 5.6.2 General procedure for time course reactions {with $Pd(OAc)_2/PPh_3$}

In an silicon-capped vial, equipped with magnetic bead was charged with Pd catalyst (0.025 mmol), *p*-fluorophenylboronic acid (167 mg, 1.20 mmol), 2,4-dibromopyridine (236.89, 1.00 mmol) or 2,4-dichloropyridine (0.11 ml, 1.00 mmol) and caesium carbonate (650 mg, 2.00 mmol) and 1,3,5-trimethoxybenzene (168 mg, 1.00 mmol) was evacuated and backfilled with nitrogen (x 3). Degassed 1,4-dioxane/$H_2O$ (1:1, 2.5 ml) was added to the reaction vial. The reaction mixture was stirred at the reaction temperature for 5 hours. Samples (100 µL) were taken at t = 3, 5, 10, 30, 60, 90, 120, 210, 300 mins. Each sample was quenched in $CH_2Cl_2$ (2 ml) then passed over a Celite® plug (~1 cm). The solvent was removed under reduced pressure and the residue dissolved in chloroform-*d* and analysed by $^{1}H$ and $^{19}F$ NMR spectroscopy.

### 5.6.3 Sampling of catalytic reactions

Reaction samples (100 µL) taken using a microsyringe were rapidly quenched by dissolution in $CH_2Cl_2$ and filtered through a pipette filled with a celite plug (~1cm). After filtration, samples removed solvent under reduced pressure and the residue was dissolved in chloroform-*d* (0.5 ml) for NMR spectroscopy.

## 5.7 General procedure for time course reactions – MALDI-MS

In an silicon-capped vial, equipped with magnetic bead was charged with Pd catalyst (0.025 mmol), *p*-fluorophenylboronic acid (167 mg, 1.20 mmol), 2,4-dibromopyridine (236.89, 1.00 mmol) or 2,4-dichloropyridine (0.11 ml, 1.00 mmol) and caesium carbonate (650 mg, 2.00 mmol) and 1,3,5-trimethoxybenzene (168 mg, 1.00 mmol) was evacuated and backfilled with nitrogen (x 3). Degassed 1,4-dioxane/$H_2O$ (1:1, 2.5 ml) was added to the reaction vial. The reaction mixture was stirred at the reaction temperature for 5 hours. Samples (40 µL) were taken at t = 60, 180, 300, 1440 mins. Each sample was quenched in $CH_2Cl_2$ (10 ml) then passed over a Celite® plug (~1 cm). Samples analysed by MALDI-MS with matrix solvent.

# Appendix

## MS spectra of the Compounds (MALDI-MS)

***1.*** **Catalytic reaction of 2,4-dibromopyridine and *p*-fluorophenylboronic acid with *P3.***

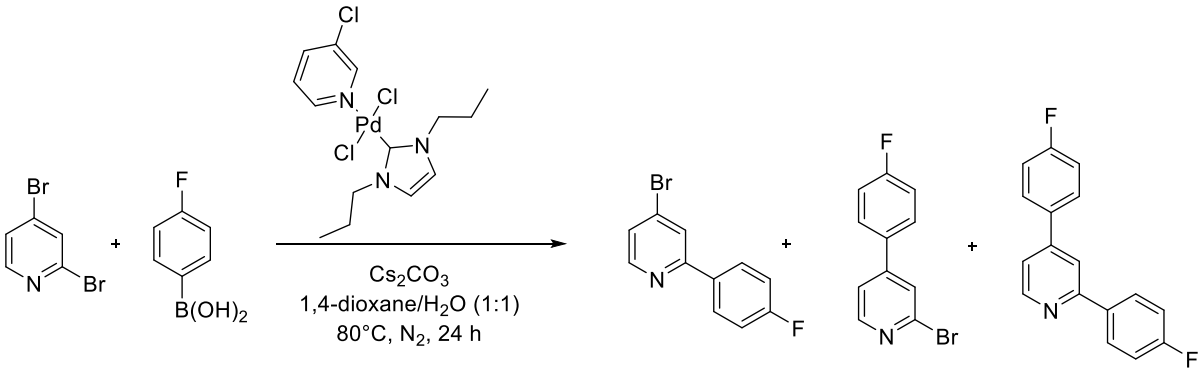


**Scheme 53.** Catalytic reaction of 2,4-dibromopyridine or 2,4-dichloropyridine and *p*-fluorophenylboronic acid with ***P3*** and analysed by MALDI-MS.

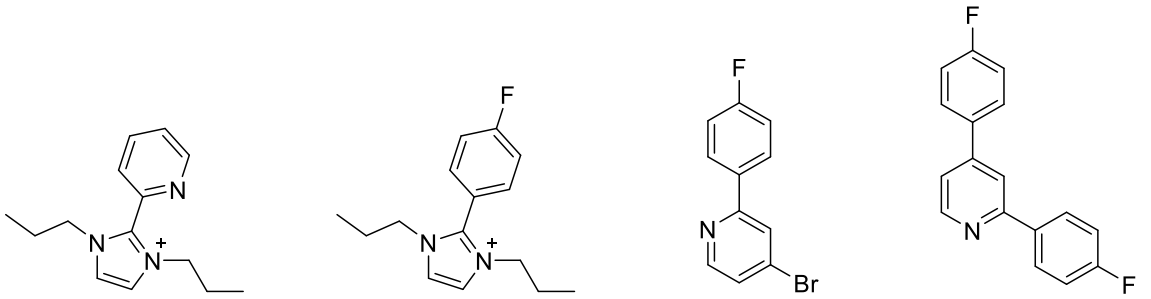


Figure 47. Imidazolium species and mono-arylated and 2,4-arylated products confirmed by MALDI-MS.

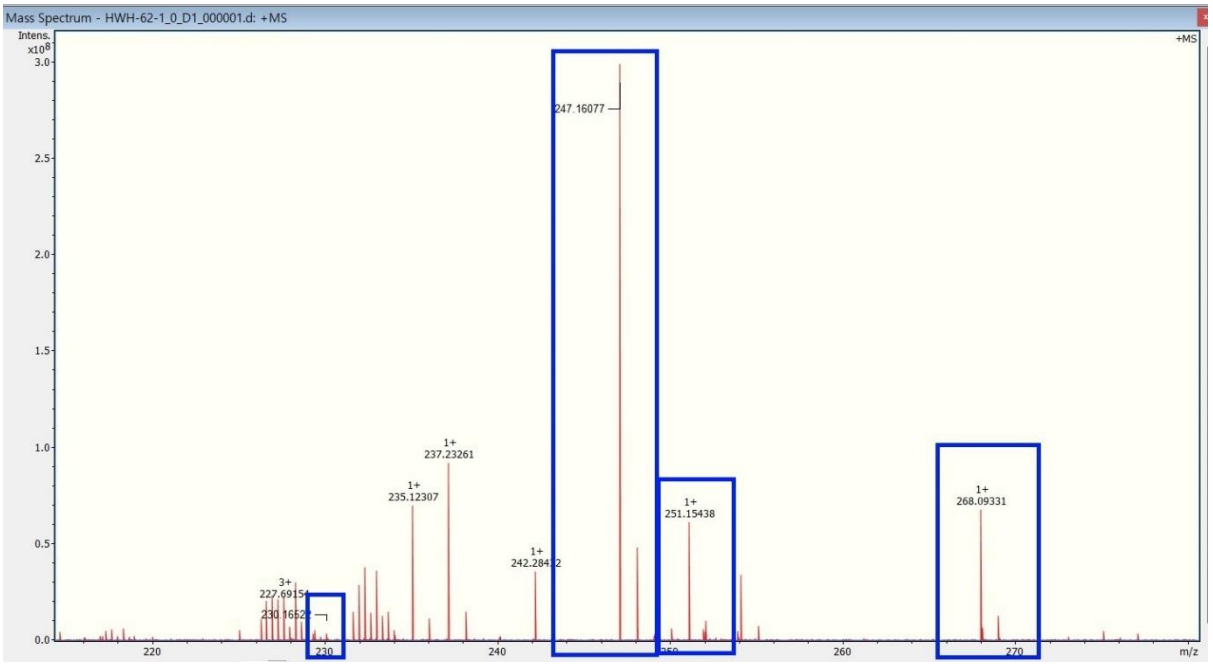


Figure 48. The 2,4-Ar and NHC-arylated species shown at the first an hour. The others shown at the first 5 hours.

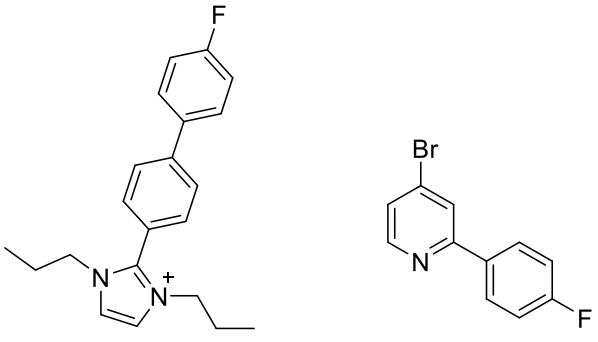


Figure 49. Mono-arylated product (2-Ar or 4-Ar) and imidazolium species confirmed by MALDI-MS.

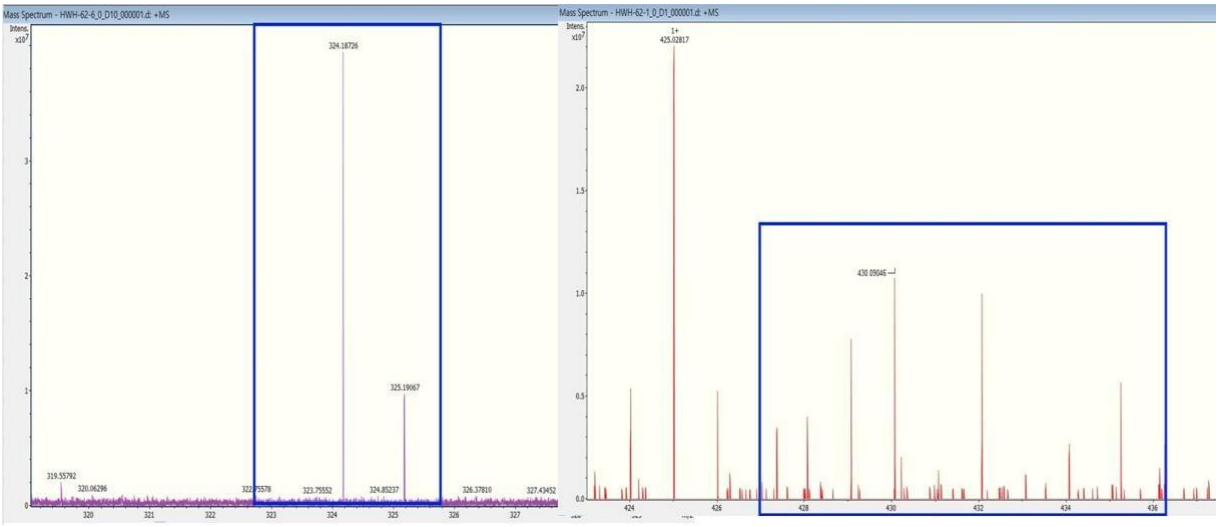


Figure 50. The mono-arylated product and imidazolium species shown at the first 5 hours.

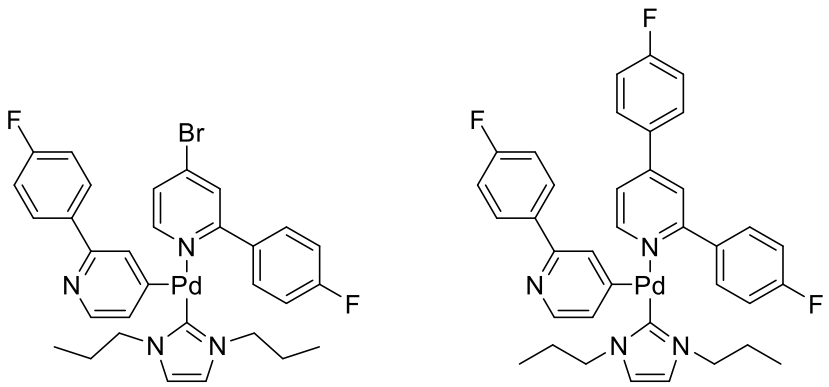


Exact Mass: 681.07 Exact Mass: 697.18

Figure 51. Imidazolium species confirmed by MALDI-MS.

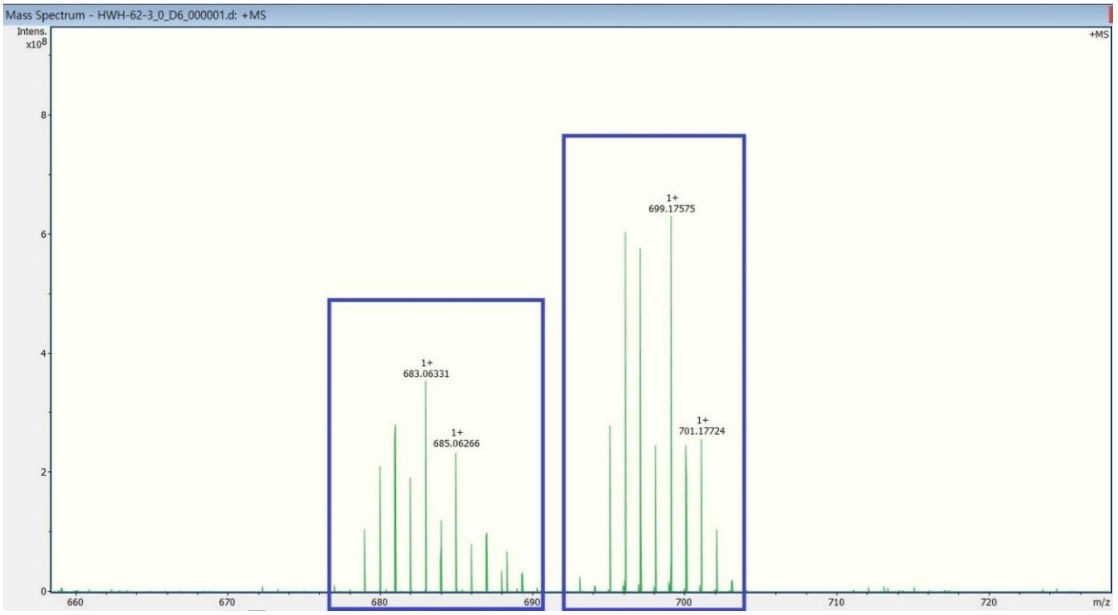


Figure 52. Two imidazolium species shown at the first 3 hours.

### *2.* Catalytic reaction of 2,4-dibromopyridine and *p*-fluorophenylboronic acid with *P1.*

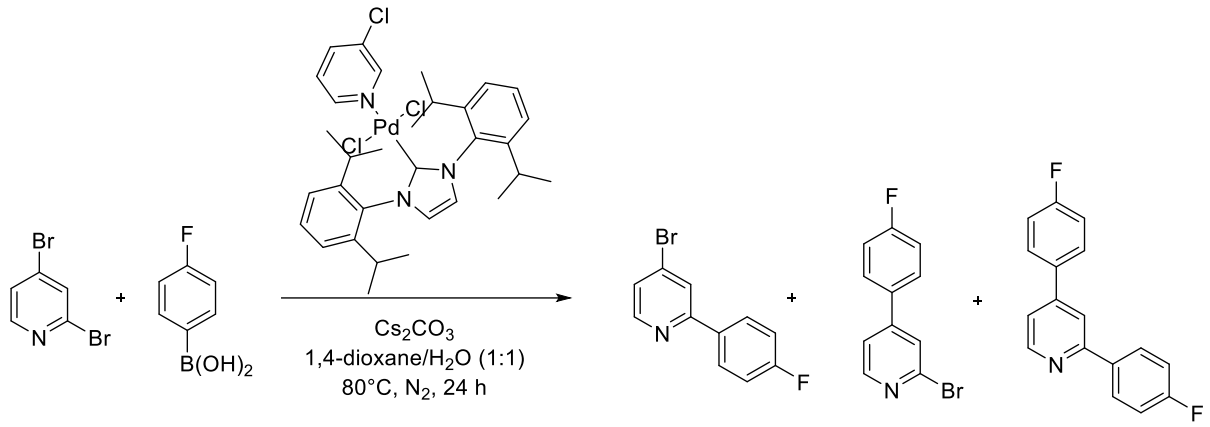


Scheme 54. Catalytic reaction of 2,4-dibromopyridine and *p*-fluorophenylboronic acid with ***P3*** and analyse by MALDI-MS.

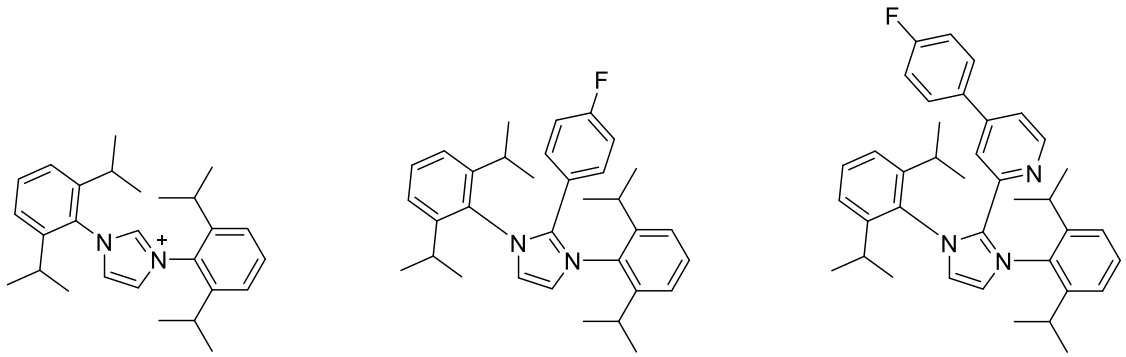


Exact Mass: 389.30 Exact Mass: 483.32 Exact Mass: 560.34

Figure 53. Imidazolium species confirmed by MALDI-MS.

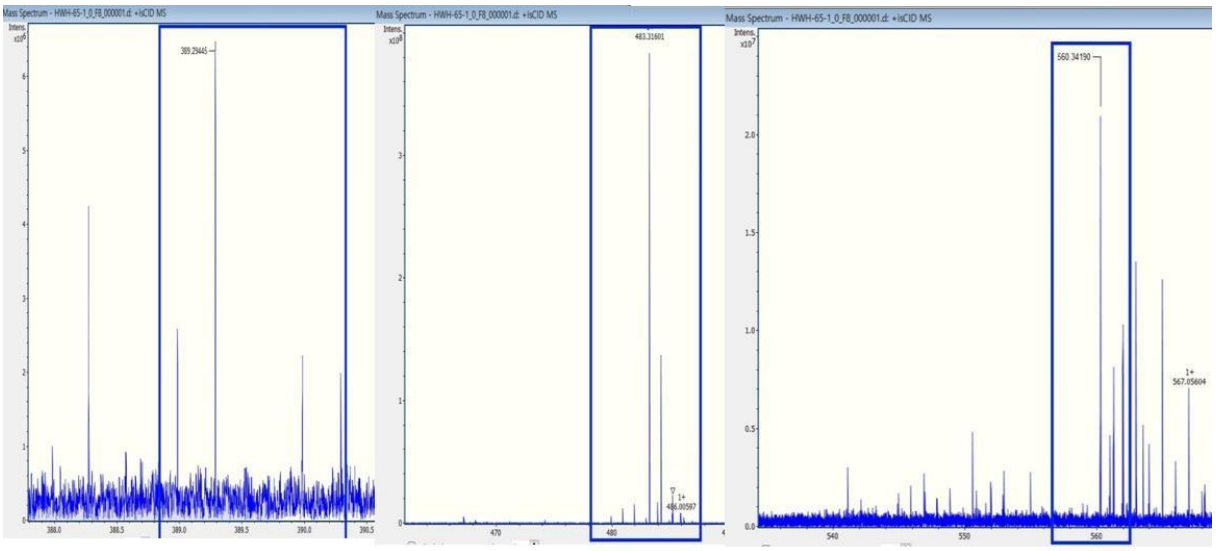

Figure 54. The two imidazolium species shown at the first 5 hours and the imidazolium chloride (NHC) shown until end of the reaction.

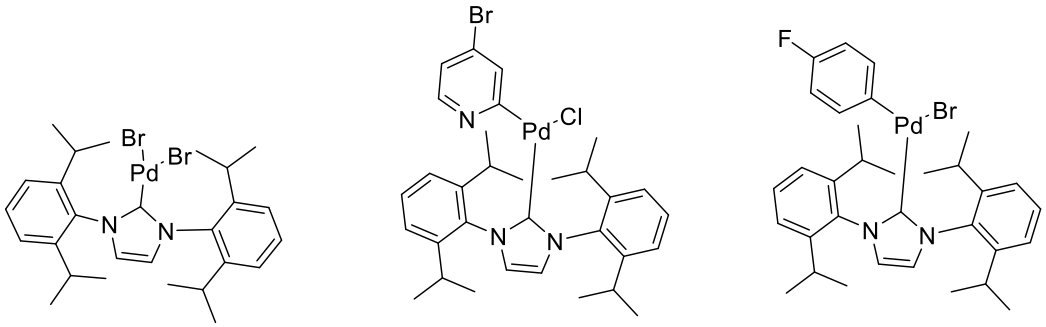


Figure 55. Imidazolium species confirmed by MALDI-MS.

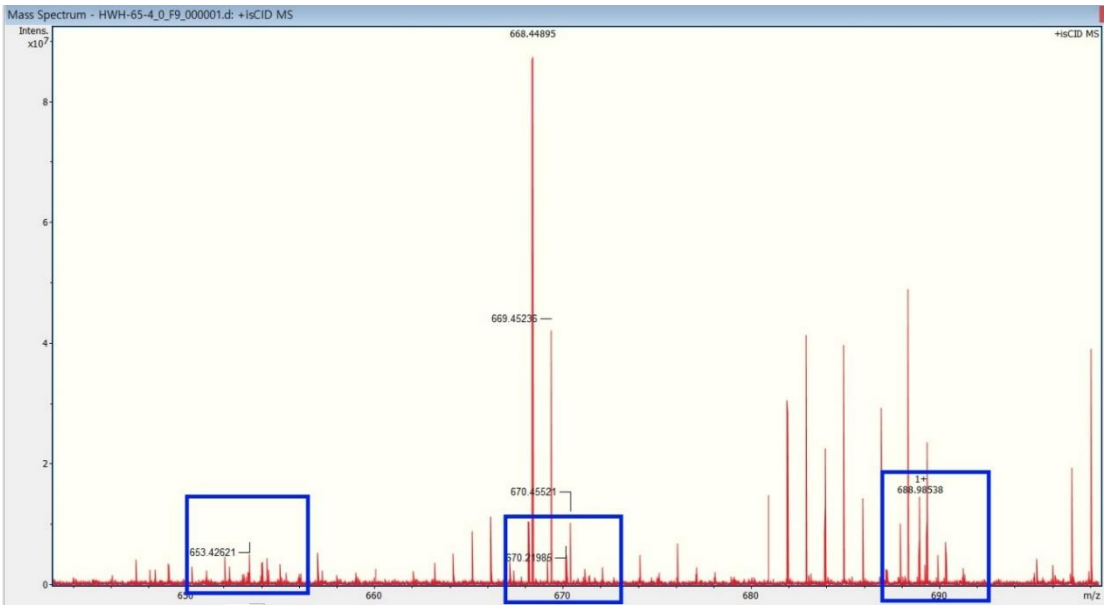


Figure 56. All the imidazolium species in figure 54 signals shown at the 5 hours.

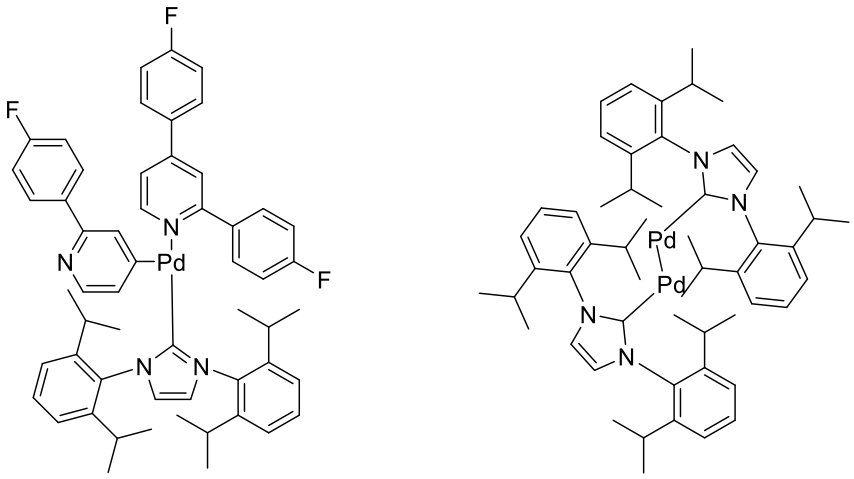


Figure 57. Pd-imidazolium species confirmed by MALDI-MS.

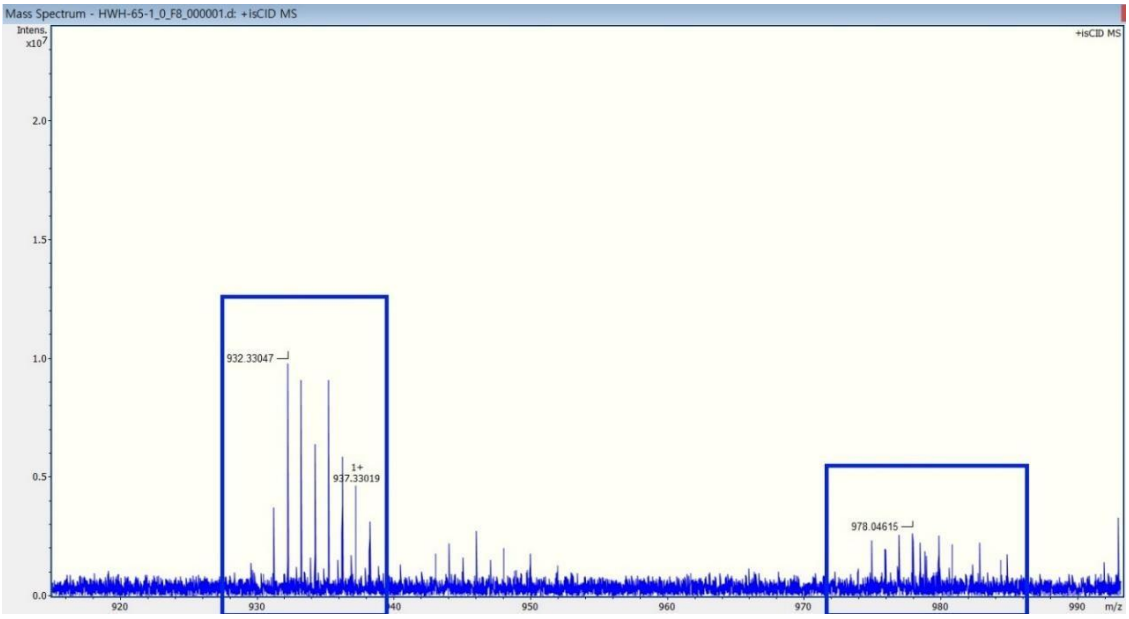


Figure 58. The Pd-imidazolium species shown at the first 10 minutes and 2Pd-NHC species shown atthe 1-5 hours.

### 3. Catalytic reaction of 2,4-dichloropyridine and *p*-fluorophenylboronic acid with *P3*.

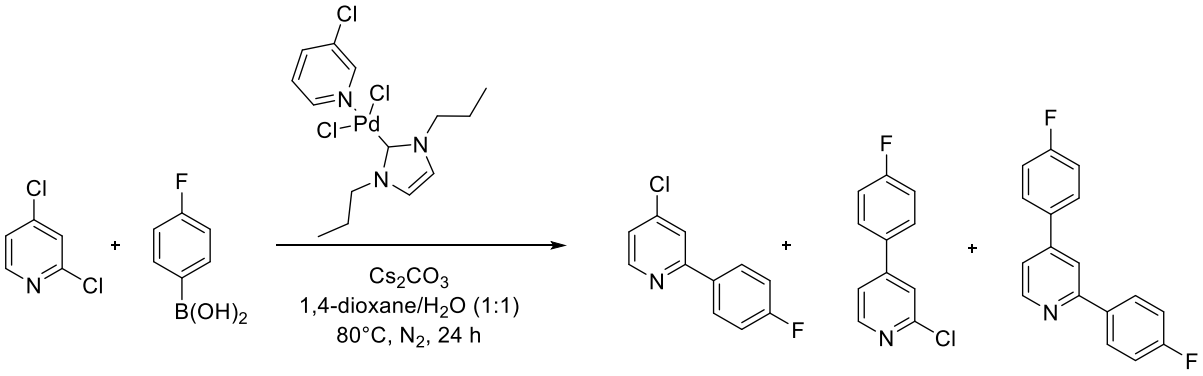


Scheme 55. Catalytic reaction of 2,4-dichloropyridine and *p*-fluorophenylboronic acid with ***P3*** and analysed by MALDI-MS.

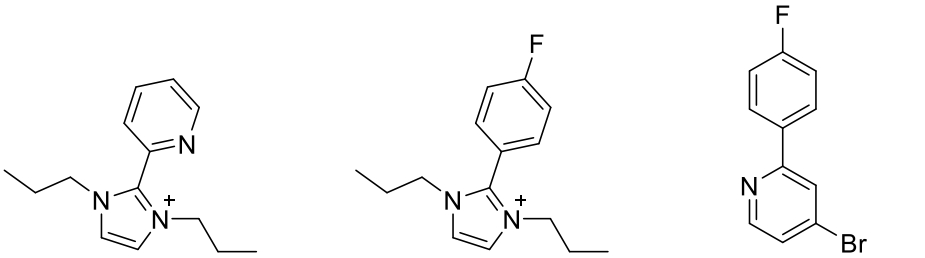


Exact Mass: 230.17 Exact Mass: 247.16 Exact Mass: 250.97

Figure 59. Three imidazolium species confirmed by MALDI-MS during the reaction.

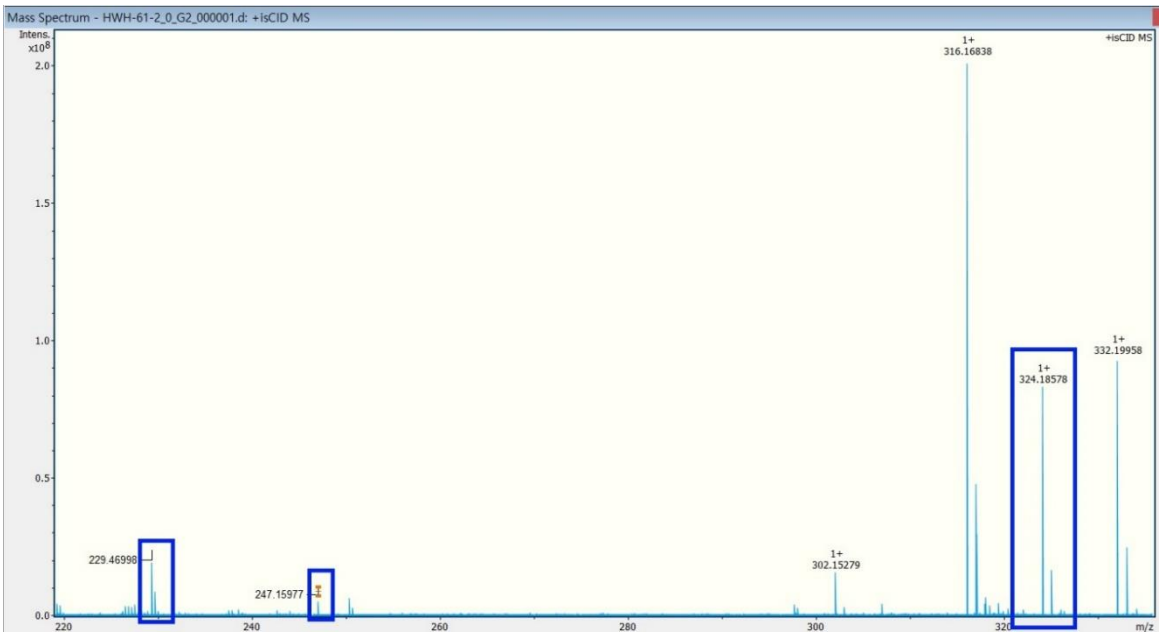


Figure 60. All of the imidazolium species signal in figure 58 shown during whole of the reaction.

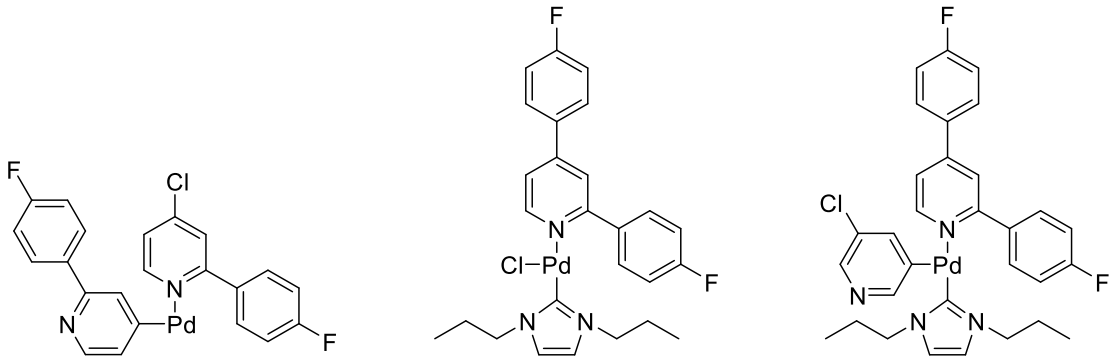


Exact Mass: 484.98 Exact Mass: 560.09 Exact Mass: 637.12

Figure 61. Pd species confirmed by MALDI-MS.

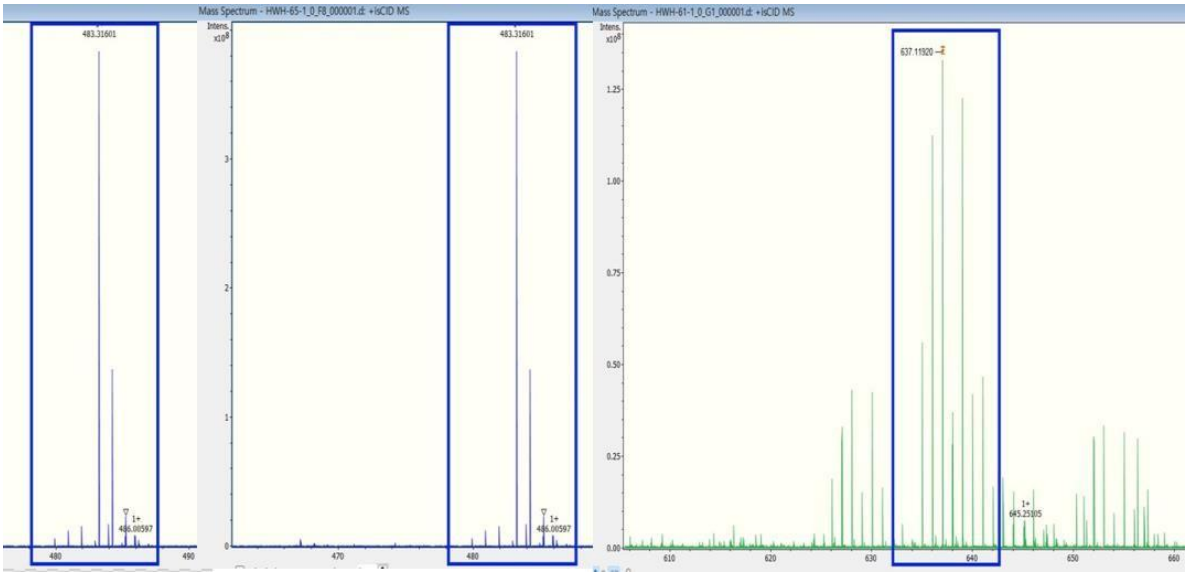


Figure 62. All the Pd species in figure 62 shown during the whole reaction.

**4. Catalytic reaction of 2,4-dichloropyridine and *p*-fluorophenylboronic acid with *P1*.**

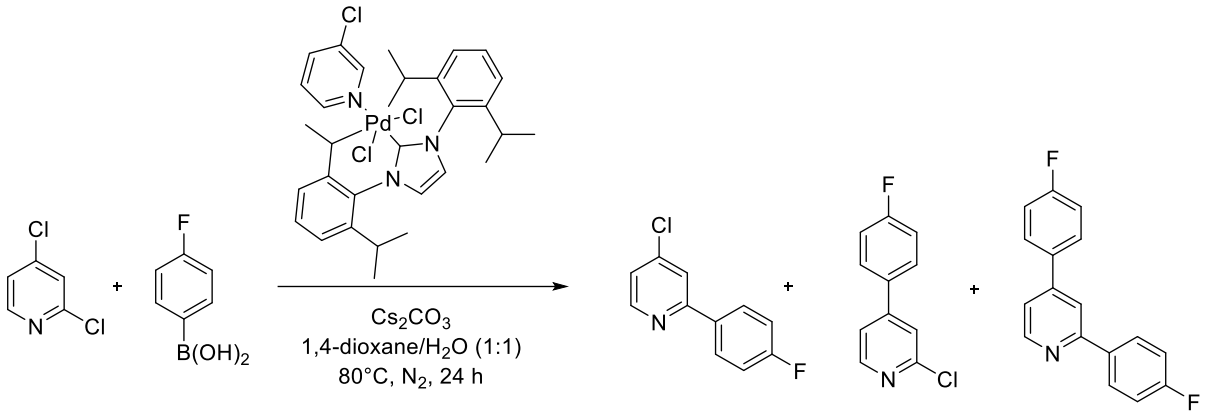


Scheme 56. Catalytic reaction of 2,4-dichloropyridine and *p*-fluorophenylboronic acid with ***P1*** and analysed by MALDI-MS.

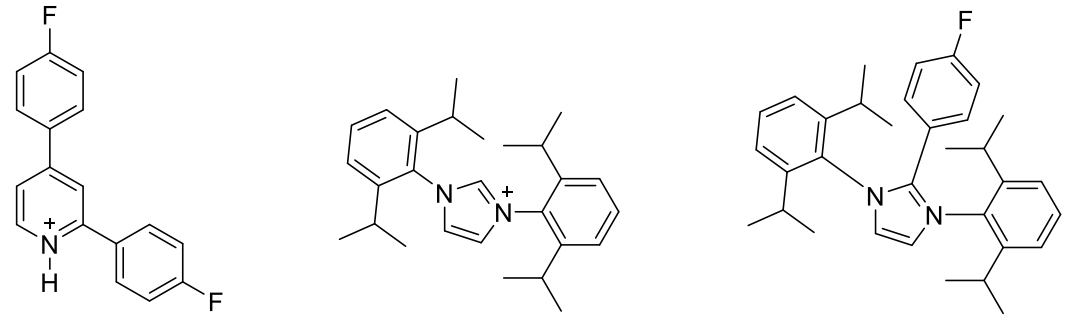


Exact Mass: 268.09 Exact Mass: 389.30 Exact Mass: 483.32

Figure 63. 2,4-Ar and Imidazolium species confirmed by MALDI-MS.

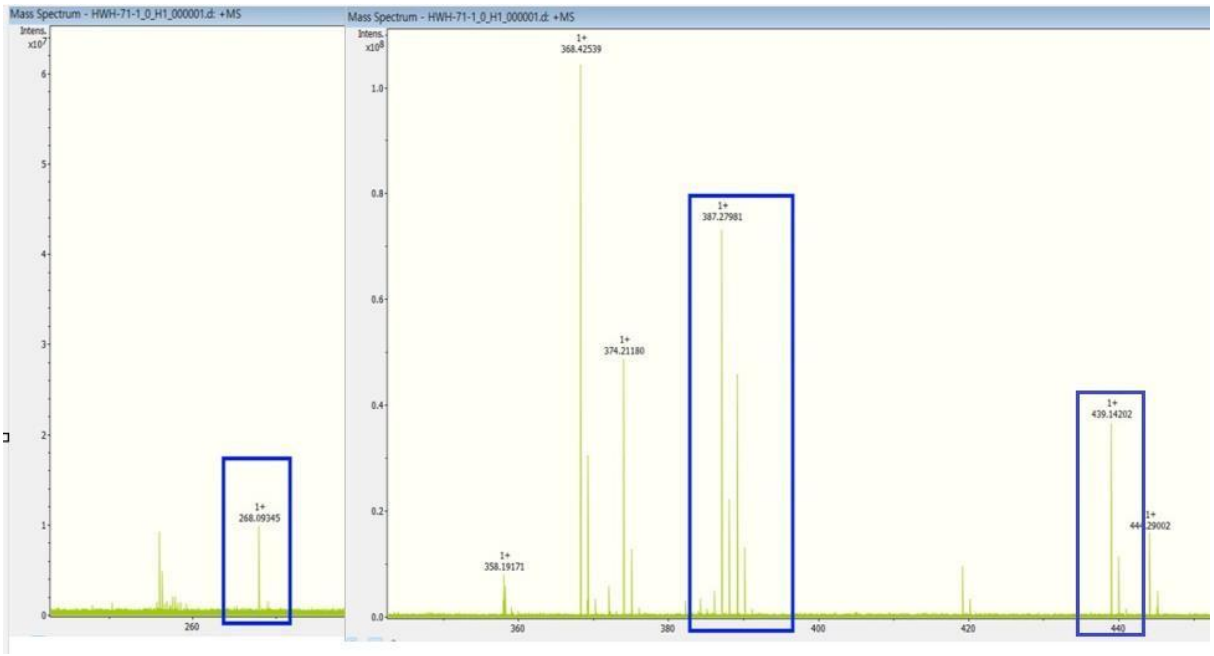

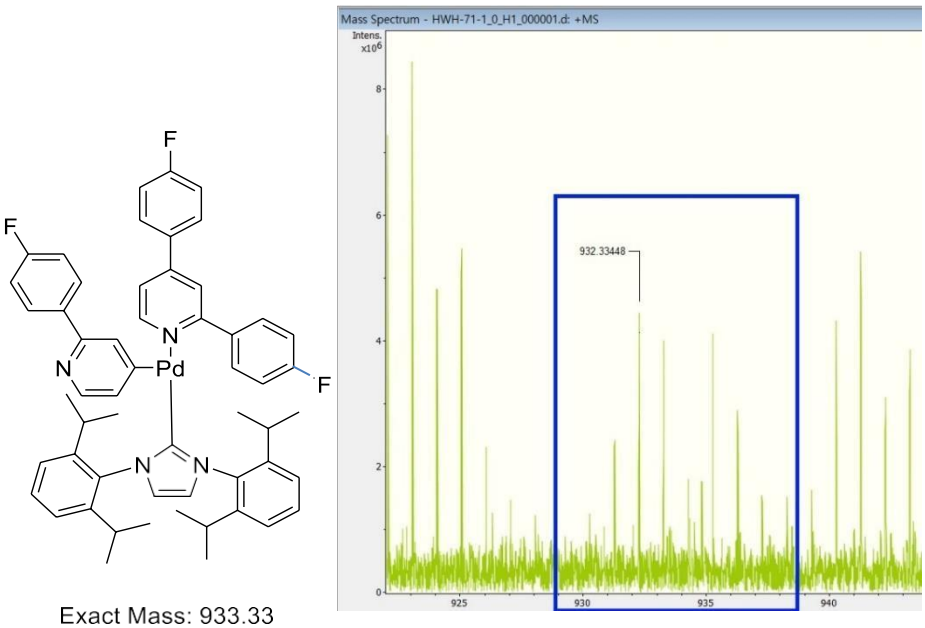


Exact Mass: 933.33

Figure 65. Pd species shown at the first 10 minutes.

## 5. SMCCs Data files

Han_209068340_NMR data_zipped files.zip

## *References*


(1) Gujral, S.; Khatri, S.; Riyal, P. Suzuki Cross Coupling Reaction-A Review. *Indo Glob. J. Pharm. Sci.* **2012**, *2*, 351–367. https://doi.org/10.35652/IGJPS.2012.41.

(2) Miyaura, N.; Yamada, K.; Suzuki, A. A New Stereospecific Cross-Coupling by the Palladium-Catalyzed Reaction of 1-Alkenylboranes with 1-Alkenyl or 1-Alkynyl Halides. *Tetrahedron Lett.* **1979**, *20* (36), 3437–3440. https://doi.org/10.1016/S0040-4039(01)95429-2.

(3) Suzuki, A. Recent Advances in the Cross-Coupling Reactions of Organoboron Derivatives with Organic Electrophiles, 1995–1998. *J. Organomet. Chem.* **1999**, *576* (1), 147–168. https://doi.org/10.1016/S0022-328X(98)01055-9.

(4) Han, F.-S. Transition-Metal-Catalyzed Suzuki–Miyaura Cross-Coupling Reactions: A Remarkable Advance from Palladium to Nickel Catalysts. *Chem. Soc. Rev.* **2013**, *42* (12), 5270–5298. https://doi.org/10.1039/C3CS35521G.

(5) Miyaura, Norio.; Suzuki, Akira. Palladium-Catalyzed Cross-Coupling Reactions of Organoboron Compounds. *Chem. Rev.* **1995**, *95* (7), 2457–2483. https://doi.org/10.1021/cr00039a007.

(6) Martin, R.; Buchwald, S. L. Palladium-Catalyzed Suzuki−Miyaura Cross-Coupling Reactions Employing Dialkylbiaryl Phosphine Ligands. *Acc. Chem. Res.* **2008**, *41* (11), 1461–1473. https://doi.org/10.1021/ar800036s.

(7) *An overview of N-heterocyclic carbenes | Nature*. https://www.nature.com/articles/nature13384 (accessed 2023-10-19).

(8) Marion, N.; Navarro, O.; Mei, J.; Stevens, E. D.; Scott, N. M.; Nolan, S. P. Modified (NHC)Pd(Allyl)Cl (NHC = N-Heterocyclic Carbene) Complexes for Room-Temperature Suzuki−Miyaura and Buchwald−Hartwig Reactions. *J. Am. Chem. Soc.* **2006**, *128* (12), 4101–4111. https://doi.org/10.1021/ja057704z.

(9) *A User-Friendly, All-Purpose Pd–NHC (NHC=N-Heterocyclic Carbene) Precatalyst for the Negishi Reaction: A Step Towards a Universal Cross-Coupling Catalyst - Organ - 2006 - Chemistry – A European Journal - Wiley Online Library*. https://chemistry-europe.onlinelibrary.wiley.com/doi/full/10.1002/chem.200600206 (accessed 2023-10-31).

(10) Herrmann, W. A. N-Heterocyclic Carbenes: A New Concept in Organometallic Catalysis. *Angew. Chem. Int. Ed.* **2002**, *41* (8), 1290–1309. https://doi.org/10.1002/1521-3773(20020415)41:8<1290::AID-ANIE1290>3.0.CO;2-Y.

(11) *Stable Carbenes | Chemical Reviews*. https://pubs.acs.org/doi/full/10.1021/cr940472u (accessed 2023-10-19).

(12) Arduengo, A. J.; Harlow, R. L.; Kline, M. A Stable Crystalline Carbene. *J. Am. Chem. Soc.* **1991**, *113* (1), 361–363. https://doi.org/10.1021/ja00001a054.

(13) Crabtree, R. H. NHC Ligands versus Cyclopentadienyls and Phosphines as Spectator Ligands in Organometallic Catalysis. *J. Organomet. Chem.* **2005**, *690* (24), 5451–5457. https://doi.org/10.1016/j.jorganchem.2005.07.099.

(14) Wheaton, C. A.; Bow, J.-P. J.; Stradiotto, M. New Phosphine-Functionalized NHC Ligands: Discovery of an Effective Catalyst for the Room-Temperature Amination of Aryl Chlorides with Primary and Secondary Amines. *Organometallics* **2013**, *32* (21), 6148–6161. https://doi.org/10.1021/om400684n.

(15) *Stability and reactivity of N-heterocyclic carbene complexes - ScienceDirect*. https://www.sciencedirect.com/science/article/pii/S0010854504001341 (accessed 2023-10-19).

(16) Breslow, R.; Haynie, R.; Mirra, J. THE SYNTHESIS OF DIPHENYLCYCLOPROPENONE. *J. Am. Chem. Soc.* **1959**, *81* (1), 247–248. https://doi.org/10.1021/ja01510a060.

(17) *Cyclopropenylidenes: From Interstellar Space to an Isolated Derivative in the Laboratory | Science*. https://www.science.org/doi/full/10.1126/science.1126675 (accessed 2023-10-19).

(18) Bandar, J. S.; Lambert, T. H. Aminocyclopropenium Ions: Synthesis, Properties, and Applications. *Synthesis* **2013**, *45* (18), 2485–2498. https://doi.org/10.1055/s-0033-1338516.

(19) Kuchenbeiser, G.; Donnadieu, B.; Bertrand, G. Stable Bis(Diisopropylamino)Cyclopropenylidene (BAC) as Ligand for Transition Metal Complexes. *J. Organomet. Chem.* **2008**, *693* (5), 899–904. https://doi.org/10.1016/j.jorganchem.2007.11.056.

(20) *Insights Into the Carbene-Initiated Aggregation of [Fe(cot)2] - Lavallo - 2011 - Angewandte Chemie - Wiley Online Library*. https://onlinelibrary.wiley.com/doi/full/10.1002/ange.201005212 (accessed 2023-11-30).

(21) Harris, D. C.; Gray, H. B. Synthesis, Characterization, and Cleavage Reactions of Substituted Cyclopropenium Salts of Di-.Mu.-Chlorotetrachlorodiplatinate(2-) and Di-.Mu.-

Chloro-Tetrachlorodipalladate(2-). *Inorg. Chem.* **1974**, *13* (9), 2250–2255. https://doi.org/10.1021/ic50139a038.

(22) Cowman, C. D.; Thibeault, J. C.; Ziolo, R. F.; Gray, H. B. Structural and Electronic Spectroscopic Investigation of [(Me2N)3C3]2[Pt2Cl6]. *J. Am. Chem. Soc.* **1976**, *98* (11), 3209–3214. https://doi.org/10.1021/ja00427a026.

(23) Bruns, H.; Patil, M.; Carreras, J.; Vázquez, A.; Thiel, W.; Goddard, R.; Alcarazo, M. Synthesis and Coordination Properties of Nitrogen(I)-Based Ligands. *Angew. Chem. Int. Ed.* **2010**, *49* (21), 3680–3683. https://doi.org/10.1002/anie.200906168.

(24) Petuškova, J.; Bruns, H.; Alcarazo, M. Cyclopropenylylidene-Stabilized Diaryl and Dialkyl Phosphenium Cations: Applications in Homogeneous Gold Catalysis. *Angew. Chem. Int. Ed.* **2011**, *50* (16), 3799–3802. https://doi.org/10.1002/anie.201100338.

(25) *Metal Complexes of N-Heterocyclic Carbenes—A New Structural Principle for Catalysts in Homogeneous Catalysis - Herrmann - 1995 - Angewandte Chemie International Edition in English - Wiley Online Library*. https://onlinelibrary.wiley.com/doi/abs/10.1002/anie.199523711 (accessed 2023-10-31).

(26) Öfele, K. 1,3-Dimethyl-4-Imidazolinyliden-(2)-Pentacarbonylchrom Ein Neuer Übergangsmetall-Carben-Komplex. *J. Organomet. Chem.* **1968**, *12* (3), P42–P43. https://doi.org/10.1016/S0022-328X(00)88691-X.

(27) Wanzlick, H.-W.; Kleiner, H.-J. Nucleophile Carben-Chemie Darstellung Des Bis-[1.3-Diphenyl-Imidazolidinyliden-(2)]. *Angew. Chem.* **1961**, *73* (14), 493–493. https://doi.org/10.1002/ange.19610731408.

(28) Norman, J. P.; Larson, N. G.; Neufeldt, S. R. Different Oxidative Addition Mechanisms for 12- and 14-Electron Palladium(0) Explain Ligand-Controlled Divergent Site Selectivity. *ACS Catal.* **2022**, *12* (15), 8822–8828. https://doi.org/10.1021/acscatal.2c01698.

(29) A. Herrmann, W.; Reisinger, C.-P.; Spiegler, M. Chelating N-Heterocyclic Carbene Ligands in Palladium-Catalyzed Heck-Type reactions1N-Heterocyclic Carbenes, Part 17.-For the Preceding Communication of This Series, See [3].1. *J. Organomet. Chem.* **1998**, *557* (1), 93–96. https://doi.org/10.1016/S0022-328X(97)00736-5.

(30) Gstöttmayr, C. W. K.; Böhm, V. P. W.; Herdtweck, E.; Grosche, M.; Herrmann, W. A. Ein Definierter N-Heterocyclischer Carbenkomplex Für Die Palladium-Katalysierte Suzuki-Kreuzkupplung von Chlorarenen Bei Raumtemperatur. *Angew. Chem.* **2002**, *114* (8), 1421–

1423. https://doi.org/10.1002/1521-3757(20020415)114:8<1421::AID-ANGE1421>3.0.CO ;2- E.

(31) *Synthesis and Characterization of N-Heterocyclic Carbene Phospha-Palladacycles and Their Properties in Heck Catalysis | Organometallics* . https://pubs.acs.org/doi/full/10.1021/om049001g (accessed 2023-10-31).

(32) *Synthesis, Characterization, and Catalytic Activity of N-Heterocyclic Carbene (NHC) Palladacycle Complexes | Organic Letters*. https://pubs.acs.org/doi/full/10.1021/ol0342 64c (accessed 2023-10-31).

(33) *Synthetic and Structural Studies of (NHC)Pd(allyl)Cl Complexes (NHC = N-heterocyclic carbene) | Organometallics*. https://pubs.acs.org/doi/full/10.1021/om03431 9e (accessed 2023-10-31).

(34) *N-Heterocyclic Carbene Palladium Complexes Bearing Carboxylate Ligands and Their Catalytic Activity in the Hydroarylation of Alkynes | Organometallics* . https://pubs.acs.org/doi/full/10.1021/om049843f (accessed 2023-10-31).

(35) Jensen, D. R.; Schultz, M. J.; Mueller, J. A.; Sigman, M. S. A Well-Defined Complex for Palladium-Catalyzed Aerobic Oxidation of Alcohols: Design, Synthesis, and Mechanistic Considerations. *Angew. Chem. Int. Ed.* **2003**, *42* (32), 3810–3813. https://doi.org/10.1002/anie.200351997.

(36) Balanta, A.; Godard, C.; Claver, C. Pd Nanoparticles for C–C Coupling Reactions. *Chem. Soc. Rev.* **2011**, *40* (10), 4973–4985. https://doi.org/10.1039/C1CS15195A.

(37) *A review of soluble transition-metal nanoclusters as arene hydrogenation catalysts - ScienceDirect*. https://www.sciencedirect.com/science/article/pii/S13811169020012 55 (accessed 2023-11-01).

(38) *Reduced Transition Metal Colloids: A Novel Family of Reusable Catalysts? | Chemical Reviews*. https://pubs.acs.org/doi/full/10.1021/cr010350j (accessed 2023-11-01).

(39) C. Hurst, E.; Wilson, K.; S. Fairlamb, I. J.; Chechik, V. N-Heterocyclic Carbene Coated Metal Nanoparticles. *New J. Chem.* **2009**, *33* (9), 1837–1840. https://doi.org/10.1039/B905559B.

(40) Vignolle, J.; Don Tilley, T. N-Heterocyclic Carbene -Stabilized Gold Nanoparticles and Their Assembly into 3D Superlattices. *Chem. Commun.* **2009**, *0* (46), 7230–7232. https://doi.org/10.1039/B913884F.

(41) *Au25 Clusters as Electron-Transfer Catalysts Induced the Intramolecular Cascade Reaction of 2-nitrobenzonitrile | Scientific Reports*. https://www.nature.com/articles/srep032 14 (accessed 2023-11-02).

(42) Fu, F.; Xiang, J.; Cheng, H.; Cheng, L.; Chong, H.; Wang, S.; Li, P.; Wei, S.; Zhu, M.; Li, Y. A Robust and Efficient Pd3 Cluster Catalyst for the Suzuki Reaction and Its Odd Mechanism. *ACS Catal.* **2017**, *7* (3), 1860–1867. https://doi.org/10.1021/acscatal.6b02527.

(43) *A Dichotomy in Cross-Coupling Site Selectivity in a Dihalogenated Heteroarene: Influence of Mononuclear Pd, Pd Clusters, and Pd Nanoparticles—the Case for Exploiting Pd Catalyst Speciation | J. Am. Chem. Soc.* https://pubs.acs.org/doi/full/10.1021/jacs.1c052 94 (accessed 2023-10-31).

(44) M. Fowler, J.; Britton, E.; M. Pask, C.; E. Willans, C.; J. Hardie, M. Cyclotriveratrylene-Tethered Trinuclear Palladium( Ii )–NHC Complexes; Reversal of Site Selectivity in Suzuki–Miyaura Reactions. *Dalton Trans.* **2019**, *48* (39), 14687–14695. https://doi.org/10.1039/C9DT03400E.

(45) Zhang, B.; Chen, R.; Jiang, H.; Zhou, Q.; Qiu, F.; Han, D.; Li, R.; Tang, W.; Zhong, A.; Zhang, J.; Yu, X. Palladium-Catalyzed Highly Regioselective 2-Alkynylation of 2,x-Dihalopyridines. *Tetrahedron* **2016**, *72* (22), 2813–2817. https://doi.org/10.1016/j.tet.2016.03.027.

(46) Crudden, C. M.; Allen, D. P. Stability and Reactivity of N-Heterocyclic Carbene Complexes. *Coord. Chem. Rev.* **2004**, *248* (21), 2247–2273. https://doi.org/10.1016/j.ccr.2004.05.013.

(47) Leuthäußer, S.; Schwarz, D.; Plenio, H. Tuning the Electronic Properties of N-Heterocyclic Carbenes. *Chem. – Eur. J.* **2007**, *13* (25), 7195–7203. https://doi.org/10.1002/chem.200700228.

(48) Gusev, D. G. Electronic and Steric Parameters of 76 N-Heterocyclic Carbenes in Ni(CO)3(NHC). *Organometallics* **2009**, *28* (22), 6458–6461. https://doi.org/10.1021/om900654g.

(49) Norman, J. P.; Neufeldt, S. R. The Road Less Traveled: Unconventional Site Selectivity in Palladium-Catalyzed Cross-Couplings of Dihalogenated N-Heteroarenes. *ACS Catal.* **2022**, *12* (19), 12014–12026. https://doi.org/10.1021/acscatal.2c03743.

(50) Grasa, G. A.; Viciu, M. S.; Huang, J.; Nolan, S. P. Amination Reactions of Aryl Halides with Nitrogen-Containing Reagents Mediated by Palladium/Imidazolium Salt Systems. *J. Org. Chem.* **2001**, *66* (23), 7729–7737. https://doi.org/10.1021/jo010613+.

(51) *Global and local reactivity of N-heterocyclic carbenes with boron and phosphorus atoms: An analysis based on spin polarized density functional framework - ScienceDirect*. https://www.sciencedirect.com/science/article/pii/S0166128009007453 (accessed 2023-12-06).

(52) Özdemir, İ.; Demir, S.; Gök, Y.; Çetinkaya, E.; Çetinkaya, B. Synthesis of Novel Palladium–Carbene Complexes as Efficient Catalysts for Amination of Aryl Chlorides in Ionic Liquid. *J. Mol. Catal. Chem.* **2004**, *222* (1), 97–102. https://doi.org/10.1016/j.molcata.2004.07.024.

(53) Schaub, T.; Backes, M.; Radius, U. Nickel(0) Complexes of N-Alkyl-Substituted N-Heterocyclic Carbenes and Their Use in the Catalytic Carbon−Carbon Bond Activation of Biphenylene. *Organometallics* **2006**, *25* (17), 4196–4206. https://doi.org/10.1021/om0604223.

(54) Gstöttmayr, C. W. K.; Böhm, V. P. W.; Herdtweck, E.; Grosche, M.; Herrmann, W. A. A Defined N-Heterocyclic Carbene Complex for the Palladium-Catalyzed Suzuki Cross-Coupling of Aryl Chlorides at Ambient Temperatures. *Angew. Chem. Int. Ed.* **2002**, *41* (8), 1363–1365. https://doi.org/10.1002/1521-3773(20020415)41:8<1363::AID-ANIE1363>3.0.CO;2-G.

(55) *A Highly Efficient Catalyst for the Telomerization of 1,3-Dienes with Alcohols: First Synthesis of a Monocarbenepalladium(0)–Olefin Complex - Jackstell - 2002 - Angew. Chem. Int. Ed.* https://onlinelibrary.wiley.com/doi/full/10.1002/1521-3773%2820020315%2941%3A6%3C986%3A%3AAID-ANIE986%3E3.0.CO%3B2-M (accessed 2023-11-09).

(56) O'Brien, C. J.; Kantchev, E. A. B.; Valente, C.; Hadei, N.; Chass, G. A.; Lough, A.; Hopkinson, A. C.; Organ, M. G. Easily Prepared Air- and Moisture-Stable Pd–NHC (NHC=N-Heterocyclic Carbene) Complexes: A Reliable, User-Friendly, Highly Active Palladium Precatalyst for the Suzuki–Miyaura Reaction. *Chem. – Eur. J.* **2006**, *12* (18), 4743–4748. https://doi.org/10.1002/chem.200600251.

(57) Scott, N. W. J.; Ford, M. J.; Jeddi, N.; Eyles, A.; Simon, L.; Whitwood, A. C.; Tanner, T.; Willans, C. E.; Fairlamb, I. J. S. A Dichotomy in Cross-Coupling Site Selectivity in a Dihalogenated Heteroarene: Influence of Mononuclear Pd, Pd Clusters, and Pd Nanoparticles—the Case for Exploiting Pd Catalyst Speciation. *J. Am. Chem. Soc.* **2021**, *143* (25), 9682–9693. https://doi.org/10.1021/jacs.1c05294.

(58) Norman, J. P.; Larson, N. G.; Entz, E. D.; Neufeldt, S. R. Unconventional Site Selectivity in Palladium-Catalyzed Cross-Couplings of Dichloroheteroarenes under Ligand-Controlled and Ligand-Free Systems. *J. Org. Chem.* **2022**, *87* (11), 7414–7421. https://doi.org/10.1021/acs.joc.2c00665.

(59) Karas, Michael.; Bachmann, Doris.; Hillenkamp, Franz. Influence of the Wavelength in High-Irradiance Ultraviolet Laser Desorption Mass Spectrometry of Organic Molecules. *Anal. Chem.* **1985**, *57* (14), 2935–2939. https://doi.org/10.1021/ac00291a042.

(60) *Electrospray Ionization for Mass Spectrometry of Large Biomolecules | Science*. https://www.science.org/doi/abs/10.1126/science.2675315 (accessed 2023-11-17).

(61) Nadler, W. M.; Waidelich, D.; Kerner, A.; Hanke, S.; Berg, R.; Trumpp, A.; Rösli, C. MALDI versus ESI: The Impact of the Ion Source on Peptide Identification. *J. Proteome Res.* **2017**, *16* (3), 1207–1215. https://doi.org/10.1021/acs.jproteome.6b00805.

(62) Petroselli, G.; Mandal, M. K.; Chen, L. C.; Ruiz, G. T.; Wolcan, E.; Hiraoka, K.; Nonami, H.; Erra-Balsells, R. Mass Spectrometry of Rhenium Complexes: A Comparative Study by Using LDI-MS, MALDI-MS, PESI-MS and ESI-MS. *J. Mass Spectrom.* **2012**, *47* (3), 313–321. https://doi.org/10.1002/jms.2965.

(63) Wiliams, J. R. Investigation of Palladium-NHC Catalysts to Probe the Mechanistic Action and Direct Site-Selectivity in Cross-Coupling Reactions, University of Leeds, 2023. https://etheses.whiterose.ac.uk/33304/.

(64) Clarke, M. L.; Heydt, M. The Importance of Ligand Steric Effects on Transmetalation. *Organometallics* **2005**, *24* (26), 6475–6478. https://doi.org/10.1021/om050724p.

(65) Pranckevicius, C.; Liu, L. L.; Bertrand, G.; Stephan, D. W. Synthesis of a Carbodicyclopropenylidene: A Carbodicarbene Based Solely on Carbon. *Angew. Chem. Int. Ed.* **2016**, *55* (18), 5536–5540. https://doi.org/10.1002/anie.201600765.

(66) Thaddeus, P.; Vrtilek, J. M.; Gottlieb, C. A. Laboratory and Astronomical Identification of Cyclopropenylidene, C3H2. *Astrophys. J.* **1985**, *299*, L63–L66. https://doi.org/10.1086/184581.

*(67) Cyclopropenylidene - Reisenauer - 1984 - Angew. Chem. Int. Ed.* https://onlinelibrary.wiley.com/doi/abs/10.1002/anie.198406411 (accessed 2023-12-05).

(68) Weiss, R.; Priesner, C.; Wolf, H. SE Reactions on the C-Ring: σ-Attack. *Angew. Chem. Int. Ed. Engl.* **1978**, *17* (6), 446–447. https://doi.org/10.1002/anie.197804461.

(69) Weiss, R.; Hertel, M.; Wolf, H. Synthesis of a Donor-Substituted Tris(Cyclopropenylio)Cyclopropenylium Salt. *Angew. Chem. Int. Ed. Engl.* **1979**, *18* (6), 473–474. https://doi.org/10.1002/anie.197904731.

(70) *Cyclopropenylidenes: From Interstellar Space to an Isolated Derivative in the Laboratory | Science*. https://www.science.org/doi/full/10.1126/science.1126675 (accessed 2023-11-30).

(71) Lavallo, V.; Canac, Y.; Donnadieu, B.; Schoeller, W. W.; Bertrand, G. Cyclopropenylidenes: From Interstellar Space to an Isolated Derivative in the Laboratory. *Science* **2006**, *312* (5774), 722–724. https://doi.org/10.1126/science.1126675.

(72) Lavallo, V.; Ishida, Y.; Donnadieu, B.; Bertrand, G. Isolation of Cyclopropenylidene – Lithium Adducts: The Weiss–Yoshida Reagent. *Angew. Chem. Int. Ed.* **2006**, *45* (40), 6652–6655. https://doi.org/10.1002/anie.200602701.

(73) *Formation and propagation of well-defined Pd nanoparticles (PdNPs) during C–H bond functionalization of heteroarenes: are nanoparticles a moribund form of Pd or an active catalytic species? - ScienceDirect*. https://www.sciencedirect.com/science/article/pii/S0040402014008485 (accessed 2023-12-05).

(74) *A mild and selective Pd-mediated methodology for the synthesis of highly fluorescent 2-arylated tryptophans and tryptophan-containing peptides: a cata ... - Chemical Communications (RSC Publishing) DOI:10.1039/C3CC48481E* . https://pubs.rsc.org/en/content/articlehtml/2014/cc/c3cc48481e (accessed 2023-12-05).

(75) Reay, A. J.; Neumann, L. K.; Fairlamb, I. J. S. Catalyst Efficacy of Homogeneous and Heterogeneous Palladium Catalysts in the Direct Arylation of Common Heterocycles. *Synlett* **2016**, *27* (8), 1211–1216. https://doi.org/10.1055/s-0035-1561436.

(76) *Palladium(I) Dimer Enabled Extremely Rapid and Chemoselective Alkylation of Aryl Bromides over Triflates and Chlorides in Air - Kalvet - 2017 - Angew. Chem. Int. Ed.* https://onlinelibrary.wiley.com/doi/full/10.1002/anie.201701691 (accessed 2023-12-05).

(77) *Modular Functionalization of Arenes in a Triply Selective Sequence: Rapid C(sp2) and C(sp3) Coupling of C−Br, C−OTf, and C−Cl Bonds Enabled by a Single Palladium(I) Dimer - Keaveney - 2018 - Angew. Chem. Int. Ed.* https://onlinelibrary.wiley.com/doi/full/10.1002/anie.201808386 (accessed 2023-12-05).

(78) DAVID,EDWARD, T. From Stable Carbenes to Stable Blatter-Type Radicals. E-Thesis, Durham University, 2018. http://etheses.dur.ac.uk/12830/.

(79) Coulson, D. R. Ready Cleavage of Triphenylphosphine. *Chem. Commun. Lond.* **1968**, No. 23, 1530. https://doi.org/10.1039/c19680001530.

(80) Monfredini, A.; Santacroce, V.; Marchiò, L.; Maggi, R.; Bigi, F.; Maestri, G.; Malacria, M. Semi-Reduction of Internal Alkynes with Prototypical Subnanometric Metal Surfaces: Bridging Homogeneous and Heterogeneous Catalysis with Trinuclear All-Metal Aromatics. *ACS Sustain. Chem. Eng.* **2017**, *5* (9), 8205–8212. https://doi.org/10.1021/acssuschemeng.7b01847.

(81) Deyris, P.-A.; Cañeque, T.; Wang, Y.; Retailleau, P.; Bigi, F.; Maggi, R.; Maestri, G.; Malacria, M. Catalytic Semireduction of Internal Alkynes with All-Metal Aromatic Complexes. *ChemCatChem* **2015**, *7* (20), 3266–3269. https://doi.org/10.1002/cctc.201500729.

(82) Monfredini, A.; Santacroce, V.; Deyris, P.-A.; Maggi, R.; Bigi, F.; Maestri, G.; Malacria, M. Boosting Catalyst Activity in Cis -Selective Semi-Reduction of Internal Alkynes by Tailoring the Assembly of All-Metal Aromatic Tri-Palladium Complexes. *Dalton Trans.* **2016**, *45* (40), 15786–15790. https://doi.org/10.1039/C6DT01840H.